The dysregulation of BRCA1, PTEN, or CHK1 influences therapy resistance of breast cancer cells by affecting DNA repair and DNA replication stress signaling

Dissertation

Zur Erlangung der Würde des Doktors der Naturwissenschaften
des Fachbereichs Biologie der Fakultät für Mathematik, Informatik und Naturwissenschaften
der Universität Hamburg

vorgelegt von

Sandra Nadine Classen

aus Pinneberg, Deutschland

Hamburg, 2023

Dissertation reviewer

First reviewer: Prof. Dr. Tim Gilberger

Second reviewer: Prof. Dr. Kerstin Borgmann

Date of disputation: 01.11.2023

Eidesstattliche Versicherung - Declaration on oath

Hiermit erkläre ich an Eides statt, dass ich die vorliegende Dissertationsschrift selbst verfasst und keine anderen als die angegebenen Quellen und Hilfsmittel benutzt habe.

I hereby declare, on oath, that I have written the present dissertation by my own and have not used other than the acknowledged resources and aids.

Hamburg, 10.05.2023
City, Date

S. Clo

Signature

Erklärung

Ich versichere, dass dieses gebundene Exemplar der Dissertation und das in elektronischer Form eingereichte Dissertationsexemplar (über den Docata-Upload) und das bei der Fakultät (zuständiges Studienbüro bzw. Promotionsbüro Physik) zur Archivierung eingereichte gedruckte gebundene Exemplar der Dissertationsschrift identisch sind.

I, the undersigned, declare that this bound copy of the dissertation and the dissertation submitted in electronic form (via the Docata upload) and the printed bound copy of the dissertation submitted to the faculty (responsible Academic Office or the Doctoral Office Physics) for archiving are identical.

Hamburg, 10.05.2023

City, Date

Signature

Table of contents

Abbreviation

53BP1	Tumor suppressor p53-binding protein 1
AKT	Protein kinase B
ATM	Ataxia telangiectasia mutated
ATP	Adenosine triphosphate
ATR	Ataxia telangiectasia and Rad3-related protein
ATRIP	ATR-interacting protein
BARD1	BRCA1 associated RING domain 1
BIR	Break-induced replication
BLM	Bloom syndrome protein
BRCA1/2	Breast cancer gene 1/2
BRCT	BRCA1 C-terminal
C-terminus	Carboxyl-terminus
Cas9	CRISPR associated protein 9
CD	Cluster of differentiation
CDC25A	Cell division cycle 25A
CDK	Cyclin-dependent kinase
CENP-C	Centromeric protein C
Cera	Ceralasertib (ATR inhibitor)
cGAS	Cyclic GMP–AMP synthase
CHK1	Checkpoint kinase 1
CIN	Chromosomal instability
CRISPR	Clustered regularly interspaced short palindromic repeats
CtIP	CtBP-interacting protein
CTLA-4	Cytotoxic T-lymphocyte antigen-4
D-loop	Displacement-loop
DDR	DNA damage response
DNA	Deoxyribonucleic acid
DNA2	DNA replication ATP-dependent helicase/nuclease DNA2
DNA-PKcs	DNA-dependent protein kinase catalytic subunit
dNTP	Deoxynucleotide triphosphate
DSB	Double strand break
EG5	Kinesin-related motor protein Eg5
EMA	European Medicines Agency
ER	Estrogen receptor

EXO1	Exonuclease 1
FANCI	Fanconi anemia complementation group I
FDA	U.S. Food and Drug Administration
h	hours
Her2	Human epidermal growth factor receptor 2
HLTF	Helicase-like transcription factor
HR	Homologous recombination
HU	Hydroxyurea
ICI	Immune checkpoint inhibitor
IFN	Interferon
IR	Ionizing radiation
Ki67	Marker of proliferation Ki-67
LumA	Luminal A
LumB	Luminal B
MCM2	Minichromosome maintenance protein 2
METABRIC	Molecular Taxonomy of Breast Cancer International Consortium
MMC	Mitomycin C
MRE11	Double strand break repair nuclease MRE11
MRN-complex	MRE11-RAD50-NBS1-complex
MSI	Microsatellite instability
mTOR	Mammalian target of rapamycin
N-terminus	Amino-terminus
NBS1	Nijmegen breakage syndrome protein 1
nCIN	Numerical chromosomal instability
NHEJ	Non-homologous end joining
NLS	Nuclear localization signal
OLA1	Obg-Like ATPase 1
Ori	Origin of replication
p-	Phospho-
PALB2	Partner and localizer of BRCA2
PARP1	Poly-[ADP-ribose] polymerase 1
PCNA	Proliferating cell nuclear antigen
PD-L1	Programmed death-ligand 1
PDO	Patient-derived organoid
PI3K	Phosphoinositide 3-kinases
PIP2	Phosphatidylinositol-4,5-bisphosphate
PIP3	Phosphatidylinositol-3,4,5-trisphosphat

PLK1	Polo-like kinase 1
PR	Progesterone receptor
PRIMPOL	Primase and DNA directed polymerase
PTEN	Phosphatase and tensin homolog
RACK1	Receptor for activated protein C kinase 1
RAD50	Double Strand Break Repair Protein RAD50
RAD51	Recombinase Rad51
RAP80	Receptor-associated protein 80
RECQ1	ATP-dependent DNA helicase Q1
RING	Really interesting new gene
RNA	Ribonucleic acid
RPA	Replication protein A
RT	Radiotherapy
SCD	Serine containing domain
sCIN	Structural chromosomal instability
Ser	Serine
SMARCAD1	SWI/SNF-related, matrix-associated actin-dependent regulator of chromatin, subfamily A containing DEAD/H box 1
SMARCAL1	SWI/SNF-related matrix-associated actin-dependent regulator of chromatin subfamily A-like protein 1
SSA	Single strand annealing
SSB	Single strand break
ssDNA	Single strand deoxyribonucleic acid
STING	Stimulator of interferon genes
Tala	Talazoparib (PARP1 inhibitor)
TGCA	The Cancer Genome Atlas
Thr	Threonin
TNBC	Triple negative breast cancer
TopBP1	DNA topoisomerase II binding protein 1
WEE1	WEE1 G2 checkpoint kinase
WT	Wild type
WRN	Werner syndrome helicase
ZRANB3	Zinc finger, RAN-binding domain containing 3

Abstract

Breast cancer is the most frequently diagnosed cancer worldwide. Despite good available therapeutic options, more than half a million women still die each year due to breast cancer. A major reason contributing to this high number is the development of therapy resistances. Thus, identification of proteins and associated pathways that are involved in resistance development are a focus of the cancer research field. A common mechanism by which tumor cells become resistant to therapy is their tolerance to genomic instability, which leads to accumulation of tumor-promoting mutations. DNA replication stress and defects in DNA repair pathways have been shown to contribute to genomic instability, thereby supporting the development of resistance to chemotherapeutics and radiotherapy. Since increased replication stress is a hallmark of cancer cells, it has been identified as a promising target for new therapeutic approaches. The aim of this thesis was to exploit how the replication stress response contributes to therapy resistance, depending on the dysregulation of the three selected candidate proteins BRCA1, PTEN, and CHK1.

BRCA1 is a key protein of the DNA repair pathway homologous recombination and involved in DNA replication fork protection of stalled forks. An isogenic MCF7 *BRCA1* mutated cell system with therapy resistant and sensitive clones was generated. The observed resistance to different DNA damaging sources correlated to low level of replication stress, efficient DNA repair and high CHK1 activation. CHK1, one of the main proteins of the replication stress response and highly expressed in chromosomal unstable tumors, counteracts exogenously induced replication stress by anti-cancer therapies. Similar results were observed in *BRCA1* proficient MDA-MB-231 cells with resistant and sensitive sublines. An inhibition of the ATR-CHK1 axis led to sensitization of the resistant cell lines.

PTEN prevents genomic instability through association with replication forks. Analysis of the TCGA dataset revealed that a low PTEN expression correlated with a high chromosomal instability score and significantly worse overall survival in breast cancer patients. Low PTEN expression was associated with increased replication stress, manifested by increased origin firing in several breast cancer cell lines. Additionally, PTEN expression correlated with the fork stability upon replication stress induction. The elevated replication stress led to increased sensitivity against PARP1 inhibition.

The observed results show that the replication stress response is a suitable target to sensitize resistant cancer cells to radio- and chemotherapy, which was independent of the analyzed breast cancer subtype and *BRCA* status. This suggests that a wide range of breast cancer patients could benefit from combination therapies that target the replication stress response.

Zusammenfassung

Brustkrebs ist weltweit die am häufigsten diagnostizierte Krebsart. Trotz guter Behandlungsmöglichkeiten sterben mehr als eine halbe Million Frauen jedes Jahr daran. Ein Grund für diese hohe Zahl ist die Entstehung von Therapieresistenzen. Die Identifizierung von Proteinen und damit verbundenen Signalwegen, die an der Resistenzentwicklung beteiligt sind, ist daher ein Schwerpunkt der Krebsforschung. Genomische Instabilität von Tumorzellen begünstigt das Auftreten weiterer tumorfördernder Mutationen und daraus resultierende Resistenzen. DNA-Replikationsstress und Defekte in der Reparatur von DNA-Schäden tragen zur genomischen Instabilität bei und begünstigen die Entwicklung von Chemo- und Strahlenresistenz. Da erhöhter Replikationsstress ein Merkmal von Krebszellen ist, ist es ein vielversprechendes Ziel für neue therapeutische Ansätze. Das Ziel dieser Arbeit war es, den Beitrag der Replikationsstressreaktion für die Therapieresistenz, in Abhängigkeit von der Deregulierung der drei Kandidatenproteine BRCA1, PTEN und CHK1 zu untersuchen.

BRCA1 ist ein Schlüsselprotein des DNA-Reparaturweges homologe Rekombination und beteiligt am Schutz vom angehaltenen DNA-Replikationsgabeln. Es wurde ein isogenes MCF7 *BRCA1*-mutiertes Zellsystem mit therapieresistenten und -empfindlichen Klonen erzeugt. Die beobachtete Resistenz korrelierte mit geringem Replikationsstress, effizienter DNA-Reparatur und erhöhter CHK1-Aktivierung. CHK1, eines der wichtigsten Proteine der Replikationsstress-reaktion, wirkt durch hohe Expression dem durch Krebstherapien induziertem Replikationsstress entgegen. Diese Beobachtungen konnten in *BRCA1*-kompetenten MDA-MB-231-Zellen mit resistenten und empfindlichen Sublinien bestätigt werden. Eine Inhibition der ATR-CHK1-Achse führte zur Sensibilisierung der resistenten Zelllinien.

PTEN verhindert eine genomische Instabilität durch Assoziation mit Replikationsgabeln. Eine Analyse des TCGA-Datensatzes ergab, dass eine niedrige PTEN-Expression mit hoher chromosomalen Instabilität und einer signifikant schlechteren Gesamtüberlebensrate bei Brustkrebspatientinnen korreliert. Verschiedene Zelllinien mit niedriger PTEN-Expression wiesen erhöhten Replikationsstress auf, der sich durch die vermehrte Aktivierung von ruhenden Replikationsursprüngen äußerte. Darüber hinaus wurde eine Korrelation von PTEN-Expression und Stabilität der Replikationsgabel nach Induktion von Replikationsstress beobachtet. Erhöhter Replikationsstress führte zu einer höheren Empfindlichkeit gegenüber PARP1-Inhibition.

Diese Ergebnisse zeigen, dass die Replikationsstressreaktion ein geeignetes Ziel ist, um resistente Krebszellen gegenüber Radio- und Chemotherapie zu sensibilisieren, unabhängig vom Brustkrebs-Subtyp und *BRCA* Status. Dies deutet darauf hin, dass ein breites Spektrum von Brustkrebspatientinnen von Kombinationstherapien profitieren könnte, die auf die Replikationsstressreaktion abzielen.

1. Introduction

Cancer is a very common disease with estimated 19.3 million new diagnosed cases worldwide in 2020 [1]. With the still incredibly high number of about 10 million deaths in 2020, it is a leading cause of death in many countries [1]. The general feature underlying most cancers is an abnormal cell division, thereby promoting uncontrolled cellular growth and the ability to spread to nearby or distant organs across the human body [2]. As this can occur in almost any organ and cell type, cancer is a very heterogeneous and complex disease that displays many different hallmarks which are still under extensive investigation [3]. The increase in longevity leads to a growing number of patients being diagnosed with cancer each year and the upsetting high number of cancer deaths highlights the importance of the entire field of cancer research.

1.1 Breast cancer

Breast cancer has become the most frequently diagnosed cancer with 2.26 million newly diagnosed patients worldwide in 2020 [1]. Approximately 685.000 breast cancer patients died due to the disease in 2020, making breast cancer the leading cancer associated cause of death for women in 18 out of 20 investigated regions across the world [1]. Thus, more research to improve therapeutic options for breast cancer patients is necessary.

1.1.1 Breast cancer subtype is associated with prognosis and therapy indication

Breast cancer is a very heterogeneous disease that has been classified into five main subtypes: luminal A (LumA), normal-like, luminal B (LumB), human epidermal growth factor receptor 2 (Her2)-positive (Her2+), and triple-negative breast cancer (basal-like) (TNBC) (Figure 1) [4]. These molecular subtypes were identified and defined in 2000 by microarray analysis [5]. The definition includes the expression of different receptors, which vary depending on the subtype and have major implications for therapy options [6-8]. LumA and LumB, as well as normal-like cancer cells, express hormone receptors (estrogen and/or progesterone), only distinguished by the proliferation marker Ki67 [8, 9]. LumA and normal-like tumors show low marker of proliferation Ki-67 (Ki67) expression. In contrast, LumB tumors have a high Ki67 expression and may also express Her2 [9]. These hormone receptor positive breast cancer subtypes are usually treated with hormone therapy, e.g., tamoxifen [10]. Her2+ tumors are classified as hormone receptor negative but show high Her2 expression. Her2 can be specifically targeted by therapeutic drugs like trastuzumab [11]. TNBC is another subtype, which has no expression of either hormone or Her2 receptors. Therefore, no targeted drugs are available, and these tumors are mainly treated with systemic chemotherapies, e.g.,

taxanes or anthracyclines and radiotherapy (RT) [12]. While response rates to chemotherapy are initially high, many patients develop resistance to standard of care therapy later on. Recurrences and visceral metastasis in mainly lung, liver, and brain occur frequently, contributing to an overall bad prognosis for many patients [13]. Thus, a great number of studies focus on the treatment of TNBC patients, as they have the worst prognosis amongst the different breast cancer subtypes (Figure 1) [12].

Lately, it has become evident that certain patients with a primary LumA tumor develop resistance against the standard of care treatment options and show recurrent tumors, which may change their subtype [9, 14]. Once a recurrent tumor is diagnosed, the survival rates for luminal, as well as Her2+, are close to the rates for TNBCs five years post recurrence [15]. The rates were 10 % for patients with a TNBC, around 35 % for patients with a luminal tumor, and 30 % for Her2+ breast cancer patients [15].

This observation indicates that for a subgroup of the breast cancer subtypes with good cure rates, identification of markers that could predict therapy failure and recurrence probability are desirable.
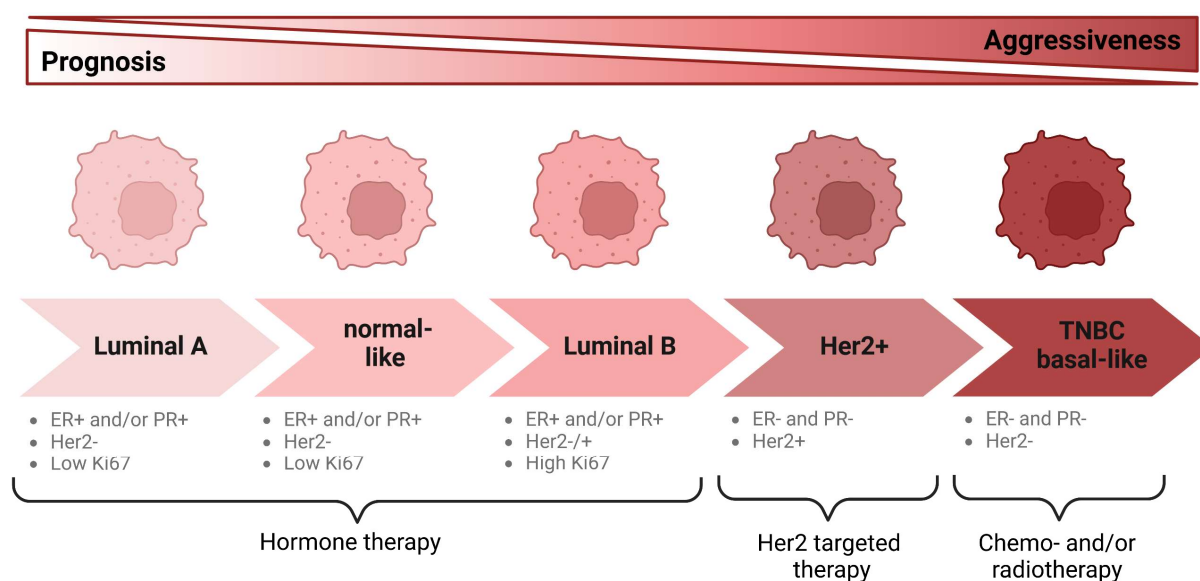

Figure 1: Overview of breast cancer subtypes with associated molecular features, prognosis, aggressiveness, and therapy implications. Adapted version from [4]. Created with BioRender.com. ER: Estrogen receptor; Her2: Human epidermal growth factor receptor 2; Ki67: Marker of proliferation Ki-67; PR: progesterone receptor; TNBC: Triple-negative breast cancer.

1.1.2 Consequences of BRCA1, PTEN, and CHK1 mutations in hereditary breast cancer

Several genes have been identified to be mutated in hereditary breast cancer and are associated with a high penetrance. These genes include *breast cancer gene 1 and 2* (*BRCA1/2*) and *phosphatase and tensin homolog* (*PTEN*) [16-18]. Hereditary breast cancers account for about 10% of all cases and more than 25% of those are caused by mutations in the *BRCA1* and *BRCA2* genes [19]. Mutations in *PTEN* are less frequent in hereditary breast cancers (≤ 5%), but *PTEN* loss is acquired in more than 30% of sporadic breast tumors [20]. BRCA1 and PTEN are both involved in the regulation of checkpoint kinase 1 (CHK1), which is a regulator for the cell cycle progression and has additional functions in deoxyribonucleic acid (DNA) repair as well as the replication stress response. CHK1 itself is not frequently mutated in breast cancer and has also not been associated with a high penetrance [21].

Associated risk for breast cancer development: The risk of developing breast cancer during a lifetime has been investigated by several groups for these genes. For carrier of *BRCA1/2* or *PTEN* mutations the risk to develop breast cancer is as high as up to 85% [22]. The results for *CHK1* are controversial. One study did not find any evidence that hereditary variants of *CHK1* are linked to an increased risk for the development of breast cancer [21]. In contrast, other studies have indicated before that alterations of *CHK1* may contribute to an increased breast cancer risk [23]. For *BRCA1* and *PTEN* it has further been shown that mutations may correlate with a certain breast cancer subtype. Low expression or loss of PTEN, as well as BRCA1 has been associated with a TNBC subtype [24, 25]. For *BRCA1* mutated tumors it is estimated that approximately 50-80% of them are TNBCs [24].

Molecular consequences on involved pathways: The severe consequences of the mutations in *BRCA1*, *PTEN*, or *CHK1* are explained by their important functions in multiple pathways to ensure the cellular homeostasis. BRCA1 is an essential protein that is involved in different cellular processes. The most described and well-known function is found in the DNA repair process homologous recombination (HR) [26]. It also acts in the protection of stalled replication forks and centrosome duplication (Figure 2) [27, 28]. Functions of PTEN are the antagonizing effect on the phosphoinositide 3-kinases (PI3K)-protein kinase B (AKT)-mammalian target of rapamycin (mTOR) pathway and supporting centrosome stability [29, 30]. Additional discovered functions are associated with the DNA damage and replication stress responses (Figure 2) [31-33]. CHK1 has important functions in cell cycle control, which is especially important in response to DNA damage and replication stress [34]. Further, CHK1 directly promotes DNA repair by HR [35] and acts as an inhibitor for cyclin-dependent kinase 1 (CDK1) at the centrosomes (Figure 2) [36]. All three proteins are important key regulators of pathways that ensure the chromosomal and thereby the genomic stability of a cell.

1.2 Chromosomal instability

Chromosomal instability (CIN) is one of the processes that have been identified to cause genomic instability and thereby contributes to tumorigenesis and tumor progression [2]. CIN is characterized by aberrant chromosomal segregation, leading to aneuploidy, which is characterized by amplifications or losses of entire or parts of chromosomes [37]. The amplification or loss of whole chromosomes is defined as numerical CIN (nCIN). Loss or amplification of parts of the chromosomes is referred to as structural CIN (sCIN), which also
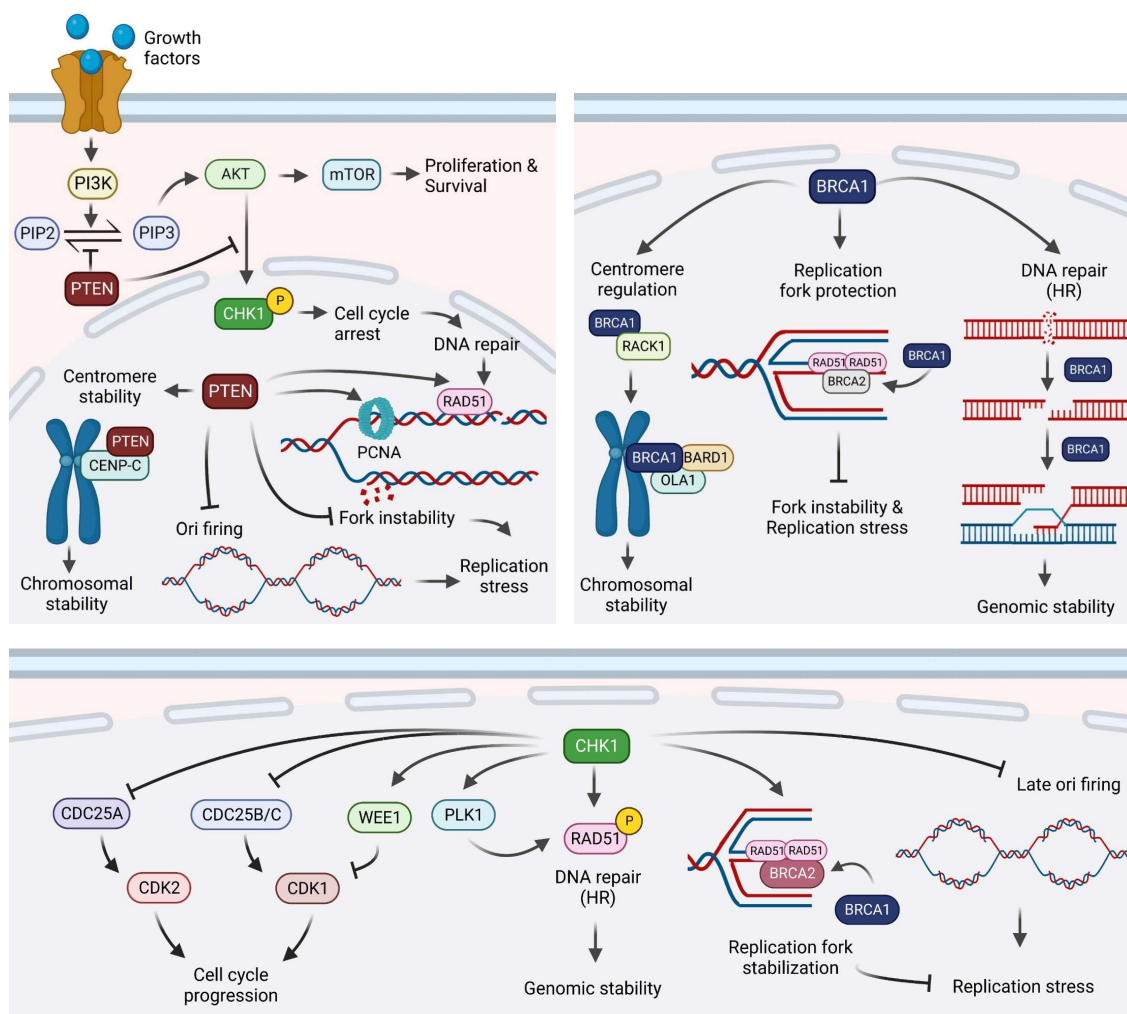
Figure 2: Functions of PTEN, BRCA1, and CHK1 in different cellular pathways. Created with BioRender.com. AKT: Protein kinase B; BARD1: BRCA1 associated RING domain 1; BRCA1/2: Breast cancer gene 1/2; CDC25A/B/C: Cell division cycle 25A/B/C; CDK1/2: Cyclin-dependent kinase 1/2; CENP-C: Centromeric protein C; CHK1: Checkpoint kinase 1; HR: Homologous recombination; mTOR: Mammalian target of rapamycin; OLA1: Obg-like ATPase 1; P: Phospho-; Ori: Origin of replication; PCNA: Proliferation cell nuclear antigen; PI3K: Phosphoinositide 3-kinase; PIP2: Phosphatidylinositol-4,5-bisphosphate; PIP3: Phosphatidylinositol-3,4,5-trisphosphat; PLK1: Polo-like kinase 1; PTEN: Phosphatase and tensin homolog; RACK1: Receptor for activated protein C kinase 1; RAD51: Recombinase Rad51; WEE1: G2 checkpoint kinase WEE1.

includes the translocation of chromosomal parts [37]. Another process contributing to genomic instability is microsatellite instability (MSI). It is defined as a change in the number of repetitive short sequences (microsatellites) from the inherited number and is mainly caused by defects in the DNA repair pathway mismatch repair [38]. MSI occurs most frequently in colorectal, endometrial and gastric cancers [38]. CIN has been stated as a major driver of tumorigenesis and tumor progression, as the loss or amplification of chromosomes or parts of it may result in deletion of tumor suppressor genes or amplification of oncogenes [39]. Thus, tumors with high CIN are associated with high aggressiveness, therapy resistance, and an overall worse prognosis for cancer patients [40, 41].

1.2.1 Chromosomal instability in breast cancer

A study from Carter et al. estimated that more than 50% of their breast cancer cohort samples showed a genome doubling, independent of the subtype [42]. Thus, all breast cancer subtypes can display CIN. Further, *BRCA*-mutated or TNBC tumors have been shown to be associated with the highest CIN level [43]. In the case of TNBCs, an extremely high level of CIN does not correlate with the prognosis in a linear matter. Indeed, the higher the CIN, the better the response to chemotherapy treatment and patient outcome [43]. This finding was confirmed by the study from Birkbak et al., in which they show that intermediate CIN scores lead to decreased recurrence-free survival compared to the groups of low and extremely high CIN scores [44]. They conducted the CIN70 score for their analysis, which was introduced by Carter et al. in 2006 [45]. Almost 2000 tumor samples from nine different tumor entities were screened for functional aneuploidy and examined for correlating gene expression patterns. This revealed a signature of 70 involved genes, which is now commonly used to identify CIN in tumor samples and is referred to as the CIN70 score [45].

Most of the therapeutic approaches for the treatment of TNBCs, including taxanes and RT, lead to increased and intolerable CIN levels in a cancer cell and, thus cancer cell death. At the same time, high CIN already sensitizes cancer cells to the treatment with RT and taxanes [46, 47]. This explains why many TNBCs initially show good response rates to these treatment options. Yet, the problem of frequently developed resistances and recurrences remains to be solved [48]. As the CIN state of cancer cells may give important indications for therapy response and prognosis, the mechanisms how CIN arises and is maintained in cancer cells has been highly investigated.

1.2.2 Emergence of chromosomal instability

Several mechanisms contributing to CIN have been identified so far. These include amongst many other pathways: mitotic checkpoint failure, centrosome aberrations, DNA replication stress, and DNA damage response (DDR) [48-50].

Consequences of *BRCA1* mutations: *BRCA1* mutations can contribute to CIN due to the involvement of BRCA1 in most of the mentioned pathways (Figure 2). An early study from Xu et al. in 1999 investigated the involvement of BRCA1 in the tumorigenesis in normal fibroblasts [51]. They discovered that the loss of exon 11 in the *BRCA1* gene led to a defect in the G2/M checkpoint and amplification of centrosomes, resulting in incorrect segregation of the chromosomes. They concluded that *BRCA1* defects caused severe genomic instability due to CIN and thus contribute to tumorigenesis in cells [51]. Later, it was shown that BRCA1 associates at centromeres together with BRCA1 associated RING domain 1 (BARD1) and obg-Like ATPase 1 (OLA1) [52, 53] and that a dysregulated expression of any of the three proteins led to incorrect centromere duplications [54]. Further, the interaction of the N-terminus of BRCA1 with receptor for activated protein C kinase 1 (RACK1) is essential for guiding BRCA1 to the centromeres [55]. The other two functions of BRCA1 in the DNA repair and replication stress response (Chapter 1.3.1 & 1.4.2) highlight that a non-functional BRCA1 protein can contribute to the emergence of CIN in more than one pathway and ultimately promote genomic instability (Figure 2). How replication stress contributes to CIN was described by Burell et al. in 2013. The induction of replication stress caused sCIN and nCIN to arise in colorectal cancer cells that displayed no CIN before [49]. They further show that replication fork progression was affected in cells with high CIN, accompanied by increased replication fork stalling and asymmetric fork progression [49].

Impact of PTEN dysregulation: PTEN dysregulation also contributes to CIN due to its multiple nuclear functions (Figure 2). One function is the direct interaction with the centromeric protein C (CENP-C), which is an important protein of the kinetochore [33]. During mitosis, mitotic spindles attach to the kinetochore protein structure for chromosomal segregation. That is why mutations which disrupt the interaction of PTEN and CENP-C cause instability of the centromeres and lead to breakage of the centromeres [33]. Additionally, PTEN regulates the mitotic kinesin-related motor protein Eg5 (EG5), which is responsible for the correct formation of the spindles and thus for the alignment of the chromosomes [29]. The study revealed that *PTEN* depletion led to aberrant EG5 phosphorylation, which resulted in spindle assembly failure and chromosome misalignment [29]. Like BRCA1, PTEN is not only contributing to CIN by direct association with the centromeres of the chromosomes, but also by additional functions in other cellular pathways, like DNA repair and replication stress response (Figure 2; Chapter 1.3.1 and 1.4.2).

Influence of CHK1 dysregulation: CHK1 is also a key protein of many pathways that lead to CIN upon disruption. The ataxia telangiectasia and Rad3-related protein (ATR)-CHK1 axis is a key regulator of the replication stress response (Chapter 1.4), and a deregulation of both proteins has been shown to result in elevated CIN [56]. Upon detection of DNA damage, ATR and CHK1 control the stalling of replication forks and the firing of origins of replication. CHK1

also delays the cell cycle progression to prevent the formation of under-replicated DNA and allow the DNA repair pathways to repair the detected DNA damages [57, 58]. Lastly, CHK1 actively promotes the repair of DNA double strand breaks (DSBs) by phosphorylation of the recombinase Rad51 (RAD51) at threonine (Thr)309, which seems to be essential for the loading of RAD51 on the DNA to perform HR (Figure 2) [35]. It has been shown that unrepaired DNA damages contribute to CIN, especially since two DSBs on different chromosomes are sufficient to create chromosomal translocations [59]. Thus, deficiency or disruption of DNA repair pathways may lead to elevated CIN in a cancer cell.

1.3 DNA repair

The repair of occurring DNA damages is the most crucial process in a cell. The accurate repair is essential for the survival of normal cells and the prevention of a neoplastic transformation. Incorrect repair may lead to inactivation of tumor suppressor genes or activation of proto-oncogenes [60]. The most lethal DNA damage that a cell can acquire is a DSB. The repair is complex and the risk for severe chromosomal aberrations to occur is high. There are three main pathways that can repair DSBs: Non-homologous end joining (NHEJ), single strand annealing (SSA), and HR. However, the only pathway that repairs DSBs without errors is HR, as it uses the homologous sister chromatid as template [61, 62]. This is why HR can only occur during the S and G2 phase of the cell cycle, due to the requirement of the sister chromatid to be present. NHEJ is the major repair pathway during the other cell cycle phases [63]. This thesis focuses on HR, since a deficiency in HR is frequently associated with breast cancer and BRCA1 is a key regulator.

1.3.1 Homologous recombination

The accurate repair of DSBs prevents the occurrence of mutations, chromosomal aberrations, and ensures the survival of the cell. DSBs can arise endogenously, for example when a replication fork runs into a single strand break (SSB). They can also be induced exogenously by DNA damaging chemicals or ionizing radiation (IR) [64].

Once a DSB is detected in a cell, the appropriate DNA repair pathway has to be chosen. This is achieved by tumor suppressor p53-binding protein 1 (53BP1) and BRCA1, controlling the end resection dependent on the cell cycle phase. In the S phase, 53BP1 is removed in a BRCA1-dependent manner from DSB sites. 53BP1 inhibits the end resection by CtBP-interacting protein (CtIP) and leads the cell towards NHEJ [65]. BRCA1 associates at DSB sites due to the interaction with the Abraxas and receptor-associated protein 80 (RAP80) complex that binds to ubiquitinated histones [66]. If BRCA1 is recruited to a DSB, it forms a complex with CtIP to promote the 5'-3'-end resection to generate 3'-overhangs. This is achieved by interaction with the MRE11-RAD50-NBS1 (MRN)-complex, which consists of

double-strand break repair nuclease MRE11 (MRE11), double Strand Break Repair Protein RAD50 (RAD50), and nijmegen breakage syndrome protein 1 (NBS1) [67]. Additional nucleases and helicases, like DNA replication ATP-dependent helicase/nuclease DNA2 (DNA2), exonuclease 1 (EXO1), werner syndrome helicase (WRN), and bloom syndrome protein (BLM) join to further promote excessive 5'-3'-end resection that is needed for HR [68]. This step represents the initiation step of the HR. The 3'-overhangs are then subsequently coated with replication protein A (RPA) to protect the single strand DNA (ssDNA) from nucleolytic degradation and formation of secondary DNA structures [63]. Next, RPA must be replaced by RAD51, the essential protein to mediate the strand invasion in the sister chromatid. The complex of BRCA1-partner and localizer of BRCA2 (PALB2)-BRCA2 recruits RAD51 and initiates the loading on to the ssDNA [26]. The newly formed RAD51-filament can then start the search for the homologous region on the sister chromatid [69]. Upon detection of the homologous region, a small displacement-loop (D-loop) can be formed, where one strand of the sister chromatid is displaced, and a primer-template junction is created to enable DNA synthesis and repair [70]. Once the synthesis is finished, the newly synthesized DNA can be displaced from the D-loop, followed by annealing to the complementary sequence of the non-invading stand [70]. This sub pathway of the HR is called synthesis-dependent strand annealing. This process avoids the crossover of DNA, and is thus the preferred pathway for DSB repair. The other two sub pathways of HR are the double Holliday junction model, and break-induced replication (BIR). Both are prone to the generation of DNA crossovers, potentially leading to mutations and genomic alterations [71].

Additional factors influencing the HR are modifications of the involved proteins, like phosphorylation. For example, it has been shown that CHK1 is responsible for the phosphorylation of RAD51 at Thr309 [35]. This phosphorylation seems to be essential for the DNA association of RAD51 and thereby for the ability to perform HR [35]. Recently, it has been suggested that CHK1 is also involved in the mediation of polo-like kinase 1 (PLK1) activity [72]. This activity promotes HR by phosphorylation of RAD51 at serine (Ser)14, which is required for the CHK1-dependent Thr309 phosphorylation [72]. CHK1 passively contributes to HR, by stalling the cell cycle progression to allow DNA damage to be repaired [34]. PTEN has less direct functions on HR, but rather influences the DNA repair by regulation of CHK1 [32]. It also seems to be involved in the recruitment of RAD51 and other DNA repair associated factors to the chromatin, as a loss of *PTEN* leads to reduced detection of these proteins in nuclear fractions [33, 73].

However, the involvement of BRCA1 in most of the key steps of HR makes it an essential protein for the pathway. Thus, mutations in *BRCA1* are associated with a HR deficiency, which can have severe effects on the cell and offer indications for possible therapy options.

1.3.2 The BRCA1 gene and associated functions

In 1990, Hall and colleagues first described an association of early-onset familial breast cancer with the chromosome 17q21 [17]. This gene was soon named *BRCA1* and has been extensively studied ever since. The *BRCA1* gene encodes a protein with 1863 amino acids and contains several important protein domains (Figure 3) [74].

Starting from the N-terminus, the first domain is the really interesting new gene (RING) domain, which conducts the direct interaction with the BARD1 protein [75]. This heterodimer functions as an E3-ubiquitin ligase and has been shown to be involved in several cellular processes, including chromatin remodeling, DNA repair, and response to chemotherapeutic drugs [76, 77]. Mutations in the entire N-terminal region, including the RING domain, have been associated with an increased breast cancer risk before and are likely associated with loss of the E3-ubiquitin ligase activity [78]. It has been shown that the function of the heterodimer influences the response to chemotherapeutics in DT40 cells [77]. A non-functional E3-ubiquitin ligase activity led to resistance against mitomycin C (MMC), but at the same time, showed sensitivity to camptothecin. The authors suggested that this effect is due to the BRCA1-BARD1-dependent claspin-CHK1 activation, an essential step in the replication stress response [77]. The chromatin remodeling function has been demonstrated by Densham et al., as they indicated the following model: The E3-ubiquitin ligase activity modifies the chromatin and thereby promotes binding of SWI/SNF-related, matrix-associated actin-dependent
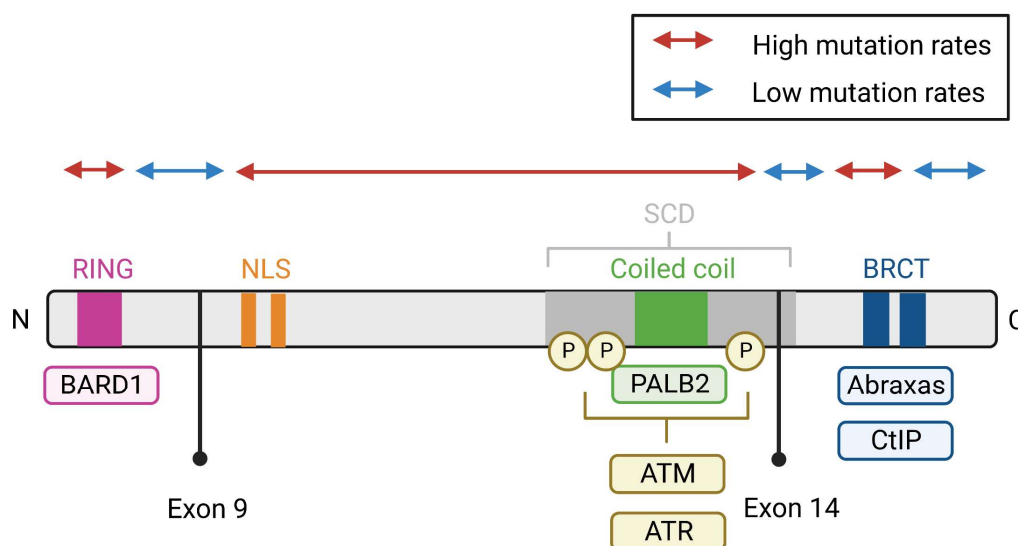
Figure 3: *BRCA1* gene with functional domains, associated proteins, and mutation rates. Adapted version from [83]. Created with Biorender.com. ATM: Ataxia telangiectasia mutated; ATR: Ataxia telangiectasia and Rad3-related protein; BARD1: BRCA1 associated RING domain 1; BRCT: BRCA1 C-terminal domain; C: C-terminus; CtIP: CtBP-interacting protein; N: N-terminus; NLS: Nuclear localization signal; P: Phosphorylation site; PALB2: Partner and localizer of BRCA2; RING: Really interesting new gene; SCD: Serine containing domain.

regulator of chromatin, subfamily A containing DEAD/H box 1 (SMARCAD1), a chromatin remodeler itself. The binding of SMARCAD1 is required for repositioning of 53BP1, which allows end resection and HR initiation to occur [76]. Many questions regarding the targets, functions, and consequences of loss of the E3-ubiquitin ligase activity on prognosis and therapeutic implications remain elusive.

Next to the RING domain, the nuclear localization signal (NLS) of BRCA1 is encoded, which ensures the transport into the nucleus via interaction with importin α [79]. The domain is essential to ensure the correct localization of the BRCA1 protein due to the critical functions of BRCA1 being located in the nucleus.

The next functional domain is the coiled-coil domain, which has important functions in the complex formation with PALB2 [80]. Lately, it has been shown that mutations affecting the BRCA1-PALB2 interaction can lead to increased cancer risk [81]. Additionally, new studies suggest that mutations in the coiled-coil domain can lead to HR deficiency and thus to sensitivity against poly-[ADP-ribose] polymerase 1 (PARP1) inhibition [82]. Spanning the coiled coil domain and surrounding regions is a serine containing domain (SCD), which includes the phosphorylation sites of ATR and ataxia telangiectasia mutated (ATM), two of the main DDR kinases [83].

In the C-terminal region, two BRCA1 C-terminal (BRCT) domains are located, which have been first identified in the *BRCA1* gene, but are conserved structures in several other known proteins [84]. The BRCT domains recognize interaction proteins that are phosphorylated with the pS-X-X-F motif, like Abraxas and CtIP, and are therefore crucial for the complex formation ability of BRCA1 [84]. Mutations in these domains have been associated with breast cancer before [74]. Interestingly, mutations in the BRCT and RING domains are occurring most frequently and seem to be of clinical relevance (Figure 3) [83]. Despite growing knowledge about mutations in the functional domains of *BRCA1*, mutations in non-functional domains remain poorly understood.

1.3.3 Clinical implications of BRCA1 mutations

A frequently described consequence of a mutation or loss of *BRCA1* is a defect in HR, which has been shown to be an important indicator for therapy choice. It is well known that specifically PARP1 inhibition is synthetic lethal for *BRCA* mutated cells [85, 86]. The concept of synthetic lethality has already been introduced in 1946 by Dobzhansky [87]. It is defined as an interaction between two genes, where mutations in one gene have no or limited effects on the viability of a cell. Mutations in both genes however, lead to cell death [88]. The synthetic lethality interaction of *BRCA1/2* mutations with PARP1 inhibition has been shown first in 2005 [85, 86]. PARP1 normally functions in an alternative DNA repair pathway, which is especially important to recognize and repair SSBs. If a cancer cell harbors a mutation in *BRCA1/2*, and due to

inhibition of PARP1 another important DNA repair pathways is impaired, the cancer cells do not have an escape from cell death [89]. It became evident soon that the synthetic lethality was not limited to tumors carrying mutations in *BRCA1/2*, but also occurred in tumors displaying a so-called "BRCAness" phenotype [90]. The main feature of BRCAness is a deficiency in HR, despite *BRCA1/2* not being mutated. This indicates that additional to screening for mutations, the functionality of pathways should be tested. These tests could lead to the identification of more patients that could benefit from therapies like PARP1 inhibition [91]. One functional readout for the performance of HR is the RAD51 foci formation at DNA damage sites, which has been suggested to be used as an indicative marker by several groups [92-94]. However, functional readouts are still not implemented in the clinic and are only rarely used for the prediction of therapy responses. In the context of personalized cancer therapy, integration of functional assays would be desirable.

Even though the first results of PARP inhibitors have been promising, the development of resistances was soon observed. Several cellular mechanisms of PARP1 inhibitor resistance have been identified. The following two are attributed to pathways that are important for this thesis. The first is the reactivation of HR, which can be achieved by either reverting mutations in *BRCA1/2*, restoring the HR activity [89] or loss of *53BP1*, which causes HR to be initiated in a BRCA1-independent manner [65]. The second mechanism is the restoration of replication fork stability in response to replication stress. *BRCA1* mutations lead to unprotected stalled replication forks, leaving them prone to uncontrolled degradation by nucleases [28]. If stalled replication forks are stabilized again due to loss of additional proteins and the replication stress level is reduced, PARP1 inhibitor resistance may occur [89].

1.4 DNA replication stress

1.4.1 Definition of replication stress

DNA replication stress is a very complex state in a cell that is usually defined as transient slowing or stalling of replication fork progression [95]. It leads to impaired DNA replication, if not handled properly [95]. The DNA replication is a critical process in cells because it ensures the correct duplication of the genome, which is inherited to the daughter cells after cell division. Failure of accurate DNA replication and cell division may lead to genomic instability, which is a hallmark of cancer [2]. Thus, increased replication stress has been identified as a major contributor to sCIN and nCIN in cells, promoting genomic instability [49]. The term 'replication stress' summarizes the occurrence of any obstacle that may arise endo- or exogenously, blocking the replication fork progression [95]. This definition and the associated features are still evolving, which is highlighted by a study from Maya-Mendoza and colleagues. They

showed that an increase in replication speed after treatment with PARP1 inhibitors led to replication stress and consequently to genomic instability [96].

Enhancement of the replication stress to a critical level in a cell may be a suitable goal for anti-cancer therapies. This hypothesis has been extensively investigated in cancer research for several years and is the focus of this thesis.

1.4.2 The mechanisms of the replication stress response

The creation of physical blocks of replication can be caused endo- or exogenously by different mechanisms. Endogenous replication stress can arise due to collision of the replication and transcription complexes, which can result in R-loop formation. The R-loop consists of one DNA-ribonucleic acid (RNA) hybrid structure and one single strand of DNA. Other sources are reactive oxygen species or secondary structures of the DNA, like hairpins or G-quaduplexes, which occur in regions with repetitive DNA sequences [95]. Endogenous replication stress may contribute to a neoplastic transformation in normal cells. In tumor cells, it may drive the tumorigenesis and progression of the tumor [2, 97]. Many drugs used as chemotherapeutics cause replication stress exogenously by the induction of replication blocks like DNA cross-links or trapping proteins on the DNA [95]. The common feature of replication stress is the presence of long ssDNA stretches (Figure 4). This is due to continued unwinding of DNA by the
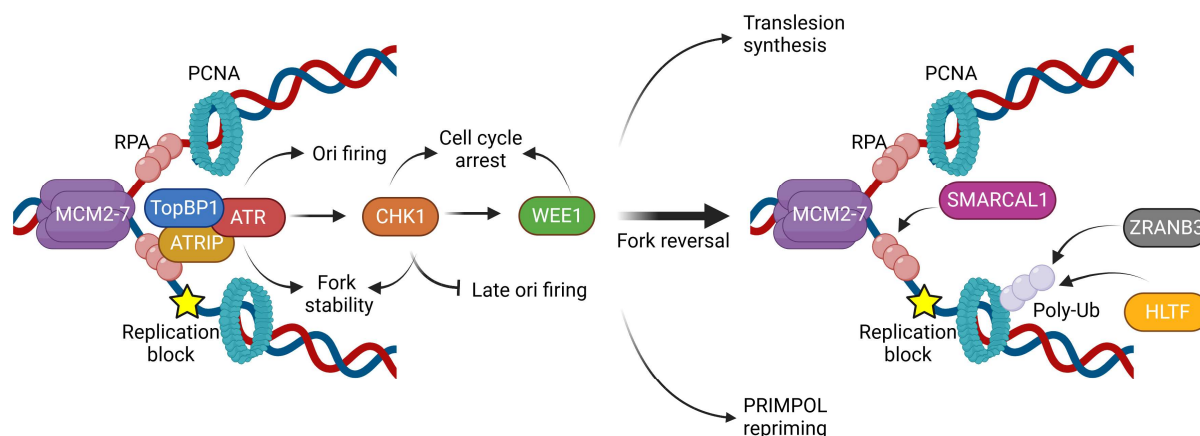

Figure 4: Overview of the replication stress response. The pathway is explained in detail in chapter 1.4.2**.** Adapted version from [95, 104]. Created with BioRender.com. ATR: Ataxia telangiectasia and Rad3-related protein; ATRIP: ATR-interacting protein; BRCA1/2: Breast cancer gene 1/2; CHK1: Checkpoint kinase 1; HLTF: Helicase-like transcription factor; MCM2-7: Minichromosome maintenance protein 2-7; Ori: Origin of replication; PCNA: Proliferation cell nuclear antigen; PRIMPOL: Primase and DNA directed polymerase; RAD51: Recombinase Rad51; RPA: Replication protein A; SMARCAL1: SWI/SNF-related matrix-associated actin-dependent regulator of chromatin subfamily A-like protein 1; TopBP1: DNA topoisomerase II binding protein 1; Poly-Ub: Polyubiquitin; WEE1: WEE1 G2 checkpoint kinase; ZRANB3: Zinc finger, RAN-binding domain containing 3.

associated minichromosome maintenance protein (MCM) helicase, while the DNA polymerase has already been stalled [98]. The ssDNA stretches must be immediately covered by RPA, leading to recruitment of ATR-interacting protein (ATRIP). It ultimately results in the activation of one of the main kinases of the replication stress response: ATR [99]. DNA topoisomerase II binding protein 1 (TopBP1) can then bind the complex of ATRIP and ATR to further enhance the activity of ATR [100]. The next important step in the replication stress response is the activation of CHK1 by ATR [101]. Activated ATR can phosphorylate claspin, which leads to the recruitment of inactive CHK1. Afterwards, ATR can activate CHK1 by phosphorylation [102]. The fully activated replication stress response then counteracts the blockade of replication fork progression in multiple ways.

The first pathway is the regulation of the cell cycle progression. Activated CHK1 can tightly regulate the S phase checkpoint by cell division cycle 25A (CDC25A) degradation, which inhibits the activation of CDKs and thereby stops cell cycle progression [103]. Additionally, CHK1 activates G2 checkpoint kinase WEE1 (WEE1), which can also regulate the CDKs, further contributing to the inhibition of the cell cycle progression [104]. The cell cycle arrest gives the cell time to overcome the replication stress and complete DNA replication to prevent the occurrence of under-replicated DNA [105]. If the DNA replication is not completed before the mitosis, genomic instability might be a consequence [105].

The second pathway is the control of origin firing. CHK1 has inhibitory functions on late origin firing during replication and thereby directs the cell to rather restart stalled replication forks, instead of activating more origins of replication. This saves energy and resources necessary for DNA synthesis, like deoxynucleotide triphosphates (dNTPs) [106, 107]. However, in some conditions, it can also be beneficial for the cell to fire new origins in close proximity to stalled forks, leading to a rescue of these replication forks. ATR can directly control this firing of dormant origins by phosphorylation-dependent regulation of the MCM complex and fanconi anemia complementation group I (FANCI) [108, 109].

A third and more complex pathway is the stabilization and restart of stalled replication forks, which is orchestrated by ATR [110]. Stalled forks need to be stabilized, as a fork collapse may result in a DSB. The most common form of replication fork protection is the reversal of stalled replication forks (Figure 4) [104]. Alternative pathways are the translesion synthesis and primase and DNA directed polymerase (PRIMPOL) repriming. Both are error prone as they simply push the replication fork progression through the DNA lesion. Thus, replication fork reversal is the preferred pathway [104]. The main three proteins involved in fork reversal are SWI/SNF-related matrix-associated actin-dependent regulator of chromatin subfamily A-like protein 1 (SMARCAL1), recruited by ssDNA bound RPA, zinc finger, RAN-binding domain containing 3 (ZRANB3), recruited by polyubiquitinated proliferating cell nuclear antigen (PCNA), and helicase-like transcription factor (HLTF) (Figure 4). They all catalyze the fork

reversal by adenosine triphosphate (ATP) hydrolysis [104]. Once the fork is reversed, ATR-CHK1 promotes the recruitment of several proteins that are also involved in HR, like BRCA1, BRCA2, and RAD51, to protect the reversed fork structure from degradation by nucleases (Figure 5) [28, 111, 112]. Cells lacking functional fork protection displayed uncontrolled nucleolytic degradation of the DNA at reversed replication forks, mediated by the nucleases MRE11 and EXO1 [112]. If proteins of the fork reversal pathway like SMARCAL and ZRANB3 are additionally mutated in *BRCA1* deficient cells, less DSBs occur. This indicates that fork reversal supports genomic instability in *BRCA1* mutated cells [113]. If a cell can overcome the replication stress, stalled replication forks may be restarted by mechanisms that are mediated by ATP-dependent DNA helicase Q1 (RECQ1) via WRN and DNA2 (Figure 5) [114, 115]. Once the replication stress raises to a critical point, which cannot be rescued by the replication stress response, replication catastrophe occurs, leading to cell death [116]. One hypothesis how replication catastrophe is initiated is the exhaustion of RPA, since uncovered ssDNA is prone to breakage and degradation by nucleases [116]. This is a reason why the regulation of dormant origin firing is crucial, as more open forks also require more RPA, thereby further reducing the pool of available RPA [116].

In addition to the mentioned proteins, there are other tumor suppressor genes that have been previously associated with the replication stress response. One of them is PTEN, which has been described to directly interact with RPA and MCM2 under replicative stress [117, 118]. It
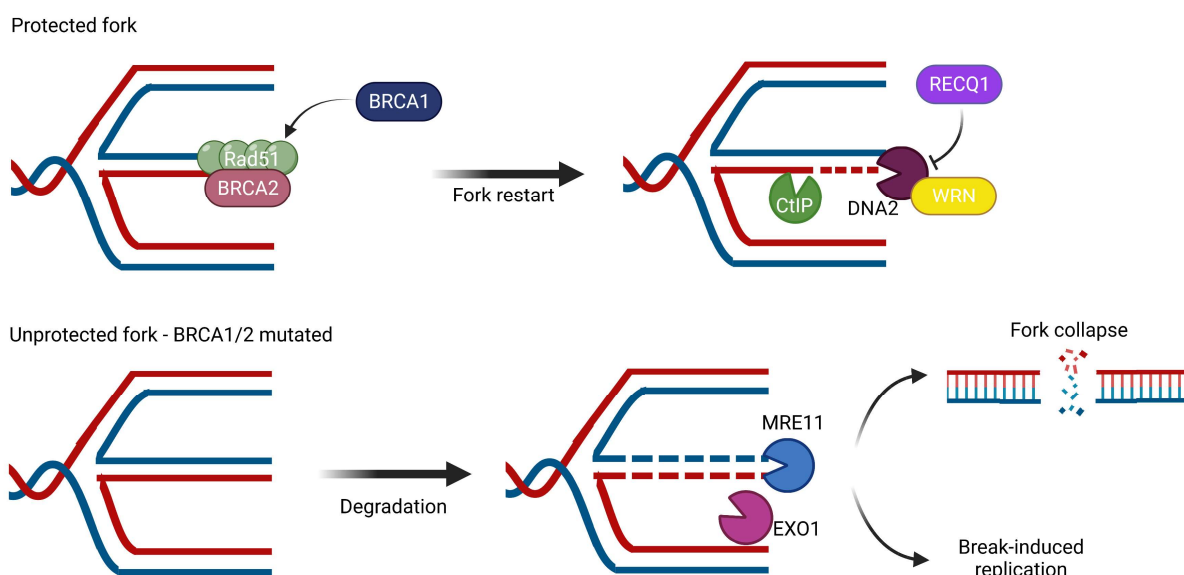
Figure 5: Replication fork protection and consequences of *BRCA1* or *2* mutations. The pathways are explained in detail in chapter 1.4.2. Adapted version from [104]. Created with BioRender.com. BRCA1/2: Breast cancer gene 1/2; CtIP: CtBP-interacting protein; DNA2: DNA replication ATP-dependent helicase/nuclease DNA2; EXO1: Exonuclease 1; MRE11: Double-strand break repair nuclease MRE11; RAD51: Recombinase Rad51; RECQ1: ATP-dependent DNA helicase Q1; WRN: Werner syndrome helicase.

has been further shown that PTEN is required for the loading of RAD51 at stalled replication forks [73]. The loss of *PTEN* has also been associated with impaired CHK1 activation, which resulted in accumulation of DNA damage [32, 119].

Replication stress is believed to be specifically elevated in many cancer cells compared to the corresponding normal tissue cells. Consequently, there are high expectations to use available or newly developed targeted drugs in new combinations to target the replication stress response. The idea is to drive cancer cells into replication catastrophe and cancer cell death [104, 120].

1.4.3 Clinical application of the replication stress response for cancer therapy

Cancer cells can display high level of replication stress due to different reasons. These include the activation of oncogenes, loss of G1/S checkpoint or defective DNA repair pathways [121, 122]. Depending on the affected mechanism, different level of replication stress can be present in cancer cells. Thus, a classification of low, moderate, and high replication stress cancers would be beneficial and could indicate the response to different therapeutic options. Replication stress has been shown to be also present in breast cancer, and several combinational therapies targeting the replication stress response are investigated in clinical trials in advanced stage tumors, including TNBCs [123, 124]. Measuring replication stress is not trivial though, as markers that are commonly used, like phosphorylation of histone H2AX (yH2AX), are not exclusively caused by replication stress [95]. More indicative marker for replication stress would be: (I) The phosphorylation of CHK1 at Ser345 or RPA at Ser33, as those sites are ATR-dependent. (II) RPA foci detection at the appropriate time point, as the ssDNA stretches that occur due to replication stress have to be covered by RPA immediately. (III) Direct visualization of the DNA replication by the DNA fiber assay. Nucleotide analogous are incorporated in the DNA, which can be stained and measured to reveal the replication fork speed and DNA structures. They can be counted to assess, e.g., the number of stalled replication forks [95]. Those methods are all functional readouts which are usually not integrated as a standard tool for therapy prediction. Therefore, more recent studies try to use specific replication stress signatures or scores based on The Cancer Genome Atlas (TCGA) and other large available datasets, which can be implemented easier in clinical routines [125, 126].

The induction of replication stress is a general mechanism of many anti-cancer therapies [127]. Depending on the drug, different replication blocks are generated. Examples are: (I) DNA crosslinks between the two DNA strands that are generated by platinum-based and alkylating drugs, making it impossible for the replication complex to pass by. A replication fork meeting a DNA crosslink has to stall until the crosslink is repaired. (II) Nucleotide analogous that are incorporated into the DNA and directly cause replication fork stalling. At the same time, they

inhibit the cellular dNTP synthesis, reducing the available dNTP pool for replication, further enhancing the replication stress level [127]. (III) Trapping of proteins on the DNA, which is achieved by topoisomerase I or II and PARP1 inhibitors [127]. (IV) Stabilizing drugs of secondary DNA structures that preferably form at repetitive DNA sequences [104].

Several other drugs do not directly inhibit the replication fork progression but rather focus on the replication stress response at different stages. Inhibitors against the key kinases of the replication stress response, like ATR, CHK1, and WEE1, are being studied extensively. Also, inhibition of the PI3K-AKT-mTOR pathway is under investigation. This pathway increases the firing of origins, decreases the HR capacity and is one of the most frequently hyper activated pathways in cancer [128, 129]. Another protein regulating the licensing and firing of origins is the MCM2-7 complex, which might also be a possible target for inhibition [130, 131]. Despite many targetable options, monotherapies with these drugs often do not lead to the expected results and development of resistances are frequent [89, 128].

Thus, many open questions regarding therapy development and improvement remain to be solved. One approach is the use of combinational therapies to avoid the occurrence of resistances and improve the outcome for the patients. An unresolved issue of these therapies is the balancing of the toxicity and clinical benefit [127]. Therefore, it is of high importance to identify the most efficient, but least toxic treatment for each tumor subgroup. In order to achieve this goal, it is important to better understand the replication stress response and enable the identification of associated marker and targets.

2. Study objective

DNA replication stress is one of the hallmarks of cancer cells and has been identified as a leading cause of genomic instability. Tumors that are genomic instable can acquire new mutations more frequently, leading to increased proliferation and higher aggressiveness. Endogenous replication stress is an almost exclusive feature of cancer cells which makes it an excellent target for anti-cancer therapies. However, the cellular replication stress response is a complex and multilayered process that has not yet been fully understood. The potential to develop new strategies or combinations of drugs to target the replication stress response is therefore very promising and the goal of this thesis.

Hypothesis 1:

Proteins involved in the DNA damage response and DNA replication can be used as predictive markers to assess the replication stress level in a cancer cell. They provide insights about pathways that could be targeted to increase the replication stress to a critical point, leading to cancer cell death.

Hypothesis 2:

Increasing the replication stress in breast cancer cells that display a chemo- and radioresistance may resensitize them to conventional therapy options. This is independent of the breast cancer subtype.

Study objective:

Promising proteins of the DNA damage response and DNA replication pathway with a potential impact on the replication stress level in breast cancer cells were selected. The three chosen candidates were: BRCA1, directly involved in DNA repair and replication fork protection, CHK1, regulating the DNA damage response in S phase, and PTEN playing a superior role regarding initiation and progression of breast cancer. Depending on the protein level or mutational status, the resistance to different DNA damaging agents was determined and it was tested how resistant cancer cells can be sensitized to these agents. Breast cancer cell lines of different subtypes were investigated to test whether the effects would be limited to a specific subtype. The main two cell lines used were the LumA cell line MCF7 and the TNBC cell line MDA-MB-231 with different subclones.

Since mainly already clinically relevant drugs were tested in this thesis, the results could give direct indication for the treatment of patients and thus possibly offer new combinational treatment options for breast cancer patients.

3. Discussion

3.1 Summary of the key findings

The aim of this thesis was to investigate how to overcome chemo- and radioresistance by targeting the replication stress response in breast cancer cells. The replication stress response represents a complex signaling pathway involving many proteins. The research project was focused on three proteins that are important in the tumor development and progression in breast cancer and are involved in maintain the chromosomal stability. BRCA1, directly involved in DNA repair via HR, CHK1, the key regulator of the intra-S phase signaling pathway, and PTEN, transmitting processes of signal transduction from the cytoplasm into the nucleus.

BRCA1 is involved in the DNA repair process HR and DNA replication fork protection of stalled forks. Isogenic cell lines with insertion and deletion *BRCA1* mutations in exons 9 or 14 were generated out of the luminal breast cancer cell line MCF7. Chemo- and radioresistance was observed in cells with a *BRCA1* mutation in exon 9 compared to the MCF7 wild type (WT). In contrast, a chemo- and radiosensitivity was observed in exon 14 mutated clones. The processes responsible for this observation in terms of DNA repair and replication stress response were analyzed. Strikingly, it was shown that the observed resistance to different DNA damaging sources was associated with low level of replication stress, efficient DNA repair and high CHK1 activation. Inhibition of the ATR-CHK1 cascade showed sensitization of the resistant but not the sensitive cell lines. Similar results were observed in the *BRCA1* proficient MDA-MB-231 TNBC cell line and its sublines. Again, resistant cell lines showed lower level of replication stress and higher activation of CHK1. These results confirm the two hypotheses of this thesis. They indicate that targeting the replication stress response by inhibition of the ATR-CHK1 axis sensitizes resistant cancer cells to irradiation and chemotherapeutic treatments, irrespective of the breast cancer subtype and present mutations.

PTEN is known to be primarily involved in signal transduction. Recent data showed that it also prevents genomic instability through association at replication forks. Together with other studies, the results from this thesis show that a low PTEN expression correlates with a high CIN score and significantly reduced overall survival in breast cancer patients. Different cell lines were analyzed regarding their PTEN expression and how the replication stress response was affected. A low expression of PTEN was associated with higher origin firing during replication, which is an indicator for elevated replication stress. Furthermore, PTEN expression correlated with the fork stability upon replication stress induction, mediated by hydroxyurea (HU) treatment. The elevated replication stress led to increased sensitivity against PARP1 inhibition, further confirming the hypotheses investigated in this thesis.

Taken together, these results show that targeting the replication stress response in different breast cancer subtypes could be a suitable therapeutic option for many patients, independent

of the present mutations. Especially the disruption of ATR-CHK1 signaling cascade seems to be a promising approach to sensitize previously resistant tumor cells to conventional radio-chemotherapy.

3.2 Dysregulation of proteins involved in DNA repair and replication leads to CIN

CIN summarizes serious aberrations in a cancer cell. These include the accumulation of mutations, focal rearrangements, and formation of extrachromosomal DNA or micronuclei, which may later lead to activation of the intracellular immune signaling [39, 132]. Tumors with a high CIN have been linked to an overall bad prognosis for the patient due to aggressive and invasive phenotypes, often causing therapy resistance [2, 41]. Two of the main endogenous reasons for CIN are defects in the DNA repair pathways, especially HR, and replication stress [39, 49]. The three investigated proteins in this thesis, BRCA1, PTEN, and CHK1, are all major contributors to the maintenance of chromosomal stability in a cell. Therefore, the correlation between their expression and the survival of patients with different breast cancer subtypes was analyzed using the CIN70 score. This score has been established as indicative marker for clinical applications. It is based on the top 70 identified genes, which correlate with the highest CIN, defined by total functional aneuploidy [45]. The CIN70 score is an accepted tool to predict CIN in different tumor entities and has been used in several studies before [44]. In this thesis, TCGA and Molecular Taxonomy of Breast Cancer International Consortium (METABRIC) datasets were used for the analysis.

3.2.1 Influence of BRCA1 and RAD51 dysregulation on CIN

The worst prognosis for patients with breast cancer is associated with the TNBC subtype, which is characterized by elevated CIN [8]. Studies suggest that more than 10% of all TNBC patients harbor a mutation in *BRCA1* or *2*. Additionally, it is estimated that up to 30% show a deficiency in the HR pathway, which is characterized by RAD51 not being loaded on to the DNA [133-135]. Thus, many of these tumors will display high CIN, since BRCA1 and RAD51 have essential roles in HR and the protection of stalled replication forks. Both pathways are involved in the prevention of nCIN and sCIN [136]. The study from Meyer et al., included in this thesis, showed that not only a loss or reduced expression of proteins involved in HR and replication fork protection can have negative effects on the survival, but also a high expression [137]. A high expression of RAD51 correlated with a higher CIN70 score, which further translated into a worse disease-free survival [137]. Interestingly, this observation was not limited to the TNBC subtype, which commonly displays high CIN, but was also observed in the LumA breast cancer subtype [137]. LumA tumors are usually very well treatable and

associated with high cure rates [8]. However, there is a subgroup of LumA tumors that display resistances against the standard treatment options or patients develop a resistant recurrence later [9, 14]. An early identification of patients with a LumA tumor that show a high CIN70 score could offer the possibility to intensify the treatment of these patients early on to improve the outcome of the treatment.

An additional pathway in which BRCA1 is involved in is the centrosome duplication, ensuring correct progression of the cell cycle and avoiding chromosomal abnormalities [27, 51]. The interaction of the BRCA1 N-terminus with RACK1 is responsible for the localization of BRCA1 to the centromeres [55], and the function to maintain accurate centrosome number is exhibited by interaction with BARD1 and OLA1 [52, 53]. Overexpression or knockdown of any protein in this complex led to centrosome aberrations in mammary epithelium-derived cells [54, 55], indicating the importance of this BRCA1-complex to protect cells from nCIN and sCIN. Thus, dysregulation of BRCA1 and associated proteins can contribute to nCIN and sCIN via multiple pathways.

3.2.2 Low PTEN expression leads to elevated CIN

A depletion of *PTEN* has severe effects on the CIN level of a cell. It has been shown that the loss of *PTEN* resulted in a reduction of chromatin association of several proteins involved in DNA repair and replication, including CHK1 and RAD51 [33, 73]. Consistently decreasing the presence of these important proteins, led to endogenous replication stress in the cell [73]. Additionally, PTEN controls the firing of dormant origins. A depletion of *PTEN* has been shown to lead to aberrant origin firing, further enhancing replication stress in a cell [117]. However, not only a complete loss of *PTEN* can lead to increased replication stress and thus higher CIN, but also a low expression of PTEN correlated with a higher CIN70 score. This was due to increased replication stress, which was shown by the Rieckhoff et al. study that is part of this thesis [138]. Further, PTEN has a function in the process of chromosomal segregation, which is key to avoid the occurrence of nCIN [33, 139]. An important structure to ensure that this process proceeds correctly are the centromeres of the chromosomes [140]. The C-terminus of PTEN has been shown to directly interact with the centromere protein CENP-C during the interphase, contributing to centromere stability and correct chromosome segregation [29, 33]. These multiple complex functions, which prevent CIN, led to PTEN being named as "the new guardian of the genome" [141, 142], similar to the well-known tumor suppressor p53, which has first been stated as "the guardian of the genome" in 1992 by Lane [143].

3.2.3. Influence of aberrant CHK1 expression and activation on CIN

The activation of the ATR-CHK1 pathway is a crucial step in the initiation of the cellular replication stress response, which controls the cell cycle progression, origin firing, and

protection of stalled replication forks [34]. Due to CHK1 playing a key role in all these processes, the correlation to CIN and disease-free survival was analyzed. Like the data from RAD51, a high CHK1 expression was associated with increased CIN70 scores and worse disease-free survival in TNBC, as well as LumA tumors [137]. These results highlight that an overexpression of certain DNA repair and replication stress response proteins in high CIN tumors can have a negative prognostic implication for the patients [137]. High CHK1 expression has been associated with high proliferation rates before, due to high Ki67 staining and tumor stage three association in TNBCs [144]. Additionally, a study showed that the upregulation of CHK1 expression contributes to a worse prognosis for TNBC patients [145]. Another function of CHK1 has been described by Krämer and colleagues, where they show that CHK1 is located at centrosomes and acting as an inhibitor for CDK1, thereby preventing premature entry into mitosis [36]. Thus, an aberrant expression level of CHK1 has dramatic consequences for the cell. A mutation or downregulation has been shown to be associated with aggressive variants of human lymphoid neoplasms [146]. It was frequently detected in colon and endometrial cancers, rendering a CHK1 frame shift mutation responsible for microsatellite instability [147]. Thus, an overexpression as well as a mutation or loss of *CHK1* may have negative consequences for certain groups of patients.

In summary, all analyzed proteins have the ability to contribute to nCIN and sCIN in a cell via multiple pathways. The analysis of TCGA and METABRIC datasets revealed that a correlation between the protein expression and CIN70 score was present in the patient data. The results confirm that the expression of the analyzed proteins can have a direct impact on patient survival. Furthermore, analysis of the CIN should not be limited to tumor subtypes which have been previously described as highly chromosomal instable, such as TNBCs. Clinical implications can also be drawn for other subtypes like patients harboring a LumA tumor. This may provide the opportunity to adapt treatment options for a more aggressive subset of usually well-treatable breast cancer subtypes.

3.3 *BRCA1* exon 9 or 14 mutations modify DNA repair and replication stress response

BRCA1 is a well-studied tumor suppressor gene with many important functions in different pathways. It is involved in all three major steps of the DNA repair pathway HR and in protecting stalled replication forks from collapsing [26]. A collapsed replication fork could result in formation of a DSB, which is the most dangerous event in a cell [26]. Most studies focus on complete loss or mutations affecting exclusively functional domains of the BRCA1 protein. Consequences of mutations located in other regions of the gene are poorly understood. Therefore, *BRCA1* exon 9 and 14 mutated clones were generated using clustered regularly

interspaced short palindromic repeats/CRISPR associated protein 9 (CRISPR/Cas9). The parental cell line was MCF7 (derived from a human breast adenocarcinoma – classified as LumA subtype) [148-150]. Both exons are not located in any known functional domain of the protein. *BRCA1* mutations were introduced successfully in all analyzed clones, which was confirmed by next generation sequencing [148].

3.3.1 BRCA1 exon 9 mutation is associated with resistance to DNA damage

First, the effect of the introduced *BRCA1* mutations on HR was analyzed. As expected, all clones showed a reduced capacity to perform HR in the plasmid reconstruction assay, since a mutation in a major protein of the HR pathway was introduced [148, 150]. Yet, the *BRCA1* exon 9.2 clone showed an increased resistance against treatment with MMC, PARP1 inhibition by talazoparib (tala), and IR in the colony formation assay. The *BRCA1* exon 14.3 clone displayed increased sensitivity against all these DNA damaging sources compared to the parental MCF7 WT. The clone *BRCA1* exon 14.1 showed similar responses as the MCF7 WT with a tendency of increased sensitivity. These results were quite surprising, since it was expected that the *BRCA1* mutations would cause an increased sensitivity against DNA damage in all the clones, due to the observed impaired HR capacity [148, 150]. This is especially true for PARP1 inhibition, since *BRCA* mutated cancer cells have been shown to react with synthetic lethality to treatments with PARP1 inhibitors before [85, 86]. Yet, the *BRCA1* mutated clone 9.2 showed an increased resistance against PARP1 inhibition, despite a lower HR capacity than the MCF7 WT [148, 150]. The combination of a HR defect with PARP1 inhibition should lead to cancer cell death, because PARP1 is a key molecule of a second DNA repair pathway [85, 86]. For that reason, the functionality of the HR was further assessed in the clones, because determination of the HR capacity by the plasmid reconstruction assay has its limits. This method usually only introduces one single DSB in a cell, not leading to the activation of the whole DDR [151]. Thus, a functional readout of the HR pathway was conducted. It has been previously published that the ability to form RAD51 foci correlates with HR-proficiency [92-94]. This is due to the essential step of HR being the loading of the recombinase RAD51 on the resected DNA ends [69]. The analysis of RAD51 foci formation in the *BRCA1* mutated clones revealed that none of the clones had a complete deficiency in HR. However, the resistant *BRCA1* exon 9.2 clone could form RAD51 foci most efficiently 6h after MMC treatment. It also showed the highest resolution of RAD51 foci 24h after treatment. Thus, the resistance in the *BRCA1* exon 9.2 clone could be partially explained by higher HR performance compared to the sensitive *BRCA1* exon 14 clones [148]. It seemed unlikely that the highly significant differences in survival of the three different *BRCA1* clones after DNA damage induction by IR, MMC, and tala were only explained by these rather small

differences in the ability to repair DSBs by HR. For that reason, the functions of the BRCA1 protein in the replication stress response were further investigated.

3.3.2. BRCA1 exon 9.2 clone shows less replication stress

Cells that are known to have an impaired HR capacity are expected to react with synthetic lethality to PARP1 inhibition [85, 86]. In 2009, the first clinical trial using a PARP1 inhibitor (olaparib) showed promising results in patients carrying a *BRCA1/2* mutation [152]. Since then, multiple other specific PARP1 inhibitors have been developed and approved by the U.S. Food and Drug Administration (FDA) and the European Medicines Agency (EMA) for different mono- and combinational treatment settings [89]. Soon, resistances were observed in patients, and different mechanisms of PARP1 inhibitor resistance have been extensively studied. Stabilization of stalled DNA replication forks in response to treatment with PARP1 inhibitors has been identified as one of the mechanisms contributing to resistance [89]. Since BRCA1 is involved in the protection of stalled replication forks, it was investigated how this function of BRCA1 was affected by the introduced mutations and if the observed resistances could be associated to the stabilization of stalled replication forks.

Treating actively replicating cells with HU causes a depletion of the dNTP pool in the cell, leading to almost complete stalling of all ongoing replication forks [153]. It was observed that the MCF7 WT showed a degradation of the newly synthesized DNA in response to HU treatment [148]. This indicated that the protection of the stalled replication forks does not function properly. This has been shown to lead to uncontrolled degradation of unprotected DNA ends, initiated by MRE11 and further executed by EXO1 [112].

Neither of the *BRCA1* mutated clones showed this degradation, suggesting that the replication fork protection was working correctly [148]. If the replication stress response is working effectively, RPA coats ssDNA regions that are present at stalled replication forks. Subsequently, ATRIP-dependent recruitment of ATR is initiated [99]. Like RAD51, this can be detected by RPA foci formation in the nucleus of the cell. It was found that the resistant *BRCA1* exon 9.2 clone showed the highest amount of RPA foci 4h after MMC treatment, still it was able to resolve the foci to the greatest extent 24h after treatment. This indicated that the resistant *BRCA1* exon 9.2 clone could respond very well to replication stress induction and also reduce the present replication stress within the analyzed time points [148]. Additionally, this clone had the lowest amount of stalled replication forks after HU treatment. This suggested that the *BRCA1* exon 9.2 clone can efficiently restart stalled replication forks after DNA damage induction, while the MCF7 WT and *BRCA1* exon 14 mutated clones cannot [148]. Effective protection and fast restart of stalled replication forks are features of cells with low replicative stress, which seemed to be the case for the resistant *BRCA1* exon 9.2 clone. These results were confirmed by analysis of the DNA replication after DNA damage induction via IR, where

it was also observed that the lowest level of replication stress was present in the resistant *BRCA1* exon 9.2 clone [148].

Analysis of the two main functions of BRCA1 in DNA repair and replication fork protection led to one of the main conclusions of the study: Introduced mutations in *BRCA1* caused an expected sensitivity, but also unexpected resistance to different DNA damaging sources. The resistance was associated with a combination of effective DNA repair and low degree of DNA replication stress in the *BRCA1* exon 9.2 mutated clone [148].

3.4 Low PTEN expression affects DNA repair and replication stress

The tumor suppressor gene *PTEN* was first described in 1997 [154, 155]. It is frequently mutated in different cancer entities. Patients carrying a *PTEN* germline mutation have an estimated risk of up to 65-85% to develop breast cancer, which is almost comparable to mutations in *BRCA1/2* [22]. Identified by a meta-analysis of 10.231 breast cancer cases, Li et al. showed that *PTEN* mutations or low expression level were highly associated with a TNBC subtype, large tumor size, metastatic progression, and poor differentiation of the tumor cells [25]. All these factors contribute to a bad prognosis for the patient. The study of Li and colleagues was confirmed by the observation in the present study, showing that a low expression of PTEN correlated with a high CIN70 score (discussed in chapter 3.2.2).

PTEN is most widely known for its function of antagonizing the PI3K-AKT-mTOR pathway. This connects PTEN directly to the DDR, as the PI3K-dependent phosphorylation of CHK1 can be suppressed by the lipid phosphatase activity of PTEN [30, 32, 119]. In turn, CHK1 activation must be tightly controlled, as it is a key protein in the DDR, leading to CHK1-dependent CDC25A degradation. The result is a cell cycle arrest in S/G2 phase [103]. This allows the cells to repair DNA damage that have occurred and maintain genomic integrity. If this cell cycle checkpoint is not functioning correctly, the cells may acquire mutations due to increased CIN. This can lead to enhanced proliferation and resistance against anti-cancer therapies [31, 33, 119]. Thus, the aim was to further understand the effects of a low PTEN expression on the replication stress response [138].

3.4.1 PTEN expression influences replication fork stability and increases origin firing

A more recently discovered function of PTEN is the role in DNA replication [73, 117, 118]. *PTEN* depletion resulted in reduction of chromatin association of several proteins involved in DNA replication and repair, including the sliding DNA clamp PCNA, CHK1 and RAD51 [33, 73]. Decreasing the presence of these important proteins consistently led to endogenous replication stress in the cell, as replication in total was slowed down and the number of stalled replication forks increased [73]. The observations in the study included in this thesis confirmed that TNBCs seem to have low PTEN expression in general and that this affects the DNA

replication process. Five TNBC cell lines were screened (MDA-MB-231, BT-549, HS578, BT-20, and GI101) and it was shown that the mean of PTEN expression was 1.85-fold lower in these cell lines than in breast cancer cell lines with a non-TNBC subtype (SKBr3, MCF7, T47D, and BT-474) [138]. Analysis of the DNA replication process by the DNA fiber assay revealed that the elongation rate was not directly affected by lower PTEN expression. Yet, the firing of new origins of replication was significantly increased by 10%, indicating that the cells have elevated level of endogenous replication stress [138].

Testing the replication fork stability by HU treatment revealed a degradation of the newly synthesized DNA at stalled replication forks. Intriguingly, the PTEN expression correlated negatively with the DNA degradation, suggesting a PTEN expression level dependent replication fork instability in the analyzed TNBC cell lines [138]. This observation was further confirmed by the fact that three of the four tested non-TNBC cell lines did not show any replication fork instability in response to HU treatment. Transfection of a *PTEN* coding sequence containing plasmid (pPTENiZs2puro++tTR+) into the MDA-MB-231-BR cell line showed a 2.2-fold increase of PTEN associated with the chromatin. This led to a rescue of the endogenous replication stress. The replication speed was enhanced in the *PTEN* transfected cells, and the rate of newly fired origins was reduced in the untreated condition, implying that by restoration of a higher PTEN expression the endogenous replication stress can be mitigated [138]. The observation of a direct correlation between the PTEN expression level and stability of stalled replication forks is supported by other studies. They showed that functions of PTEN will start to fail if it is not physically available to a certain amount in the cell [156]. It might be the reason why PTEN is generally highly expressed in a cell. The distribution patterns vary in different cell cycle phases, implying that PTEN is involved in many pathways and important for maintaining the genomic stability of a cell [156].

3.4.2. Low PTEN expression impairs the recruitment of DDR proteins to the chromatin

It has been shown that complete loss of *PTEN* led to uncoupling of DNA polymerase and helicase progression in response to exogenously induced replication stress [117]. This was due to aberrant MCM2 activation, which is a core protein of the pre-replication complex and a substrate for the phosphatase activity of PTEN [117]. Formation and loading of the MCM2-7 complex on to the DNA is required for activating replication origin licensing and firing [130, 131]. The hyper activated MCM2 helicase function led to continuous unwinding of DNA despite a depletion of the dNTP pool by HU treatment in *PTEN* deficient cells [117]. This resulted in the emergence of very long ssDNA stretches, which needed to be covered subsequently by RPA to prevent degradation by nucleases or collapse of the replication forks [117]. However, *PTEN* deficiency is known to lead to less RPA association with the chromatin [118]. This has also been shown for PCNA, CHK1, and RAD51 previously [33, 73]. Impaired recruitment of

these proteins to stalled replication forks with open ssDNA stretches means that the intra-S checkpoint cannot be triggered correctly, circling back to the function of PTEN in the DDR [73, 157]. In the present study western blot analysis revealed that there was indeed a reduced recruitment of DNA repair and replication proteins to the chromatin [138]. This was true for CHK1 and PALB2 in the TNBC cell line panel with low PTEN expression in an untreated condition. In response to HU treatment, the recruitment of CHK1 and activated CHK1 to the chromatin was impaired. However, the upstream kinase of the intra-S phase checkpoint ATR was not affected. This implies that the effects of low PTEN expression on CHK1 are not mediated by the upstream kinase ATR [138].

PTEN deficient cells have previously been shown to fail at the recruitment of DDR proteins to sites of DSBs in response to DNA damage induction by IR. This was especially pronounced for RAD51, which led to persisting 53BP1 foci at DNA damage sites 24h after IR [158]. 53BP1 is one of the first proteins recruited to DSBs and is involved in the selection of DNA repair pathway (NHEJ or HR) [65, 159, 160]. This finding indicates that DNA repair does not function correctly in *PTEN* deficient cells, and that PTEN plays a critical role in the DDR in response to exogenously induced genotoxic stress [158].

Thus, the study included in this thesis showed that TNBC cell lines with low PTEN expression have increased endogenous replication stress. It is mainly caused by uncontrolled firing of new origins of replication. Additionally, PTEN expression correlated with the degradation of newly synthesized DNA after treatment with HU, accompanied by impaired recruitment of DDR proteins to the chromatin [138].

3.5 Overcoming resistance by targeting the replication stress response

Enhanced replication stress has been shown to increase the genomic instability of cancer cells [49], which has been indicated to be a hallmark of cancer in 2011 by Hanahan and Weinberg [2]. High CIN increases the likelihood of tumors to acquire mutations in tumor suppressor- or oncogenes, which will further drive the progression of the tumor [161]. Thus, replication stress has been identified as a reasonable target for anti-cancer therapies since cancer cells generally show higher degrees of replication stress compared to normal tissue cells [104, 120].

3.5.1 Therapy resistance due to avoidance of replication stress

Replication stress is commonly defined as transient slowing or stalling of replication forks, which can be caused by any obstacle occurring endo- or exogenously, blocking replication fork progression [95]. However, it has become evident that an increase in replication speed after treatment with PARP1 inhibitors can also cause replication stress and lead to genomic instability [96]. In response to stalled replication forks, RPA binds to arising ssDNA and subsequently induces the ATRIP-dependent recruitment of ATR [99]. Activation of ATR results

in phosphorylation of CHK1, leading to cell cycle arrest in S/G2 phase [103]. This gives the cell time to protect and restart stalled replication forks, in which many proteins of the HR are involved in [28, 107, 111, 112].

As discussed in chapter 3.3.2, the present study showed that resistance to IR, MMC, and PARP1 inhibition was associated with a lower degree of replication stress in *BRCA1*-mutated MCF7 cells [148]. Similar results were observed in the second study included in this thesis [137]. The *BRCA1* proficient TNBC cell line MDA-MB-231 and its sublines –BR and –SA (brain-seeking and bone-seeking [162]) showed reduced HR capacities in the plasmid-reconstruction assay, but functional RAD51 foci formation after MMC treatment. Similar to the results from the Classen et al. study, a resistance against MMC and PARP1 inhibition was observed in MDA-MB-231 WT and -SA, not correlating to HR capacity [137]. RPA foci were significantly lower in the resistant cell lines 24h after treatment, suggesting less replicative stress. Additionally, analysis of the fork stability revealed that MCF7 showed a degradation of the newly synthesized DNA in response to HU treatment. This was consistent with the Classen et al. study [137, 148]. The MDA-MB-231 cell lines also showed a degradation, but to a lesser extent than the MCF7 cells [137, 148]. However, the two resistant cell lines (MDA-MB-231 WT and –SA) showed no degradation of the newly synthesized DNA in response to MMC treatment. The two more sensitive cell lines did show degradation (MDA-MB-231 –BR and MCF7). It further indicated that resistance is not simply linked to HR capacity, but rather to efficient replication fork protection in response to DNA damage. Similar results have also been observed by other groups. Chaudhuri and colleagues could show in a *BRCA2* deficient mouse model and PEO1 cells that resistance to cisplatin and PARP1 inhibition was determined by the replication fork stability rather than DNA repair capacity [163]. Another study showed that in *BRCA1* deficient MDA-MB-231 and -436 cells, fork stability can be promoted by additionally downregulating proteins involved in the replication fork reversal, like SMARCAL1, ZRANB3 and HLTF. This led to increased resistance against cisplatin and PARP1 inhibition [113]. Resistance to radiation has also been associated with replication stress before. Bold et al. showed that in head and neck squamous cell carcinoma cell lines resistance to radiation was correlated with replication fork stability [164]. In both studies included in this thesis, the mechanism how radio- and chemoresistant cell lines maintain a low level of replication stress was investigated.

3.5.2 Suppression of replication stress due to CHK1 activation

Replication stress describes the disturbance of DNA replication, which results in slowing and stalling of replication forks. Both, endogenous and exogenous reasons can be responsible for causing disruption. The activation of the replication stress response involves the activation of ATR, which leads to activation of its downstream target CHK1 [165]. If the activation of the

ATR-CHK1 pathway is impaired, a cell cycle arrest cannot be initiated to allow complete replication of the DNA. Entering the mitosis with under-replicated DNA may lead to genomic instability [105]. Activated CHK1 prevents replication stress mainly due to the inhibition of dormant origin firing. This allows the cell to complete DNA replication by restating stalled forks, rather than opening new origins of replication [106, 107].

The Classen et al. study included in this thesis showed that the resistance to different DNA damaging sources was partly due to a lower degree of replication stress. To investigate the underlying mechanism of how the resistant *BRCA1* exon 9.2 clone could maintain a stable low replication stress level, the ATR-CHK1 pathway was analyzed by western blot. The analysis revealed that ATR activation was not significantly different in the *BRCA1* exon 9.2 clone compared to the exon 14 mutated clones or the MCF7 WT [148]. However, the activation of CHK1 was significantly increased in the resistant *BRCA1* exon 9.2 clone, indicating that CHK1 is activated in an ATR-independent manner. It has been shown previously that CHK1 can be activated ATR-independently by DNA-dependent protein kinase catalytic subunit (DNA-PKcs) in ATR-inhibited cells [166]. Yet, the inhibition of ATR by ceralasertib (cera) led to significant increase of replication stress in the *BRCA1* exon 9.2 clone. This was indicated by high increase in RPA foci formation after combined treatment of cera + IR, while the *BRCA1* exon 14 clones and MCF7 WT were not affected by the combinational treatment [148]. These results demonstrate that a disruption of the ATR-CHK1 axis at any point can sensitize cells to treatments they were shown to be resistant against before. Other groups have observed that response to ATR inhibition can be very different to CHK1 inhibition, which was surprising. Long time, it was thought that both kinases acting in the same pathway should cause similar consequences for the cell [167].

Similar observations were found in the study from Meyer et al. included in this thesis. The low level of replication stress was accompanied by significantly higher CHK1 activation in response to induced DNA damage by MMC treatment in the resistant MDA-MB-231 WT and –SA cell lines, compared to the sensitive cell lines –BR and MCF7 [137]. It was further demonstrated by CHK1 inhibition that the activation of CHK1 was responsible for the maintenance of low replication stress level and the associated resistance. The analysis of the total DNA damage by the general DNA damage marker γH2AX showed that inhibition of CHK1 by MK8776 + MMC treatment led to a significant increase in persisting DNA damage 24h post treatment compared to MMC treatment alone [137]. Further, the analysis of the cellular survival by colony formation assay revealed that the resistant cell lines could be sensitized to MMC by additional inhibition of CHK1. The sensitive cell lines did not show any sensitizing effect to MMC due to the combined treatment [137]. The data from the third study included in this thesis further highlight the importance of CHK1 in the replication stress response. The elevated replication

stress in TNBC cells with low PTEN expression was explained partially by the impaired recruitment and activation of CHK1 at the chromatin [138].

Collectively, the data from all three studies suggest that resistance to different DNA damaging sources is caused by efficient DNA repair and low level of replication stress. An increase of replication stress in response to exogenously induced DNA damage is counteracted by elevated CHK1 activation in the analyzed resistant cell lines. Thus, targeting CHK1 or related proteins involved in the replication stress response may be a promising strategy to overcome resistance that is mediated by replication stress [137, 138, 148].

3.5.3 Replication stress as a therapeutic target

The discovery of a direct connection between replication stress and genomic instability has extended the knowledge about the severe impact of replication stress on a cell [49]. Exploiting different strategies to target the replication stress response as anti-cancer treatment are currently investigated in different pre-clinical studies and first clinical trials. There are different strategies and stages of the replication stress response that could be potentially targeted.

One early stage is the control of licensing and firing of origins of replication, which is controlled by the MCM2-7 complex [130, 131]. MCM2 overexpression has been correlated with overall worse prognosis for breast cancer patients and is frequently found in TNBCs [168, 169]. One reason for MCM2 hyperactivity in TNBC could be the fact that PTEN is commonly downregulated in TNBC, which was confirmed in the study from Rieckhoff et al. in this thesis [138]. MCM2 has been shown to be a substrate for the phosphatase activity of PTEN [117]. However, inhibition of MCM2 has not been tested in clinical trials yet, despite several available inhibitors. Great efforts have been made to try and develop drugs to compensate *PTEN* loss in multiple cancer entities, as one main function of PTEN is to antagonize the PI3K-AKT-mOTR pathway. Though, not only loss of *PTEN*, but multiple other reasons for hyperactivity of the PI3K-AKT-mTOR pathway are known. It is one of the most frequently activated pathways in cancer, making it a highly investigated field of research [129, 170]. Many drugs inhibiting this signaling cascade have therefore been developed, but monotherapies with these inhibitors have only shown limited improvement on patient outcome (summarized in [128]). This is why more recently combination treatments with PI3K and PARP or other DDR inhibitors, that enhance the cellular replication stress level, have been tested. They showed promising results not only in pre-clinical models but also in first clinical trials [171-173]. These finding are in line with data from the Rieckhoff et al. study in this thesis, as PARP1 inhibition in PTEN low expression cell lines led to increased replication stress [138].

Another commonly used strategy in many anti-cancer therapies is the enhancement of replication stress to a critical level in the cell, causing replication catastrophe which leads to cell death [116]. This can be achieved by direct DNA damage induction and creation of

complex DNA lesions that cause replication stress. Examples are: (I) Platinum-based drugs that induce DNA cross-links like cisplatin. (II) Nucleotide analogs that are directly incorporated into the DNA causing failure of the replisome progression, (e.g. gemcitabine). (III) Alkylating drugs like temozolomide that block the replisome. (IV) Inhibitors of DNA replication or repair proteins like PARP (e.g. olaparib) or topoisomerase I (e.g. irinotecan) or II that are then trapped on the DNA and thereby block the replisome (e.g. etoposide). (V) Drugs stabilizing secondary DNA structures like G4-quadruplexes (e.g. pyridostatin), thereby physically blocking the replication process [104]. Like inhibitors of the PI3K-AKT-mTOR pathway, monotherapies were rarely beneficial for patients, and resistances occurred frequently. This is why the stage of the activation of the replication stress response is also investigated as a major target for therapy options, with many studies focusing on combination treatments.

The main kinases involved are ATR, CHK1, DNA-PKcs, and WEE1. The ATR-CHK1 axis has multiple functions in the replication stress response. The first is the induction of cell cycle arrest via CDC25 inactivation, which can also be targeted by WEE1. This allows the DNA repair processes to repair DNA damages and to complete the DNA replication, preventing the occurrence of under-replicated DNA [103, 105]. The second is the stabilization and restart of stalled replication forks by regulating the activity of MRE11 [174]. It has also become evident that DNA-PKcs plays an important role in the stabilization of stalled replication forks and ATR signaling [175, 176].

In both studies implemented in this thesis, Classen et al. 2022, and Meyer et al. 2020, it was shown that ATR as well as CHK1 inhibition could sensitize previously resistant breast cancer cell lines. The double treatment of IR + ATR inhibition and MMC + CHK1 inhibition showed greater effects than the single treatments [137, 148]. This observation was shown for the first time in clones of the MCF7 cell line carrying mutations in non-functional domains of the *BRCA1* gene [148]. It further supports the hypothesis that combinational treatments may be more efficient in inducing tumor cell death.

There are several ongoing clinical trials with the goal to combine kinase inhibitors with other therapeutic options to improve the outcome for the patients. They focus mainly on advanced stage tumors, including breast cancer [104]. A clinical trial with the combination of ceralasertib and carboplatin or olaparib is currently ongoing. First results showed that toxicity seems manageable. The study also gave insights into pharmacokinetics and suggested schedules as well as doses for the therapy application ([124], NCT02264678). Another phase I/II clinical trial combined the CHK1 inhibitor SRA373 with gemcitabine is also showing promising results ([123], NCT02797977). The increasing number of ongoing clinical trials shows the potential of combination therapies, yet the lack of phase III trials highlights the importance of further research to gain an even better understanding of the involved processes.

3.6 Conclusion

In summary, the data compiled in this thesis based on three publications show that avoidance of replication stress by CHK1 activation is a major driver of resistance to various DNA-damaging sources. Most screens for targeted therapy in breast cancer include the screening for HR deficiency. According to the presented data, screening for CHK1 activity could also provide valuable information for treatment planning. This is independent of the *BRCA* status or breast cancer subtype. Most studies regarding therapy focus on TNBCs, while the data presented here show that also LumA tumor patients could benefit from screening for CIN and replication stress status to offer more therapeutic options for the patients. Further, inhibition of ATR or CHK1 can sensitize cell lines that were previously resistant to IR and MMC. For cell lines with mutations in non-functional domains of the *BRCA1* gene, this sensitizing effect was shown here for the first time.

3.7 Outlook

3.7.1 Implementing optimized CIN scores for personalized therapy planning

Though the CIN70 score has been used in many studies to try and predict patient outcome, the score has not been modified or adjusted with new available data sources [44, 45]. The 70 genes included in this score were chosen based on the association with high CIN, defined by total functional aneuploidy. This was irrespective of the function or pathway that these genes were involved in [45]. Larger whole genome sequencing data sets from TCGA databases have been used in a recent study to define more refined CIN signatures [125]. In this study, the signatures were also associated to the pathways that caused the specific CIN signature, indicating possible targeted strategies for tumors with different CIN signatures. They further show that sensitivity to platinum-based drugs can be predicted with a high accuracy by association to certain CIN signatures in ovarian cancers [125]. Using these new signatures could offer the possibility to classify more tumors with high CIN into different subgroups. The subgroups then could offer implications on treatment options for the patients across multiple cancer entities, as the study not only identified cancer-type specific signatures but also pan-cancer signatures [125]. The opportunity to further improve these refined CIN signatures and consistently improve prediction of therapy outcome is increasing due to the higher availability of large data sets.

3.7.2 Interplay of replication stress and immune response as therapeutic target

The discovery of immune checkpoint inhibitors (ICIs) has been beneficial for many cancer patients, especially in advanced stage melanomas and lung cancer. Most FDA approved ICIs target cytotoxic T-lymphocyte antigen-4 (CTLA-4) and programmed death-ligand 1 (PD-L1)

[177-179]. Recently, ICIs have also been used to treat metastatic breast cancer with response rates of approximately 10-20% [180]. This relatively low rate has yielded the hypothesis that ICIs could be combined with other drugs to turn non-responders into responders. There have been several studies that show a connection between the immune signaling and replication stress response in pre-clinical models [181]. Increasing level of replication stress is associated with accumulation of cytosolic DNA and micronuclei, which can activate the intracellular immune signaling cascade via the cyclic GMP–AMP synthase (cGAS)/stimulator of interferon genes (STING) pathway [50]. Consequently, proinflammatory cytokines and interferon (IFN) type I signaling is activated, which led to activation of the adaptive immune response [182]. It has already been described that *BRCA* deficiency can lead to increased cluster of differentiation 4 (CD4+) and CD8+ T cell infiltration and increased PD-L1 expression [183]. Another study showed the connection between PARP1 inhibition and activation of the intracellular immune signaling independent of the *BRCA* status, indicating that combination of PARP1 inhibition with ICIs could show improved anti-cancer effects [184]. There are currently several clinical trials investigating combinations of ICIs with DDR inhibitors and IR [185].

The avoidance of replication stress has been identified as a driver for therapy resistance in the studies included in this thesis. It can be a promising approach to investigate the influence of the intracellular immune signaling on the here described cell lines. Combining inhibitors against, e.g., ATR, and CHK1 with ICIs and IR might result in even greater effects on cellular survival rates of cancer cells. These combination treatments might enhance the number of patients that could benefit from immunotherapy.

3.7.3 Transfer of findings to a clinically relevant model system

The major problem of many pre-clinical studies is the transfer from bench to bedside. There are several different aspects that must be determined before clinical trials can even begin. These include: Safety and toxicity, application dose, timing of treatments, pharmacokinetics, and many others. This is why over 85% of drugs which showed promising results in pre-clinical settings fail to show beneficial effects in early phase clinical trials, and more than half of those drugs which succeeded in phase I clinical trials do not make it through the process of phase III clinical trials [186]. On top of that, the clinical trial fail rate in phase II and III is amongst the highest for anti-cancer drugs [187, 188]. Thus, there is an urgent need for improvement of the pre-clinical model systems to enable a faster and more precise translation from bench to bedside.

One promising model are patient-derived organoids (PDOs), which have been established over the last years for many cancer entities [189]. They are 3D grown structures directly from biopsies or surgical resected pieces of tumors from individual cancer patients. Several studies have already shown that PDOs reflect the response to different anti-cancer therapies of the

parental tumor with a high probability. Normal tissue organoids have been used to predict toxicity [190-192]. Another beneficial factor of PDOs is the presence of several different cell types, reflecting the tumor heterogeneity. Even immune cells can be co-cultured with PDOs, enabling the prediction of ICIs [193-195]. For that reason, I established this new model system in the Laboratory for Radiobiology and Experimental Radiooncology at the University Medical Center Hamburg-Eppendorf for all breast cancer subtypes (Figure 6). Further studies can now be performed in PDO culture, potentially enabling faster transfer of pre-clinical results into clinical application to improve therapeutic options for breast cancer patients.

Based on the studies included in this thesis, ATR and CHK1 inhibition have already shown promising results in sensitization of resistant cancer cells in 2D cell culture. This could be tested in 3D PDO cultures. Further, addition of ICIs to this combination could be tested to see if the sensitization effects can be enhanced. Since the therapeutic effect of ICIs depends largely on the present immune cells in a tumor, immune cells could be co-cultured with the PDOs to enhance the predictive effect of ICIs.

In parallel, normal tissue organoids could be treated with these combinations to evaluate toxic side effects. Further, the combination of drugs inhibiting other stages of the replication stress response could be tested, e.g., MCM2 inhibitors, which target the origin licensing and also have the potential to sensitize resistant cancer cells.
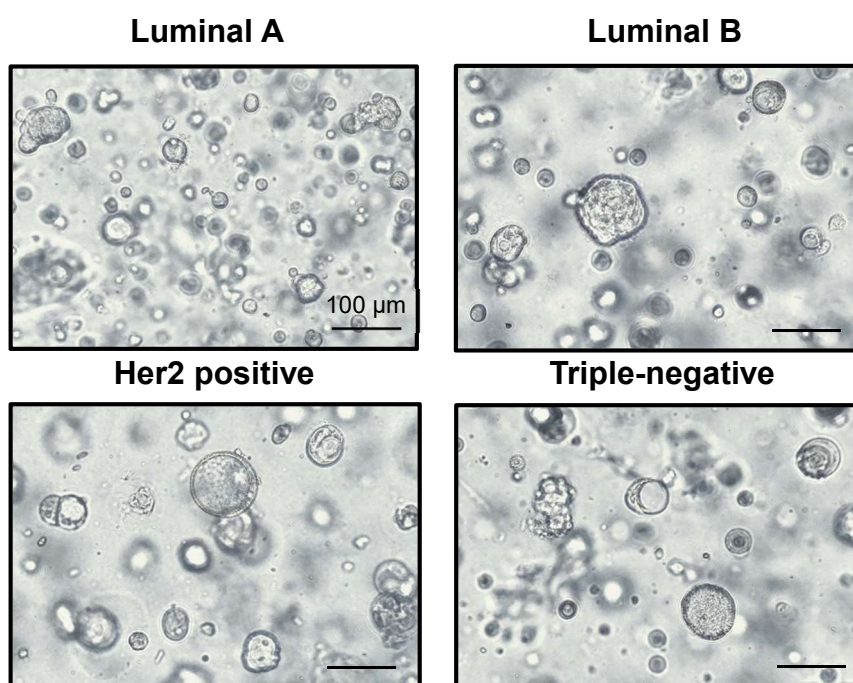

Figure 6: Patient-derived organoids of all breast cancer subtypes. Representative example bright field images of PDOs, scale bar 100 µm. Her2: Human epidermal growth factor receptor 2; PDO: Patient-derived organoid.

Contribution to publications

Publication 1 – First Author:

Published in November 2022 in the International Journal of Molecular Sciences
DOI: 10.3390/ijms232113363.

Partial Reduction in BRCA1 Gene Dose Modulates DNA Replication Stress Level and Thereby Contributes to Sensitivity or Resistance

- Active involvement in planning and conceptualization of the entire project
- Contribution by active scientific discussions and presenting the data on multiple conferences
- Performance of experiments, analysis and data visualization of
    - Figure 1D and E, Figure 3 A-G and Figure 4 B-H
    - Figure 2 A-E and Figure 4A (taken from my Master thesis)
    - Supplementary Figure S4A, S5A-C, S6, S7
- Performance of experiments for the revision of the publication
- Writing the first draft of the manuscript together with Prof. Borgmann

Publication 2 – Co-Author:

Published in January 2020 in Cells
DOI: 10.3390/cells9010238.

Prevention of DNA Replication Stress by CHK1 Leads to Chemoresistance Despite a DNA Repair Defect in Homologous Recombination in Breast Cancer

- Active involvement in conceptualization of the project by active scientific discussions
- Performance of experiments and analysis of
    - Supplementary Figure S7
- Writing and correction of the manuscript draft

Publication 3 – Co-Author:

Published in September 2020 in Cancers

DOI: 10.3390/cancers12102809

Exploiting Chromosomal Instability of PTEN-Deficient Triple-Negative Breast Cancer Cell Lines for the Sensitization Against PARP1 Inhibition in a Replication-Dependent Manner

- o Active involvement in the project by active scientific discussions
- o Support in performance of METABRIC analysis in Figure 1
- o Writing and correction of the manuscript draft

Hamburg, 10.05.2023

City, Date

Prof. Dr. Kerstin Borgmann

References

1. Ferlay, J., et al., *Cancer statistics for the year 2020: An overview.* Int J Cancer, 2021.
2. Hanahan, D. and R.A. Weinberg, *Hallmarks of cancer: the next generation.* Cell, 2011. **144**(5): p. 646-74.
3. Hanahan, D., *Hallmarks of Cancer: New Dimensions.* Cancer Discov, 2022. **12**(1): p. 31-46.
4. Rizzo, A., et al., *Systemic Treatments for Metastatic Human Epidermal Growth Factor Receptor 2-Positive Breast Cancer: Old Certainties and New Frontiers*, in *Cancer Control*. 2022, © The Author(s) 2022.
5. Perou, C.M., et al., *Molecular portraits of human breast tumours.* Nature, 2000. **406**(6797): p. 747-52.
6. Goldhirsch, A., et al., *Personalizing the treatment of women with early breast cancer: highlights of the St Gallen International Expert Consensus on the Primary Therapy of Early Breast Cancer 2013.* Ann Oncol, 2013. **24**(9): p. 2206-23.
7. Lehmann, B.D., et al., *Identification of human triple-negative breast cancer subtypes and preclinical models for selection of targeted therapies.* J Clin Invest, 2011. **121**(7): p. 2750-67.
8. Park, S., et al., *Characteristics and outcomes according to molecular subtypes of breast cancer as classified by a panel of four biomarkers using immunohistochemistry.* Breast, 2012. **21**(1): p. 50-7.
9. Abubakar, M., et al., *Combined quantitative measures of ER, PR, HER2, and KI67 provide more prognostic information than categorical combinations in luminal breast cancer.* Mod Pathol, 2019. **32**(9): p. 1244-1256.
10. Metzger Filho, O., et al., *Relative Effectiveness of Letrozole Compared With Tamoxifen for Patients With Lobular Carcinoma in the BIG 1-98 Trial.* J Clin Oncol, 2015. **33**(25): p. 2772-9.
11. Slamon, D.J., et al., *Use of chemotherapy plus a monoclonal antibody against HER2 for metastatic breast cancer that overexpresses HER2.* N Engl J Med, 2001. **344**(11): p. 783-92.
12. Dent, R., et al., *Triple-negative breast cancer: clinical features and patterns of recurrence.* Clin Cancer Res, 2007. **13**(15 Pt 1): p. 4429-34.
13. O'Reilly, D., M.A. Sendi, and C.M. Kelly, *Overview of recent advances in metastatic triple negative breast cancer.* World J Clin Oncol, 2021. **12**(3): p. 164-182.
14. McAnena, P.F., et al., *Breast cancer subtype discordance: impact on post-recurrence survival and potential treatment options.* BMC Cancer, 2018. **18**(1): p. 203.
15. Goto, W., et al., *Significance of intrinsic breast cancer subtypes on the long-term prognosis after neoadjuvant chemotherapy.* J Transl Med, 2018. **16**(1): p. 307.
16. FitzGerald, M.G., et al., *Germline mutations in PTEN are an infrequent cause of genetic predisposition to breast cancer.* Oncogene, 1998. **17**(6): p. 727-31.
17. Hall, J.M., et al., *Linkage of early-onset familial breast cancer to chromosome 17q21.* Science, 1990. **250**(4988): p. 1684-9.
18. Wooster, R., et al., *Localization of a breast cancer susceptibility gene, BRCA2, to chromosome 13q12-13.* Science, 1994. **265**(5181): p. 2088-90.
19. Melchor, L. and J. Benitez, *The complex genetic landscape of familial breast cancer.* Hum Genet, 2013. **132**(8): p. 845-63.
20. Zhang, H.Y., et al., *PTEN mutation, methylation and expression in breast cancer patients.* Oncol Lett, 2013. **6**(1): p. 161-168.
21. Lin, W.Y., et al., *Associations of ATR and CHEK1 single nucleotide polymorphisms with breast cancer.* PLoS One, 2013. **8**(7): p. e68578.
22. Tan, M.H., et al., *Lifetime cancer risks in individuals with germline PTEN mutations.* Clin Cancer Res, 2012. **18**(2): p. 400-7.
23. Pooley, K.A., et al., *Common single-nucleotide polymorphisms in DNA double-strand break repair genes and breast cancer risk.* Cancer Epidemiol Biomarkers Prev, 2008. **17**(12): p. 3482-9.

24. Chen, H., et al., *Association Between BRCA Status and Triple-Negative Breast Cancer: A Meta-Analysis.* Front Pharmacol, 2018. **9**: p. 909.

25. Li, S., et al., *Loss of PTEN expression in breast cancer: association with clinicopathological characteristics and prognosis.* Oncotarget, 2017. **8**(19): p. 32043-32054.

26. Roy, R., J. Chun, and S.N. Powell, *BRCA1 and BRCA2: different roles in a common pathway of genome protection.* Nat Rev Cancer, 2011. **12**(1): p. 68-78.

27. Hsu, L.C. and R.L. White, *BRCA1 is associated with the centrosome during mitosis.* Proc Natl Acad Sci U S A, 1998. **95**(22): p. 12983-8.

28. Schlacher, K., H. Wu, and M. Jasin, *A distinct replication fork protection pathway connects Fanconi anemia tumor suppressors to RAD51-BRCA1/2.* Cancer Cell, 2012. **22**(1): p. 106-16.

29. He, J., et al., *PTEN regulates EG5 to control spindle architecture and chromosome congression during mitosis.* Nat Commun, 2016. **7**: p. 12355.

30. Maehama, T. and J.E. Dixon, *The tumor suppressor, PTEN/MMAC1, dephosphorylates the lipid second messenger, phosphatidylinositol 3,4,5-trisphosphate.* J Biol Chem, 1998. **273**(22): p. 13375-8.

31. Liu, Y., et al., *PTEN regulates spindle assembly checkpoint timing through MAD1 in interphase.* Oncotarget, 2017. **8**(58): p. 98040-98050.

32. Puc, J. and R. Parsons, *PTEN loss inhibits CHK1 to cause double stranded-DNA breaks in cells.* Cell Cycle, 2005. **4**(7): p. 927-9.

33. Shen, W.H., et al., *Essential role for nuclear PTEN in maintaining chromosomal integrity.* Cell, 2007. **128**(1): p. 157-70.

34. Cimprich, K.A. and D. Cortez, *ATR: an essential regulator of genome integrity.* Nat Rev Mol Cell Biol, 2008. **9**(8): p. 616-27.

35. Sorensen, C.S., et al., *The cell-cycle checkpoint kinase Chk1 is required for mammalian homologous recombination repair.* Nat Cell Biol, 2005. **7**(2): p. 195-201.

36. Kramer, A., et al., *Centrosome-associated Chk1 prevents premature activation of cyclin-B-Cdk1 kinase.* Nat Cell Biol, 2004. **6**(9): p. 884-91.

37. Lengauer, C., K.W. Kinzler, and B. Vogelstein, *Genetic instabilities in human cancers.* Nature, 1998. **396**(6712): p. 643-9.

38. Hause, R.J., et al., *Classification and characterization of microsatellite instability across 18 cancer types.* Nat Med, 2016. **22**(11): p. 1342-1350.

39. Bakhoum, S.F. and L.C. Cantley, *The Multifaceted Role of Chromosomal Instability in Cancer and Its Microenvironment.* Cell, 2018. **174**(6): p. 1347-1360.

40. Bielski, C.M., et al., *Genome doubling shapes the evolution and prognosis of advanced cancers.* Nat Genet, 2018. **50**(8): p. 1189-1195.

41. Lukow, D.A. and J.M. Sheltzer, *Chromosomal instability and aneuploidy as causes of cancer drug resistance.* Trends Cancer, 2022. **8**(1): p. 43-53.

42. Carter, S.L., et al., *Absolute quantification of somatic DNA alterations in human cancer.* Nat Biotechnol, 2012. **30**(5): p. 413-21.

43. Roylance, R., et al., *Relationship of extreme chromosomal instability with long-term survival in a retrospective analysis of primary breast cancer.* Cancer Epidemiol Biomarkers Prev, 2011. **20**(10): p. 2183-94.

44. Birkbak, N.J., et al., *Paradoxical relationship between chromosomal instability and survival outcome in cancer.* Cancer Res, 2011. **71**(10): p. 3447-52.

45. Carter, S.L., et al., *A signature of chromosomal instability inferred from gene expression profiles predicts clinical outcome in multiple human cancers.* Nat Genet, 2006. **38**(9): p. 1043-8.

46. Bakhoum, S.F., et al., *Numerical chromosomal instability mediates susceptibility to radiation treatment.* Nat Commun, 2015. **6**: p. 5990.

47. Swanton, C., et al., *Chromosomal instability determines taxane response.* Proc Natl Acad Sci U S A, 2009. **106**(21): p. 8671-6.

48. Piemonte, K.M., L.J. Anstine, and R.A. Keri, *Centrosome Aberrations as Drivers of Chromosomal Instability in Breast Cancer.* Endocrinology, 2021. **162**(12).

49. Burrell, R.A., et al., *Replication stress links structural and numerical cancer chromosomal instability.* Nature, 2013. **494**(7438): p. 492-496.

50. Harding, S.M., et al., *Mitotic progression following DNA damage enables pattern recognition within micronuclei.* Nature, 2017. **548**(7668): p. 466-470.

51. Xu, X., et al., *Centrosome amplification and a defective G2-M cell cycle checkpoint induce genetic instability in BRCA1 exon 11 isoform-deficient cells.* Mol Cell, 1999. **3**(3): p. 389-95.

52. Matsuzawa, A., et al., *The BRCA1/BARD1-interacting protein OLA1 functions in centrosome regulation.* Mol Cell, 2014. **53**(1): p. 101-14.

53. Otsuka, K., et al., *The Function of BARD1 in Centrosome Regulation in Cooperation with BRCA1/OLA1/RACK1.* Genes (Basel), 2020. **11**(8).

54. Yoshino, Y., et al., *BRCA1-Interacting Protein OLA1 Requires Interaction with BARD1 to Regulate Centrosome Number.* Mol Cancer Res, 2018. **16**(10): p. 1499-1511.

55. Yoshino, Y., et al., *RACK1 regulates centriole duplication by controlling localization of BRCA1 to the centrosome in mammary tissue-derived cells.* Oncogene, 2019. **38**(16): p. 3077-3092.

56. Wilhelm, T., M. Said, and V. Naim, *DNA Replication Stress and Chromosomal Instability: Dangerous Liaisons.* Genes (Basel), 2020. **11**(6).

57. Koundrioukoff, S., et al., *Stepwise activation of the ATR signaling pathway upon increasing replication stress impacts fragile site integrity.* PLoS Genet, 2013. **9**(7): p. e1003643.

58. Wilhelm, T., et al., *Spontaneous slow replication fork progression elicits mitosis alterations in homologous recombination-deficient mammalian cells.* Proc Natl Acad Sci U S A, 2014. **111**(2): p. 763-8.

59. Richardson, C. and M. Jasin, *Frequent chromosomal translocations induced by DNA double-strand breaks.* Nature, 2000. **405**(6787): p. 697-700.

60. Rhim, J.S., *Neoplastic transformation of human cells in vitro.* Crit Rev Oncog, 1993. **4**(3): p. 313-35.

61. Jasin, M., et al., *High frequency of homologous recombination in mammalian cells between endogenous and introduced SV40 genomes.* Cell, 1985. **43**(3 Pt 2): p. 695-703.

62. Moynahan, M.E. and M. Jasin, *Mitotic homologous recombination maintains genomic stability and suppresses tumorigenesis.* Nat Rev Mol Cell Biol, 2010. **11**(3): p. 196-207.

63. Ceccaldi, R., B. Rondinelli, and A.D. D'Andrea, *Repair Pathway Choices and Consequences at the Double-Strand Break.* Trends Cell Biol, 2016. **26**(1): p. 52-64.

64. Jeggo, P.A., V. Geuting, and M. Lobrich, *The role of homologous recombination in radiation-induced double-strand break repair.* Radiother Oncol, 2011. **101**(1): p. 7-12.

65. Bunting, S.F., et al., *53BP1 inhibits homologous recombination in Brca1-deficient cells by blocking resection of DNA breaks.* Cell, 2010. **141**(2): p. 243-54.

66. Wang, B., et al., *Abraxas and RAP80 form a BRCA1 protein complex required for the DNA damage response.* Science, 2007. **316**(5828): p. 1194-8.

67. Yun, M.H. and K. Hiom, *CtIP-BRCA1 modulates the choice of DNA double-strand-break repair pathway throughout the cell cycle.* Nature, 2009. **459**(7245): p. 460-3.

68. Sturzenegger, A., et al., *DNA2 cooperates with the WRN and BLM RecQ helicases to mediate long-range DNA end resection in human cells.* J Biol Chem, 2014. **289**(39): p. 27314-27326.

69. Baumann, P. and S.C. West, *Role of the human RAD51 protein in homologous recombination and double-stranded-break repair.* Trends Biochem Sci, 1998. **23**(7): p. 247-51.

70. Elbakry, A. and M. Lobrich, *Homologous Recombination Subpathways: A Tangle to Resolve.* Front Genet, 2021. **12**: p. 723847.

71. Wright, W.D., S.S. Shah, and W.D. Heyer, *Homologous recombination and the repair of DNA double-strand breaks.* J Biol Chem, 2018. **293**(27): p. 10524-10535.

72. Peng, B., et al., *PARP1 and CHK1 coordinate PLK1 enzymatic activity during the DNA damage response to promote homologous recombination-mediated repair.* Nucleic Acids Res, 2021. **49**(13): p. 7554-7570.

73. He, J., et al., *PTEN regulates DNA replication progression and stalled fork recovery.* Nat Commun, 2015. **6**: p. 7620.

74. Miki, Y., et al., *A strong candidate for the breast and ovarian cancer susceptibility gene BRCA1.* Science, 1994. **266**(5182): p. 66-71.

75. Hashizume, R., et al., *The RING heterodimer BRCA1-BARD1 is a ubiquitin ligase inactivated by a breast cancer-derived mutation.* J Biol Chem, 2001. **276**(18): p. 14537-40.

76. Densham, R.M., et al., *Human BRCA1-BARD1 ubiquitin ligase activity counteracts chromatin barriers to DNA resection.* Nat Struct Mol Biol, 2016. **23**(7): p. 647-55.

77. Sato, K., et al., *A DNA-damage selective role for BRCA1 E3 ligase in claspin ubiquitylation, CHK1 activation, and DNA repair.* Curr Biol, 2012. **22**(18): p. 1659-66.

78. Morris, J.R., et al., *Genetic analysis of BRCA1 ubiquitin ligase activity and its relationship to breast cancer susceptibility.* Hum Mol Genet, 2006. **15**(4): p. 599-606.

79. Chen, C.F., et al., *The nuclear localization sequences of the BRCA1 protein interact with the importin-alpha subunit of the nuclear transport signal receptor.* J Biol Chem, 1996. **271**(51): p. 32863-8.

80. Sy, S.M., M.S. Huen, and J. Chen, *PALB2 is an integral component of the BRCA complex required for homologous recombination repair.* Proc Natl Acad Sci U S A, 2009. **106**(17): p. 7155-60.

81. Foo, T.K., et al., *Compromised BRCA1-PALB2 interaction is associated with breast cancer risk.* Oncogene, 2017. **36**(29): p. 4161-4170.

82. Pulver, E.M., et al., *A BRCA1 Coiled-Coil Domain Variant Disrupting PALB2 Interaction Promotes the Development of Mammary Tumors and Confers a Targetable Defect in Homologous Recombination Repair.* Cancer Res, 2021. **81**(24): p. 6171-6182.

83. Clark, S.L., et al., *Structure-Function Of The Tumor Suppressor BRCA1.* Comput Struct Biotechnol J, 2012. **1**(1).

84. Leung, C.C. and J.N. Glover, *BRCT domains: easy as one, two, three.* Cell Cycle, 2011. **10**(15): p. 2461-70.

85. Bryant, H.E., et al., *Specific killing of BRCA2-deficient tumours with inhibitors of poly(ADP-ribose) polymerase.* Nature, 2005. **434**(7035): p. 913-7.

86. Farmer, H., et al., *Targeting the DNA repair defect in BRCA mutant cells as a therapeutic strategy.* Nature, 2005. **434**(7035): p. 917-21.

87. Dobzhansky, T., *Genetics of natural populations; recombination and variability in populations of Drosophila pseudoobscura.* Genetics, 1946. **31**(3): p. 269-90.

88. Ashworth, A., C.J. Lord, and J.S. Reis-Filho, *Genetic interactions in cancer progression and treatment.* Cell, 2011. **145**(1): p. 30-8.

89. Noordermeer, S.M. and H. van Attikum, *PARP Inhibitor Resistance: A Tug-of-War in BRCA-Mutated Cells.* Trends Cell Biol, 2019. **29**(10): p. 820-834.

90. Turner, N., A. Tutt, and A. Ashworth, *Hallmarks of 'BRCAness' in sporadic cancers.* Nat Rev Cancer, 2004. **4**(10): p. 814-9.

91. Mukhopadhyay, A., et al., *Development of a functional assay for homologous recombination status in primary cultures of epithelial ovarian tumor and correlation with sensitivity to poly(ADP-ribose) polymerase inhibitors.* Clin Cancer Res, 2010. **16**(8): p. 2344-51.

92. Castroviejo-Bermejo, M., et al., *A RAD51 assay feasible in routine tumor samples calls PARP inhibitor response beyond BRCA mutation.* EMBO Mol Med, 2018. **10**(12).

93. Cruz, C., et al., *RAD51 foci as a functional biomarker of homologous recombination repair and PARP inhibitor resistance in germline BRCA-mutated breast cancer.* Ann Oncol, 2018. **29**(5): p. 1203-1210.

94. Naipal, K.A., et al., *Functional ex vivo assay to select homologous recombination-deficient breast tumors for PARP inhibitor treatment.* Clin Cancer Res, 2014. **20**(18): p. 4816-26.

95. Zeman, M.K. and K.A. Cimprich, *Causes and consequences of replication stress.* Nat Cell Biol, 2014. **16**(1): p. 2-9.

96. Maya-Mendoza, A., et al., *High speed of fork progression induces DNA replication stress and genomic instability.* Nature, 2018. **559**(7713): p. 279-284.

97. Gorgoulis, V.G., et al., *Activation of the DNA damage checkpoint and genomic instability in human precancerous lesions.* Nature, 2005. **434**(7035): p. 907-13.

98.   Byun, T.S., et al., *Functional uncoupling of MCM helicase and DNA polymerase activities activates the ATR-dependent checkpoint.* Genes Dev, 2005. **19**(9): p. 1040-52.

99.   Zou, L. and S.J. Elledge, *Sensing DNA damage through ATRIP recognition of RPA-ssDNA complexes.* Science, 2003. **300**(5625): p. 1542-8.

100.   Mordes, D.A., et al., *TopBP1 activates ATR through ATRIP and a PIKK regulatory domain.* Genes Dev, 2008. **22**(11): p. 1478-89.

101.   Guo, Z., et al., *Requirement for Atr in phosphorylation of Chk1 and cell cycle regulation in response to DNA replication blocks and UV-damaged DNA in Xenopus egg extracts.* Genes Dev, 2000. **14**(21): p. 2745-56.

102.   Kumagai, A. and W.G. Dunphy, *Claspin, a novel protein required for the activation of Chk1 during a DNA replication checkpoint response in Xenopus egg extracts.* Mol Cell, 2000. **6**(4): p. 839-49.

103.   Peng, C.Y., et al., *Mitotic and G2 checkpoint control: regulation of 14-3-3 protein binding by phosphorylation of Cdc25C on serine-216.* Science, 1997. **277**(5331): p. 1501-5.

104.   Baillie, K.E. and P.C. Stirling, *Beyond Kinases: Targeting Replication Stress Proteins in Cancer Therapy.* Trends Cancer, 2021. **7**(5): p. 430-446.

105.   Eykelenboom, J.K., et al., *ATR activates the S-M checkpoint during unperturbed growth to ensure sufficient replication prior to mitotic onset.* Cell Rep, 2013. **5**(4): p. 1095-107.

106.   Maya-Mendoza, A., et al., *Chk1 regulates the density of active replication origins during the vertebrate S phase.* EMBO J, 2007. **26**(11): p. 2719-31.

107.   Petermann, E., M. Woodcock, and T. Helleday, *Chk1 promotes replication fork progression by controlling replication initiation.* Proc Natl Acad Sci U S A, 2010. **107**(37): p. 16090-5.

108.   Chen, Y.H., et al., *ATR-mediated phosphorylation of FANCI regulates dormant origin firing in response to replication stress.* Mol Cell, 2015. **58**(2): p. 323-38.

109.   Yoo, H.Y., et al., *Mcm2 is a direct substrate of ATM and ATR during DNA damage and DNA replication checkpoint responses.* J Biol Chem, 2004. **279**(51): p. 53353-64.

110.   Lopes, M., et al., *The DNA replication checkpoint response stabilizes stalled replication forks.* Nature, 2001. **412**(6846): p. 557-61.

111.   Bhat, K.P., et al., *RADX Modulates RAD51 Activity to Control Replication Fork Protection.* Cell Rep, 2018. **24**(3): p. 538-545.

112.   Schlacher, K., et al., *Double-strand break repair-independent role for BRCA2 in blocking stalled replication fork degradation by MRE11.* Cell, 2011. **145**(4): p. 529-42.

113.   Taglialatela, A., et al., *Restoration of Replication Fork Stability in BRCA1- and BRCA2-Deficient Cells by Inactivation of SNF2-Family Fork Remodelers.* Mol Cell, 2017. **68**(2): p. 414-430 e8.

114.   Thangavel, S., et al., *DNA2 drives processing and restart of reversed replication forks in human cells.* J Cell Biol, 2015. **208**(5): p. 545-62.

115.   Zellweger, R., et al., *Rad51-mediated replication fork reversal is a global response to genotoxic treatments in human cells.* J Cell Biol, 2015. **208**(5): p. 563-79.

116.   Toledo, L., K.J. Neelsen, and J. Lukas, *Replication Catastrophe: When a Checkpoint Fails because of Exhaustion.* Mol Cell, 2017. **66**(6): p. 735-749.

117.   Feng, J., et al., *PTEN Controls the DNA Replication Process through MCM2 in Response to Replicative Stress.* Cell Rep, 2015. **13**(7): p. 1295-1303.

118.   Wang, G., et al., *PTEN regulates RPA1 and protects DNA replication forks.* Cell Res, 2015. **25**(11): p. 1189-204.

119.   Puc, J., et al., *Lack of PTEN sequesters CHK1 and initiates genetic instability.* Cancer Cell, 2005. **7**(2): p. 193-204.

120.   Ubhi, T. and G.W. Brown, *Exploiting DNA Replication Stress for Cancer Treatment.* Cancer Res, 2019. **79**(8): p. 1730-1739.

121.   Bartkova, J., et al., *DNA damage response as a candidate anti-cancer barrier in early human tumorigenesis.* Nature, 2005. **434**(7035): p. 864-70.

122.   Bartkova, J., et al., *Oncogene-induced senescence is part of the tumorigenesis barrier imposed by DNA damage checkpoints.* Nature, 2006. **444**(7119): p. 633-7.

123. Jones, R., et al., *A Phase I/II Trial of Oral SRA737 (a Chk1 Inhibitor) Given in Combination with Low-Dose Gemcitabine in Patients with Advanced Cancer.* Clin Cancer Res, 2023. **29**(2): p. 331-340.

124. Yap, T.A., et al., *Ceralasertib (AZD6738), an Oral ATR Kinase Inhibitor, in Combination with Carboplatin in Patients with Advanced Solid Tumors: A Phase I Study.* Clin Cancer Res, 2021. **27**(19): p. 5213-5224.

125. Drews, R.M., et al., *A pan-cancer compendium of chromosomal instability.* Nature, 2022. **606**(7916): p. 976-983.

126. Takahashi, N., et al., *Replication stress defines distinct molecular subtypes across cancers.* Cancer Res Commun, 2022. **2**(6): p. 503-517.

127. Dobbelstein, M. and C.S. Sorensen, *Exploiting replicative stress to treat cancer.* Nat Rev Drug Discov, 2015. **14**(6): p. 405-23.

128. Janku, F., T.A. Yap, and F. Meric-Bernstam, *Targeting the PI3K pathway in cancer: are we making headway?* Nat Rev Clin Oncol, 2018. **15**(5): p. 273-291.

129. Lawrence, M.S., et al., *Discovery and saturation analysis of cancer genes across 21 tumour types.* Nature, 2014. **505**(7484): p. 495-501.

130. Labib, K., *How do Cdc7 and cyclin-dependent kinases trigger the initiation of chromosome replication in eukaryotic cells?* Genes Dev, 2010. **24**(12): p. 1208-19.

131. Labib, K., J.A. Tercero, and J.F. Diffley, *Uninterrupted MCM2-7 function required for DNA replication fork progression.* Science, 2000. **288**(5471): p. 1643-7.

132. Tijhuis, A.E., S.C. Johnson, and S.E. McClelland, *The emerging links between chromosomal instability (CIN), metastasis, inflammation and tumour immunity.* Mol Cytogenet, 2019. **12**: p. 17.

133. Antoniou, A., et al., *Average risks of breast and ovarian cancer associated with BRCA1 or BRCA2 mutations detected in case Series unselected for family history: a combined analysis of 22 studies.* Am J Hum Genet, 2003. **72**(5): p. 1117-30.

134. Cancer Genome Atlas, N., *Comprehensive molecular portraits of human breast tumours.* Nature, 2012. **490**(7418): p. 61-70.

135. Shah, S.P., et al., *The clonal and mutational evolution spectrum of primary triple-negative breast cancers.* Nature, 2012. **486**(7403): p. 395-9.

136. Zhao, W., et al., *The BRCA Tumor Suppressor Network in Chromosome Damage Repair by Homologous Recombination.* Annu Rev Biochem, 2019. **88**: p. 221-245.

137. Meyer, F., et al., *Prevention of DNA Replication Stress by CHK1 Leads to Chemoresistance Despite a DNA Repair Defect in Homologous Recombination in Breast Cancer.* Cells, 2020. **9**(1).

138. Rieckhoff, J., et al., *Exploiting Chromosomal Instability of PTEN-Deficient Triple-Negative Breast Cancer Cell Lines for the Sensitization against PARP1 Inhibition in a Replication-Dependent Manner.* Cancers (Basel), 2020. **12**(10).

139. Cremer, T., et al., *Detection of chromosome aberrations in metaphase and interphase tumor cells by in situ hybridization using chromosome-specific library probes.* Hum Genet, 1988. **80**(3): p. 235-46.

140. McKinley, K.L. and I.M. Cheeseman, *The molecular basis for centromere identity and function.* Nat Rev Mol Cell Biol, 2016. **17**(1): p. 16-29.

141. Kritikou, E., *PTEN — a new guardian of the genome.* Nature Reviews Molecular Cell Biology, 2007. **8**(3): p. 179-179.

142. Yin, Y. and W.H. Shen, *PTEN: a new guardian of the genome.* Oncogene, 2008. **27**(41): p. 5443-53.

143. Lane, D.P., *Cancer. p53, guardian of the genome.* Nature, 1992. **358**(6381): p. 15-6.

144. Verlinden, L., et al., *The E2F-regulated gene Chk1 is highly expressed in triple-negative estrogen receptor /progesterone receptor /HER-2 breast carcinomas.* Cancer Res, 2007. **67**(14): p. 6574-81.

145. Wu, M., et al., *The clinical significance of CHEK1 in breast cancer: a high-throughput data analysis and immunohistochemical study.* Int J Clin Exp Pathol, 2019. **12**(1): p. 1-20.

146. Tort, F., et al., *Checkpoint kinase 1 (CHK1) protein and mRNA expression is downregulated in aggressive variants of human lymphoid neoplasms.* Leukemia, 2005. **19**(1): p. 112-7.

147. Bertoni, F., et al., *CHK1 frameshift mutations in genetically unstable colorectal and endometrial cancers.* Genes Chromosomes Cancer, 1999. **26**(2): p. 176-80.

148. Classen, S., et al., *Partial Reduction in BRCA1 Gene Dose Modulates DNA Replication Stress Level and Thereby Contributes to Sensitivity or Resistance.* Int J Mol Sci, 2022. **23**(21).

149. Rahlf, E., *BRCA1 verändert die Strahlenempfindlichkeit durch Modifikation des Tumorstammzellanteils in MCF7 Zellen*. 2020, Universität Hamburg, Hamburg, Germany.

150. Classen, S., *Influence of the BRCA1 downregulation on the functionality of the homologous recombination and the cellular survival after induced DNA-damage in an isogenic cell system.* 2018, Universität zu Lübeck, Lübeck, Germany.

151. Saleh-Gohari, N., et al., *Spontaneous homologous recombination is induced by collapsed replication forks that are caused by endogenous DNA single-strand breaks.* Mol Cell Biol, 2005. **25**(16): p. 7158-69.

152. Fong, P.C., et al., *Inhibition of poly(ADP-ribose) polymerase in tumors from BRCA mutation carriers.* N Engl J Med, 2009. **361**(2): p. 123-34.

153. Koc, A., et al., *Hydroxyurea arrests DNA replication by a mechanism that preserves basal dNTP pools.* J Biol Chem, 2004. **279**(1): p. 223-30.

154. Li, J., et al., *PTEN, a putative protein tyrosine phosphatase gene mutated in human brain, breast, and prostate cancer.* Science, 1997. **275**(5308): p. 1943-7.

155. Steck, P.A., et al., *Identification of a candidate tumour suppressor gene, MMAC1, at chromosome 10q23.3 that is mutated in multiple advanced cancers.* Nat Genet, 1997. **15**(4): p. 356-62.

156. Fan, X., et al., *PTEN as a Guardian of the Genome: Pathways and Targets.* Cold Spring Harb Perspect Med, 2020. **10**(9).

157. Xiao, Z., et al., *Chk1 mediates S and G2 arrests through Cdc25A degradation in response to DNA-damaging agents.* J Biol Chem, 2003. **278**(24): p. 21767-73.

158. Bassi, C., et al., *Nuclear PTEN controls DNA repair and sensitivity to genotoxic stress.* Science, 2013. **341**(6144): p. 395-9.

159. Bouwman, P., et al., *53BP1 loss rescues BRCA1 deficiency and is associated with triple-negative and BRCA-mutated breast cancers.* Nat Struct Mol Biol, 2010. **17**(6): p. 688-95.

160. Schultz, L.B., et al., *p53 binding protein 1 (53BP1) is an early participant in the cellular response to DNA double-strand breaks.* J Cell Biol, 2000. **151**(7): p. 1381-90.

161. Negrini, S., V.G. Gorgoulis, and T.D. Halazonetis, *Genomic instability--an evolving hallmark of cancer.* Nat Rev Mol Cell Biol, 2010. **11**(3): p. 220-8.

162. Yoneda, T., et al., *A bone-seeking clone exhibits different biological properties from the MDA-MB-231 parental human breast cancer cells and a brain-seeking clone in vivo and in vitro.* J Bone Miner Res, 2001. **16**(8): p. 1486-95.

163. Chaudhuri, A.R., et al., *Erratum: Replication fork stability confers chemoresistance in BRCA-deficient cells.* Nature, 2016. **539**(7629): p. 456.

164. Bold, I.T., et al., *DNA Damage Response during Replication Correlates with CIN70 Score and Determines Survival in HNSCC Patients.* Cancers (Basel), 2021. **13**(6).

165. Zhao, H. and H. Piwnica-Worms, *ATR-mediated checkpoint pathways regulate phosphorylation and activation of human Chk1.* Mol Cell Biol, 2001. **21**(13): p. 4129-39.

166. Buisson, R., et al., *Distinct but Concerted Roles of ATR, DNA-PK, and Chk1 in Countering Replication Stress during S Phase.* Mol Cell, 2015. **59**(6): p. 1011-24.

167. Toledo, L.I., et al., *A cell-based screen identifies ATR inhibitors with synthetic lethal properties for cancer-associated mutations.* Nat Struct Mol Biol, 2011. **18**(6): p. 721-7.

168. Abe, S., et al., *Targeting MCM2 function as a novel strategy for the treatment of highly malignant breast tumors.* Oncotarget, 2015. **6**(33): p. 34892-909.

169. Wojnar, A., et al., *Correlation of intensity of MT-I/II expression with Ki-67 and MCM-2 proteins in invasive ductal breast carcinoma.* Anticancer Res, 2011. **31**(9): p. 3027-33.

170.   Hoxhaj, G. and B.D. Manning, *The PI3K-AKT network at the interface of oncogenic signalling and cancer metabolism.* Nat Rev Cancer, 2020. **20**(2): p. 74-88.

171.   Gonzalez-Billalabeitia, E., et al., *Vulnerabilities of PTEN-TP53-deficient prostate cancers to compound PARP-PI3K inhibition.* Cancer Discov, 2014. **4**(8): p. 896-904.

172.   Juvekar, A., et al., *Combining a PI3K inhibitor with a PARP inhibitor provides an effective therapy for BRCA1-related breast cancer.* Cancer Discov, 2012. **2**(11): p. 1048-63.

173.   Konstantinopoulos, P.A., et al., *Olaparib and alpha-specific PI3K inhibitor alpelisib for patients with epithelial ovarian cancer: a dose-escalation and dose-expansion phase 1b trial.* Lancet Oncol, 2019. **20**(4): p. 570-580.

174.   Thompson, R., R. Montano, and A. Eastman, *The Mre11 nuclease is critical for the sensitivity of cells to Chk1 inhibition.* PLoS One, 2012. **7**(8): p. e44021.

175.   Lin, Y.F., et al., *PIDD mediates the association of DNA-PKcs and ATR at stalled replication forks to facilitate the ATR signaling pathway.* Nucleic Acids Res, 2018. **46**(4): p. 1847-1859.

176.   Ying, S., et al., *DNA-PKcs and PARP1 Bind to Unresected Stalled DNA Replication Forks Where They Recruit XRCC1 to Mediate Repair.* Cancer Res, 2016. **76**(5): p. 1078-88.

177.   Hamid, O., et al., *Safety and tumor responses with lambrolizumab (anti-PD-1) in melanoma.* N Engl J Med, 2013. **369**(2): p. 134-44.

178.   Hodi, F.S., et al., *Improved survival with ipilimumab in patients with metastatic melanoma.* N Engl J Med, 2010. **363**(8): p. 711-23.

179.   Topalian, S.L., et al., *Safety, activity, and immune correlates of anti-PD-1 antibody in cancer.* N Engl J Med, 2012. **366**(26): p. 2443-54.

180.   Nanda, R., et al., *Pembrolizumab in Patients With Advanced Triple-Negative Breast Cancer: Phase Ib KEYNOTE-012 Study.* J Clin Oncol, 2016. **34**(21): p. 2460-7.

181.   McGrail, D.J., et al., *Replication stress response defects are associated with response to immune checkpoint blockade in nonhypermutated cancers.* Sci Transl Med, 2021. **13**(617): p. eabe6201.

182.   Diamond, M.S., et al., *Type I interferon is selectively required by dendritic cells for immune rejection of tumors.* J Exp Med, 2011. **208**(10): p. 1989-2003.

183.   Parkes, E.E., et al., *Activation of STING-Dependent Innate Immune Signaling By S-Phase-Specific DNA Damage in Breast Cancer.* J Natl Cancer Inst, 2017. **109**(1).

184.   Shen, J., et al., *PARPi Triggers the STING-Dependent Immune Response and Enhances the Therapeutic Efficacy of Immune Checkpoint Blockade Independent of BRCAness.* Cancer Res, 2019. **79**(2): p. 311-319.

185.   Huang, J.L., et al., *Targeting DNA Damage Response and Immune Checkpoint for Anticancer Therapy.* Int J Mol Sci, 2022. **23**(6).

186.   Mak, I.W., N. Evaniew, and M. Ghert, *Lost in translation: animal models and clinical trials in cancer treatment.* Am J Transl Res, 2014. **6**(2): p. 114-8.

187.   Arrowsmith, J., *Trial watch: phase III and submission failures: 2007-2010.* Nat Rev Drug Discov, 2011. **10**(2): p. 87.

188.   Arrowsmith, J. and P. Miller, *Trial watch: phase II and phase III attrition rates 2011-2012.* Nat Rev Drug Discov, 2013. **12**(8): p. 569.

189.   Xu, H., et al., *Organoid technology and applications in cancer research.* J Hematol Oncol, 2018. **11**(1): p. 116.

190.   Jabs, J., et al., *Screening drug effects in patient-derived cancer cells links organoid responses to genome alterations.* Mol Syst Biol, 2017. **13**(11): p. 955.

191.   Ooft, S.N., et al., *Patient-derived organoids can predict response to chemotherapy in metastatic colorectal cancer patients.* Sci Transl Med, 2019. **11**(513).

192.   Vlachogiannis, G., et al., *Patient-derived organoids model treatment response of metastatic gastrointestinal cancers.* Science, 2018. **359**(6378): p. 920-926.

193.   Dijkstra, K.K., et al., *Generation of Tumor-Reactive T Cells by Co-culture of Peripheral Blood Lymphocytes and Tumor Organoids.* Cell, 2018. **174**(6): p. 1586-1598 e12.

194.   Kopper, O., et al., *An organoid platform for ovarian cancer captures intra- and interpatient heterogeneity.* Nat Med, 2019. **25**(5): p. 838-849.

195.   Roerink, S.F., et al., *Intra-tumour diversification in colorectal cancer at the single-cell level.* Nature, 2018. **556**(7702): p. 457-462.

List of figures

Acknowledgements

I would like to thank Prof. Dr. Kerstin Borgmann for her supervision and the opportunity to work on such interesting research projects. I want to thank her for all the support during my PhD time and many fun scientific discussions. Thanks to her, I was able to present my research results on a number of national and international conferences with great success. She always supported me to achieve my goals and kept pushing me to show my very best.

I want to thank Prof. Dr. Tim Gilberger for being the second reviewer of my dissertation.

A great thank you also goes to Prof. Dr. Kai Rothkamm, our head of laboratory, for great scientific discussions and always having an open ear.

I would also like to thank all the authors of the publications and collaboration partners for their terrific work and engagement.

I want to thank Dr. Elena Rahlf, Dr. Felix Meyer and Dr. Ann Christin Parplys for their great scientific work and the critical discussion of my research data. I want to thank them for the many laughs and great time we had together in the lab.

Thank you to Lena Poole, Britta Riepen and Alexandra Zielinski for their technical support with many experiments in the lab. Also thank you to Konstantin, Stefanie, Adriana, Fruzsina and Sabrina C. for the support with different methods and devices in the lab. I also want to thank all of them for making the time in the lab a lot of fun and being such a great team.
I would also like to thank everyone else in the lab for the nice atmosphere, great scientific discussions, and fun lab events. Thank you, Alicia, Ayham, Malte, Marie, Mo, Nadja, Nina, Ruth, Sabrina K., Shaimaa, Thorsten, Wael.

I want to thank the students that I was supervising during my PhD time and contributed to my research: Luca Hebestreit, Antonia Kiene and Victoria Aßmann.

A great thank you also to Kira, who made PhD life easier due to many fun coffee breaks and relaxing evenings.

Last but not least, I want to thank my parents who have always supported me along every phase of my life. I also want to thank Thomas for his encouragement and support during the whole time.

Associated publications

All associated scientific publications of this thesis are included in the cumulative dissertation.

Contributions to scientific conferences

Presentations:

Classen S. et al. **Auswirkungen von BRCA1-Mutationen auf Strahlenresistenz und Immunphänotyp in Brustkrebszellen.**
Conference of the Deutsche Gesellschaft für Radioonkologie e.V. 2022, Stuttgart, Germany
Awarded the Koester Prize for the best presentation at the DEGRO Annual Meeting 2022, by the DEGRO together with the Dr. Hans und Hildegard Koester Foundation.

Classen S. et al. **Altered activation of the immune response causes radioresistance in HR-impaired breast cancer cells.**
Congress of the European Society for Radiotherapy and Oncology 2022, Copenhagen, Denmark

Classen S. et al. **Replikationsstress bestimmt das zelluläre Überleben in Sphäroiden BRCA1-mutierter Zellen und Organoiden von Brustkrebstumoren.**
Conference of the Deutsche Gesellschaft für Radioonkologie e.V. 2021, digital

Classen S. et al. **The adaptive resistome in triple-negative breast cancer: Functional targeting in patient-derived organoids and cell lines**.
5th AEK Autumn School 2020, digital

Poster:

Classen S. et al. **BRCA1 mutations modify radiosensitivity through altered DNA replication stress and consequently activation of the intracellular immune response.**
11th Quinquennial Conference on Responses to DNA damage 2022, Egmond aan Zee, The Netherlands

Classen S. et al. **Identifying resistance mechanisms in breast cancer in patient-derived organoids and 3D cell culture.**
Congress of the European Society for Radiotherapy and Oncology 2021, digital

Classen S. et al. **Radioresistance is caused by altered activation of the intracellular immune response by HR-mediated replication stress in BC.**
Conference of the Deutsche Gesellschaft für Biologische Strahlenforschung e.V. 2021, digital

Classen S. et al. **The adaptive resistome in TNBC: functional targeting in patient-derived organoids and cell lines**.
Congress of the European Society for Radiotherapy and Oncology 2020, digital
Selected as a Highlight Poster, including a five-minute presentation.

Classen S. et al. **The adaptive resistome in triple-negative breast cancer: functional targeting in patient-derived organoids and homologous recombination proficient and deficient cell lines**.
11th UCCH Research Retreat 2019, Jesteburg, Germany

Appendix

The Appendix includes the three publications included in this thesis.

Partial Reduction in BRCA1 Gene Dose Modulates DNA Replication Stress Level and Thereby Contributes to Sensitivity or Resistance.
Classen S., Rahlf E., Jungwirth J., Albers N., Hebestreit L.P., Zielinski A., Poole L., Groth M., Koch P., Liehr T., Kankel S., Cordes N., Petersen C., Rothkamm K., Pospiech H. and Borgmann K.
Int. J. Mol. Sci. 2022, 23, 13363. https://doi.org/10.3390/ijms232113363

Prevention of DNA Replication Stress by CHK1 Leads to Chemoresistance Despite a DNA Repair Defect in Homologous Recombination in Breast Cancer.
Meyer F., Becker S., Classen S., Parplys A.C., Mansour W.Y., Riepen B., Timm S., Ruebe C., Jasin M., Wikman H., Petersen C., Rothkamm K. and Borgmann K.
Cells 2020, 9, 238; doi:10.3390/cells9010238

Exploiting Chromosomal Instability of PTEN-Deficient Triple-Negative Breast Cancer Cell Lines for the Sensitization Against PARP1 Inhibition in a Replication-Dependent Manner.
Rieckhoff J., Meyer F., Classen S., Zielinski A., Riepen B., Wikman H., Petersen C., Rothkamm K., Borgmann K. and Parplys A.C.
Cancers 2020, 12, 2809; doi:10.3390/cancers12102809

Article

Partial Reduction in *BRCA1* Gene Dose Modulates DNA Replication Stress Level and Thereby Contributes to Sensitivity or Resistance

Sandra Classen [1], Elena Rahlf [1], Johannes Jungwirth [2], Nina Albers [1], Luca Philipp Hebestreit [1], Alexandra Zielinski [1], Lena Poole [1], Marco Groth [3], Philipp Koch [4], Thomas Liehr [5], Stefanie Kankel [5], Nils Cordes [6,7,8,9,10], Cordula Petersen [11], Kai Rothkamm [1], Helmut Pospiech [2,12,*] and Kerstin Borgmann [1,*]

1 Laboratory of Radiobiology and Experimental Radiooncology, Center of Oncology, University Medical Center Hamburg-Eppendorf, 20246 Hamburg, Germany
2 Project Group Biochemistry, Leibniz Institute on Aging-Fritz Lipmann Institute, 07745 Jena, Germany
3 CF Next-Generation Sequencing, Leibniz Institute on Aging-Fritz Lipmann Institute, Beutenbergstrasse 11, 07745 Jena, Germany
4 CF Life Science Computing, Leibniz Institute on Aging-Fritz Lipmann Institute, Beutenbergstrasse 11, 07745 Jena, Germany
5 Institute of Human Genetics, Jena University Hospital, Friedrich Schiller University, Am Klinikum 1, 07747 Jena, Germany
6 OncoRay-National Center for Radiation Research in Oncology, Faculty of Medicine Carl Gustav Carus, Technische Universität Dresden, Fetscherstr. 74, PF 41, 01307 Dresden, Germany
7 National Center for Tumor Diseases, Partner Site Dresden: German Cancer Research Center, Im Neuenheimer Feld 280, 69120 Heidelberg, Germany
8 Department of Radiotherapy and Radiation Oncology, University Hospital Carl Gustav Carus, Technische Universität Dresden, Fetscherstr. 74, PF 50, 01307 Dresden, Germany
9 Helmholtz-Zentrum Dresden-Rossendorf, Institute of Radiooncology-OncoRay, Bautzner Landstr. 400, 01328 Dresden, Germany
10 German Cancer Consortium (DKTK), Partner Site Dresden, and German Cancer Research Center (DKFZ), Im Neuenheimer Feld 280, 69192 Heidelberg, Germany
11 Department of Radiotherapy and Radiooncology, University Medical Center Hamburg-Eppendorf, 20246 Hamburg, Germany
12 Faculty of Biochemistry and Molecular Medicine, University of Oulu, 90014 Oulu, Finland
* Correspondence: helmut.pospiech@leibniz-fli.de (H.P.); borgmann@uke.de (K.B.)

Abstract: *BRCA1* is a well-known breast cancer risk gene, involved in DNA damage repair via homologous recombination (HR) and replication fork protection. Therapy resistance was linked to loss and amplification of the *BRCA1* gene causing inferior survival of breast cancer patients. Most studies have focused on the analysis of complete loss or mutations in functional domains of *BRCA1*. How mutations in non-functional domains contribute to resistance mechanisms remains elusive and was the focus of this study. Therefore, clones of the breast cancer cell line MCF7 with indels in *BRCA1* exon 9 and 14 were generated using CRISPR/Cas9. Clones with successful introduced *BRCA1* mutations were evaluated regarding their capacity to perform HR, how they handle DNA replication stress (RS), and the consequences on the sensitivity to MMC, PARP1 inhibition, and ionizing radiation. Unexpectedly, *BRCA1* mutations resulted in both increased sensitivity and resistance to exogenous DNA damage, despite a reduction of HR capacity in all clones. Resistance was associated with improved DNA double-strand break repair and reduction in replication stress (RS). Lower RS was accompanied by increased activation and interaction of proteins essential for the S phase-specific DNA damage response consisting of HR proteins, FANCD2, and CHK1.

Keywords: BRCA1; homologous recombination; DNA damage response; CHK1; replication stress; irradiation

1. Introduction

BRCA1 and *BRCA2* are the most mutated genes in breast cancer [1,2]. For *BRCA1* it was shown that not only a loss but also an amplification of the gene, leading to increased protein expression, result in an adverse prognosis for patient survival due to therapy resistance [3].

BRCA1 is one of the critical factors in the DNA repair pathway homologous recombination (HR). It is involved in double-strand break (DSB) recognition via the interaction with abraxas 1, BRCA1 A Complex Subunit (ABRAXAS1), and receptor-associated protein 80 (RAP80) [4]. Subsequently, interaction of BRCA1 with C-terminal-binding protein-interacting protein (CtIP) and the MRE11–RAD50–NBS1 (MRN) complex creates 3′ overhangs of the DNA ends [5]. Replication protein A (RPA) then covers the single-stranded DNA (ssDNA) regions to protect them against nucleolytic degradation until it is replaced by RAD51 to allow strand invasion into the sister chromatid. RAD51 is loaded on to the DNA via the interaction of BRCA1 with PALB2 and BRCA2 [6]. Due to the involvement of BRCA1 in all the key steps of HR, a loss of BRCA1 can lead to a HR-deficiency (HRD) [7,8]. Several studies showed that overexpression of other involved DNA damage response (DDR) or HR proteins can at least partially compensate for the loss and restore the function of HR [9,10]. A defect in HR is associated with an increased sensitivity to platinum-based chemotherapies and PARP1 inhibitors in a synthetic lethal manner, though not always resulting in improved patient survival [5,8,10]. Various HRD scores were proposed to identify an HR defect, most of which employ three independent genetic markers for genomic instability [11]. Some research focuses on the formation of RAD51 foci as a critical indicator [12,13]. A further important function of BRCA1 is the stabilization of stalled DNA replication forks [14,15]. The transient stalling or slowing of replication forks is defined as a main feature of RS [16] and was previously observed in BRCA1 mutant cells [17]. An increased level of RS can cause stalled replication forks to collapse, generating DSBs and subsequently causing genomic instability [18]. RS can be counteracted by elevated CHK1 activation, which inhibits the firing of new origins of replication, allowing stalled replication forks to restart [19–22]. This may lead to therapy resistance, which was shown to be able to be overcome by CHK1 inhibition in TNBC [9]. A second pathway to overcome RS is via the Fanconi anemia protein complex, mediated by FANCD2/FANCI. Not only in response to DNA damage, but also to increased RS in the cell, FANCD2 and FANCI are ubiquitinated and start to localize at DNA damage foci regions in the nucleus [23]. Together with BRCA1/BRCA2 and RAD51, open DNA ends are protected from degradation by MRE11 or DNA2 [14,24]. Additionally, FANCD2 can protect stalled replication forks independently of FANCI by regulating the complex function of BLM [25].

The effects of complete or partial *BRCA1* loss and the importance of defined *BRCA1* mutations in regulatory regions of the gene were investigated. *BRCA1* gene gain or increased protein expression of BRCA1 was considered primarily in the context of resistance to therapy. Many mechanisms are not yet fully elucidated. Mutations located outside functional domains of the BRCA1 protein have not yet been characterized.

This study focused on understanding how mutations in *BRCA1* exon 9 and 14 influence the resistance against DNA-damaging sources by using a cell line that carries a gain of the BRCA1 gene *BRCA1* gene. *BRCA1* was modified by CRISPR/Cas9-mediated genome editing and the consequent effects on DNA repair processes were assessed by plasmid reconstruction assays and visualized by DNA repair markers such as RAD51, yH2AX, and RPA by immunofluorescence. The expression and activation of DNA damage-response proteins was measured by Western blot. The effects on replication processes were analyzed by DNA fiber assay, cell cycle distribution by FACS analysis, and cellular survival after MMC, talazoparib, and irradiation by colony formation assay.

2. Results

2.1. BRCA1 Mutations in Exon 9 and 14 Influence DDR Protein Expression and 3D Growth

Approximately 20% of breast cancer tumors show an amplification of the *BRCA1* gene [1]. Increased expression of BRCA1 was associated with inferior patient survival after therapy [3]. The cause of therapy resistance may be due to the requirement of BRCA1 for efficient DSB repair or superior protection of the DNA replication forks [14]. It is unclear whether mutations in the *BRCA1* gene in an amplified setting influence the therapy resistance.

Clones of the MCF7 cell line, in which three copies of the *BRCA1* gene are present [26] (Figure 1A and Figures S1 and S2), were generated by targeting exon 9 and 14 via CRISPR-Cas9. Clones were carrying indels at the target site detected by analysis of PCR products flanking the target sites (Figure 1B). *BRCA1* exon-9.4 clone and exon-14.2 clone showed large visible indels. All other clones differed from the MCF7 wild type (WT) in a different width of the band. Sequencing and fluorescence in situ hybridization (FISH) analysis of the eight *BRCA1* clones showed complete loss of one allele for all clones. Five clones had at least one mutation in the remaining alleles of *BRCA1* in exon 9 and three in exon 14 (Figure 1A and Figure S1B and Table 1). In each of one *BRCA1* exon 9 and 14 clone, all three copies were affected by genetic alteration. Four of the five mutant clones in *BRCA1* exon 9 had the same seven base pair (bp) deletion (c.620del7; p.207fs23stop) leading to a premature stop codon. This was most likely due to microhomology of the target sequence. *BRCA1* exon-9.4 clone showed mutations in both alleles, a 182 bp deletion (c.627del182) leading to a stop at position p.209fs7stop, and an in-frame four amino acid exchange (p.QITP205LLQI).

Table 1. *BRCA1* Mutations introduced in MCF7 cells via CRISPR/Cas9.

Cell Line	Allele 1	Allele 2	Allele 3
MCF7 WT	WT	WT	WT
MCF7 9.1	WT	7 bp deletion (c.620del7 → p.207fs23stop)	loss
MCF7 9.2	WT	7 bp deletion (c.620del7 → p.207fs23stop)	loss
MCF7 9.3	WT	7 bp deletion (c.620del7 → p.207fs23stop)	loss
MCF7 9.4	In frame 4 aa exchange (p.QITP205LLQI)	182 bp deletion (c.627del182 → p.209fs7stop)	loss
MCF7 9.5	WT	7 bp deletion (c.620del7 → p.207fs23stop)	loss
MCF7 14.1	6 bp exchange (p.RW1506GI)	14 bp deletion (c.4516 del14 → p.1506fs9stop)	loss
MCF7 14.2	WT	183 bp insertion (c.4517ins183 → p.1506ins19stop)	loss
MCF7 14.3	WT	7 bp deletion (c.4511del7 → p.1505fs40stop)	loss

List of mutations in the 3 *BRCA1* wild type (WT) alleles in the selected clones at the coding DNA (c.) and protein (p.) levels with associated position that result in complete loss (loss), deletions (del), and insertions (ins) of base pairs (bp) and cause frame shift (fs) or stop.

The *BRCA1* exon 14 clones showed four different *BRCA1* mutations: *BRCA1* exon-14.1 showed mutations in both alleles (allele 1: 6 bp exchange, leading to a change of two amino acids, p.RW1506GI; allele 2: 14 bp deletion, c.4516 del14; p.1506fs9stop), *BRCA1* exon-14.2 a 183 bp insertion (*c.4517ins183*) that led to a stop at p.1506ins19stop, and *BRCA1* exon-14.3 showed a 7 bp deletion at position c.4511del7 that also led to an early stop at p.1505fs40stop. The mutations generated most frequently resulted in truncation of the BRCA1 protein in addition to the complete loss of one allele. The effects of the mutations on BRCA1

protein expression were examined by Western blot analysis (Figure 1C). A significant decrease in BRCA1 protein expression was seen in two clones (*BRCA1* exon-9.3 and −9.5), one clone showed a slight increase (*BRCA1* exon-9.4), and all others showed expression levels comparable to WT (Figure 1C). The lymphoblast cell line HCC1937 isolated from a *BRCA1* germline mutation carrier showing residual BRCA1 expression was used for comparison [27,28].
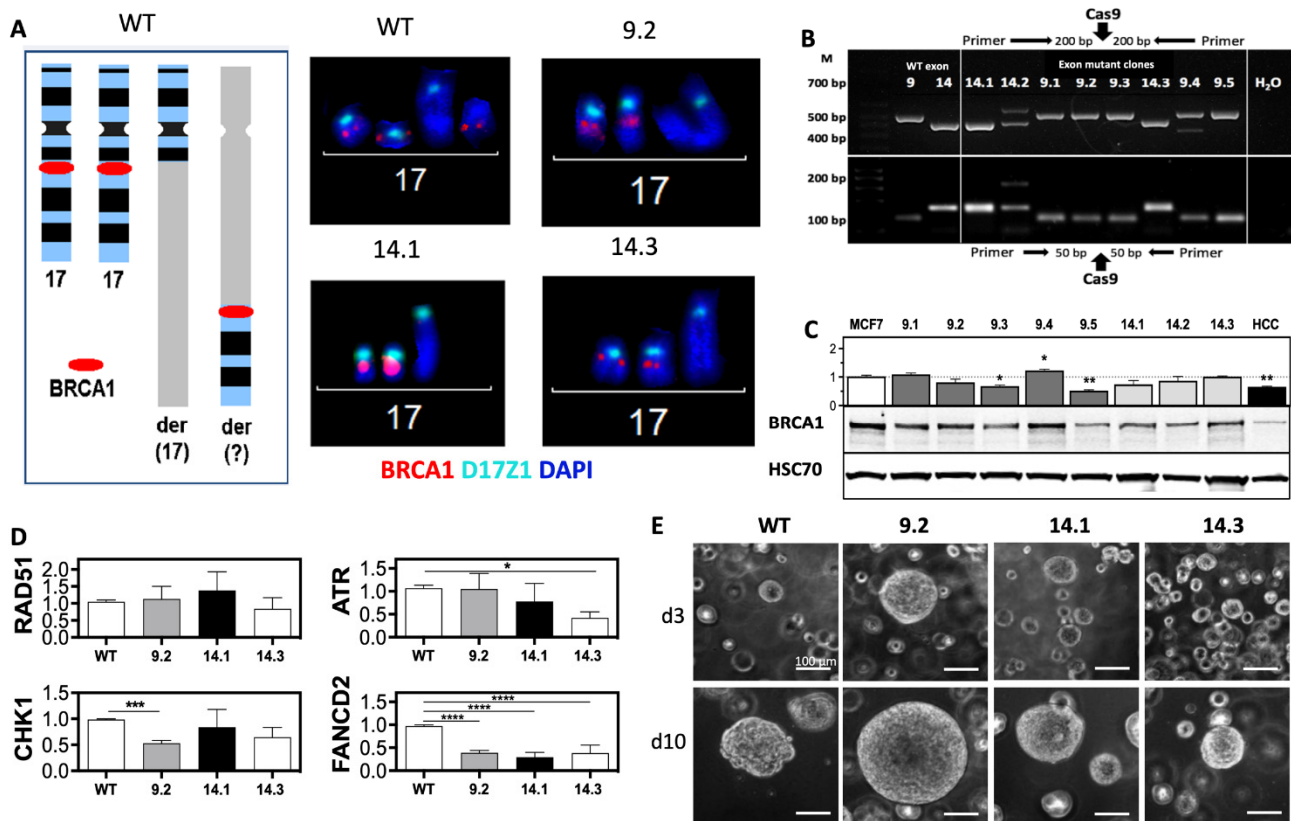

Figure 1. *BRCA1* mutations in exons 9 and 14 alter protein expression and 3D growth. (**A**) FISH analysis of *BRCA1* mutated MCF7 clones shows loss of one of the three BRCA1-alleles. (**B**) PCR screen of CRISPR/Cas9-targeted locus BRCA1 in exon 9 and 14 in MCF7 clones. Fragments with an amplicon size of 494 bp/101 bp (exon 9) and 419 bp/169 bp (exon 14) were selected for detection of large/small indels. PCR products were separated by electrophoresis. (**C,D**) BRCA1, RAD51, FANCD2, CHK1, and ATR expression from total cell extracts of exponentially growing cells were separated and analyzed by Western blot and normalized to MCF7 WT. HCC1937 (HCC) served as negative control and HSP70 and ß-ACTIN as loading controls. (**E**) 3D growth of *BRCA1* clones mutated in exon 9 or 14. Single cells were embedded in BME, and spheroids were photographed three (d3) and ten (d10) days after seeding. Scale bars represent 100 μm (20× magnification). Shown are the mean values of three independent experiments ± SEM. Asterisks (*) indicate significant differences (* $p < 0.05$; ** $p < 0.01$; *** $p < 0.001$; **** $p < 0.0001$ Student's *t*-test).

One clone with an affected allele of exon 9 (*BRCA1* exon-9.2) or exon 14 (*BRCA1* exon-14.3) and one with mutations in both remaining alleles (*BRCA1* exon-14.1) were selected. The different clones were analyzed for the expression of other factors involved in the DNA damage response (DDR) (Figure 1D). There was no change in RAD51 expression and a slight decrease in CHK1 in all *BRCA1* clones, but only reaching marginal significance in *BRCA1* exon-9.2 ($p = 0.051$). ATR expression appears to be associated with changes in *BRCA1* exon 14, as both clones showed a reduction compared with the MCF7 WT, with significance in the *BRCA1* exon-14.3 clone ($p = 0.015$). The most striking change was seen in FANCD2, which was significantly reduced by 62–71% in all *BRCA1* clones compared with the MCF7 WT ($p > 0.0001$) (Figure 1D). The growth behavior of all three clones was

compared to MCF7 WT, showing clearly visible differences under 3D conditions (Figure 1E). *BRCA1* exon-9.2 showed large, densely clustered, and sharply demarcated spheroids, *BRCA1* exon-14.1 medium, also densely clustered, and *BRCA1* exon-14.3 comparable in size to the MCF7 WT, but with slightly sharper demarcation.

2.2. Significant Reduction of HR Capacity Does Not Result in Increased MMC and PARP1i Sensitivity

The effects of the introduced *BRCA1* mutations on the molecular processes that BRCA1 is involved in were examined. BRCA1 is an important factor of HR; the capacity for DSB repair via HR was analyzed. Linearized DNA repair construct plasmid (pDR-GFP) was transfected into cells and repair capacity was detected by flow cytometry (Figure 2A,B). As expected, all *BRCA1* mutated clones showed significantly reduced HR capacity, with a relative reduction of 60% in the *BRCA1* exon-9.2 and -14.1 clones. A reduction of up to 75% in the *BRCA1* exon-14.3 clone was measured compared with the MCF7 WT. Because HR is a cell cycle-dependent process, alterations of the cell cycle profiles of the clones were analyzed (Figure 2C,D). Only minor differences were observed, with an slight increase in G1 and G2/M phase cells in the two *BRCA1* exon 14 clones while the exon 9 clone showed a cell cycle distribution comparable to the MCF7 WT (Figure 2D).
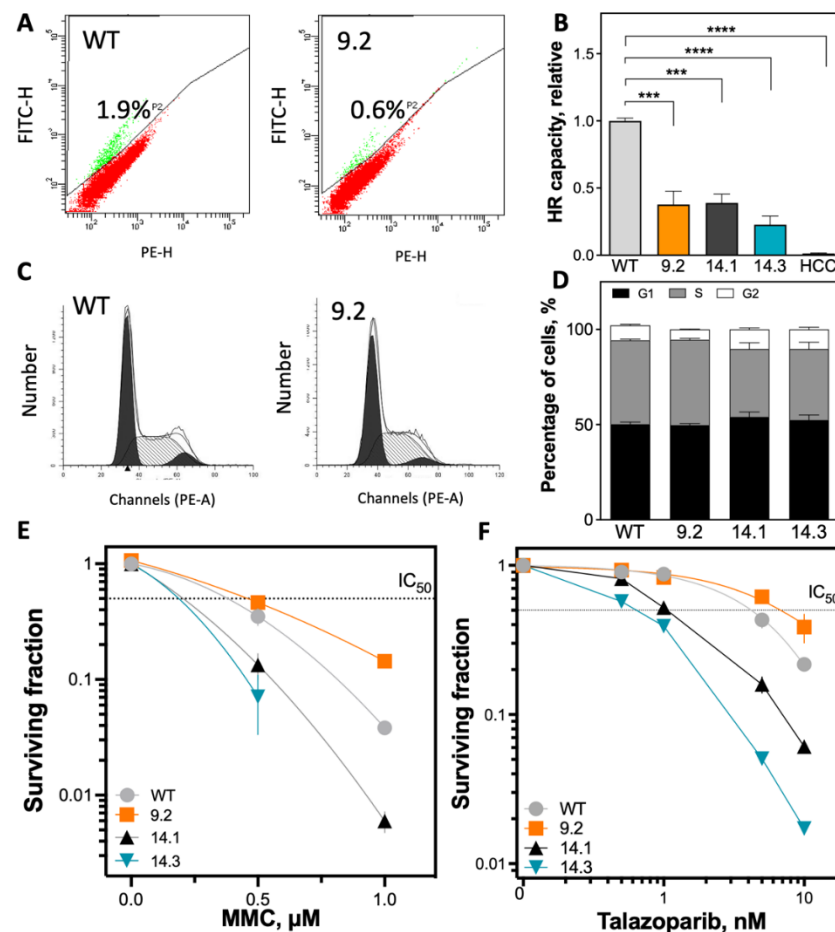
Figure 2. Significant reduction in HR capacity is not reflected by decreased survival after MMC treatment and PARP1 inhibition. (**A**,**B**) *BRCA1* mutant MCF7 clones showed significantly reduced HR capacity in the plasmid reconstruction assay. Cells were transiently transfected with the pDR-GFP plasmid and HR-competent cells (GFP-positive) were detected by flow cytometry. The determined HR capacities were normalized to the MCF7 WT cell line. The *BRCA1*-deficient cell line HCC1937 served as negative control. (**C**,**D**) No differences were detected in cell cycle profiles among *BRCA1*-mutant

clones. Cells were stained with propidium iodide and then subjected to flow cytometry analysis. (**E,F**) Differences in cellular survival after treatment with MMC or PARP1 inhibition. Cells were seeded 12 h before treatment, treated for 1 h with MMC or 24 h with talazoparib, fixed after 14 days, and the number of colonies with >50 cells was determined. Shown are the mean values of three independent experiments $\pm$ SEM. Asterisks (*) indicate significant differences; (*** $p < 0.001$; **** $p < 0.0001$, ns = not significant Student's *t*-test).

Surprisingly, the sensitivity to mitomycin C (MMC) treatment and PARP1 inhibition (PARP1i) by talazoparib was not enhanced in all *BRCA1*-mutant clones, despite the reduction in HR capacity (Figure 2E,F and Figure S3). Only the two *BRCA1* exon-14 clones showed significantly increased sensitivity to MMC treatment (IC$_{50}$: 0.21 μg/mL and 0.19 μg/mL) compared with MCF7 WT (IC$_{50}$: 0.38 μg/mL) (Figure 2E). However, the *BRCA1* exon-9.2 mutant clone showed a significant increase in MMC resistance (IC$_{50}$: 0.46 μg/mL). The MMC-sensitive *BRCA1* clones with exon 14 mutations were also sensitive to PARP1i with an IC$_{50}$ of 1.3 nM (14.1) and 0.69 nM (14.3), whereas the *BRCA1* exon-9.2 clone was resistant (IC$_{50}$: 6.8 nM) compared with MCF7 WT with an IC$_{50}$ of 4.2 nM (Figure 2F).

2.3. Efficient DSB Repair and Rapid DNA Replication Fork Restart Contributes to Therapy Resistance

RAD51 foci formation is a well-established marker to test functionality of HR [12]. Mutations in *BRCA1* are known to impair HR and thereby decrease RAD51 foci formation [29,30]. Therefore, the formation of RAD51 foci in the *BRCA1* mutant clones was examined and quantified (Figure 3A,B). All *BRCA1* clones showed formation of RAD51 foci 6 h after MMC treatment. However, the two (exon 14 clones) MMC-sensitive *BRCA1* showed an approximately 50% lower increase in RAD51 foci compared with MCF7 WT, with respective mean values of 11.5 $\pm$ 1.5 ($p = 0.0093$) and 10.1 $\pm$ 1.1 ($p = 0.0026$) compared with 18.9 $\pm$ 1.7 RAD51 foci per cell. Conversely, the resistant *BRCA1* exon-9.2 clone showed the strongest increase in RAD51 foci with a mean of 22.0 $\pm$ 1.1 foci per cell (ns. compared with MCF7 WT). Comparison of RAD51 foci 24 h after MMC showed that both *BRCA1* exon 14 clones also had a reduced ability to resolve the RAD51 foci formed during the observation period, with 10.1 $\pm$ 0.9 and 8.4 $\pm$ 0.6, respectively. In contrast, resolution of RAD51 foci was most efficient in the *BRCA1* exon-9.2 clone 24 h after MMC treatment, with a significant decrease in RAD51 foci, approximately to the level of MCF7 WT.

Initiation of HR requires a homology search and pairing of ssDNA, generated by DNA end resection, with the homologous DNA region of the intact strand. Protection of the resected ssDNA is achieved by accumulation of RPA which, as a multifunctional protein, regulates not only ssDNA but also the activity of repair factors [31]. The effect of *BRCA1* mutations in different exons on RPA foci formation 4 h after MMC treatment was determined (Figure 3C and Figure S4). All cell lines showed functionality in the formation of RPA foci. The resistant *BRCA1* exon-9.2 clone showed the highest number of RPA foci per cell with 20.4 $\pm$ 1.6 at 4 h, whereas the *BRCA1* exon-14.1 clone after MMC treatment showed the lowest number of RPA foci per cell at 12.3 $\pm$ 1.8. In contrast, the *BRCA1* exon-14.3 clone showed a value of 13.1 $\pm$ 1.4, comparable to the MCF7 WT, with 14.4 $\pm$ 1.7, 24 h after treatment. The strongest decrease in RPA foci was observed in the *BRCA1* exon-9.2 clone, while only a slight decrease occurred in the *BRCA1* exon-14.3 clone; the *BRCA1* clone-14.1 showed almost no change in RPA foci and the MCF7 WT showed an increase to 17.5 $\pm$ 1.1 RPA foci per cell. Thus, the behavior of RAD51 foci formation in the cell lines studied was confirmed. Whether the significant differences in the resolution of RAD51 and RPA foci of DNA crosslinks induced by MMC were also reflected by differences in the formation of DSBs was examined. The number of γH2AX foci 6 and 24 h after treatment with MMC was detected and evaluated (Figures 3D and S4). Clear differences between the examined cell lines were observed. The strongest increase in the number of DSB could be observed 6 h after MMC in the resistant *BRCA1* exon-9.2 clone, with 21.1 $\pm$ 1.7 compared to the MCF7 WT with 13.6 $\pm$ 1.4. The two sensitive *BRCA1* exon-14 clones showed an increase in DSBs compared to the MCF7 WT, with 11.6 $\pm$ 0.8 and 15.7 $\pm$ 1.3 γH2AX foci

per cell after 6 h MMC, respectively. The resistant *BRCA1* exon-9.2 clone showed the most pronounced reduction of DSBs 24 h after treatment, with about 50% compared with only 10% in the MCF7 WT, consistent with the survival (Figure 2E) at corresponding MMC concentration. The *BRCA1* exon-14.3 clone also showed a slight reduction in DSBs, whereas the *BRCA1* exon-14.1 showed no repair of DSBs 24 h after treatment.
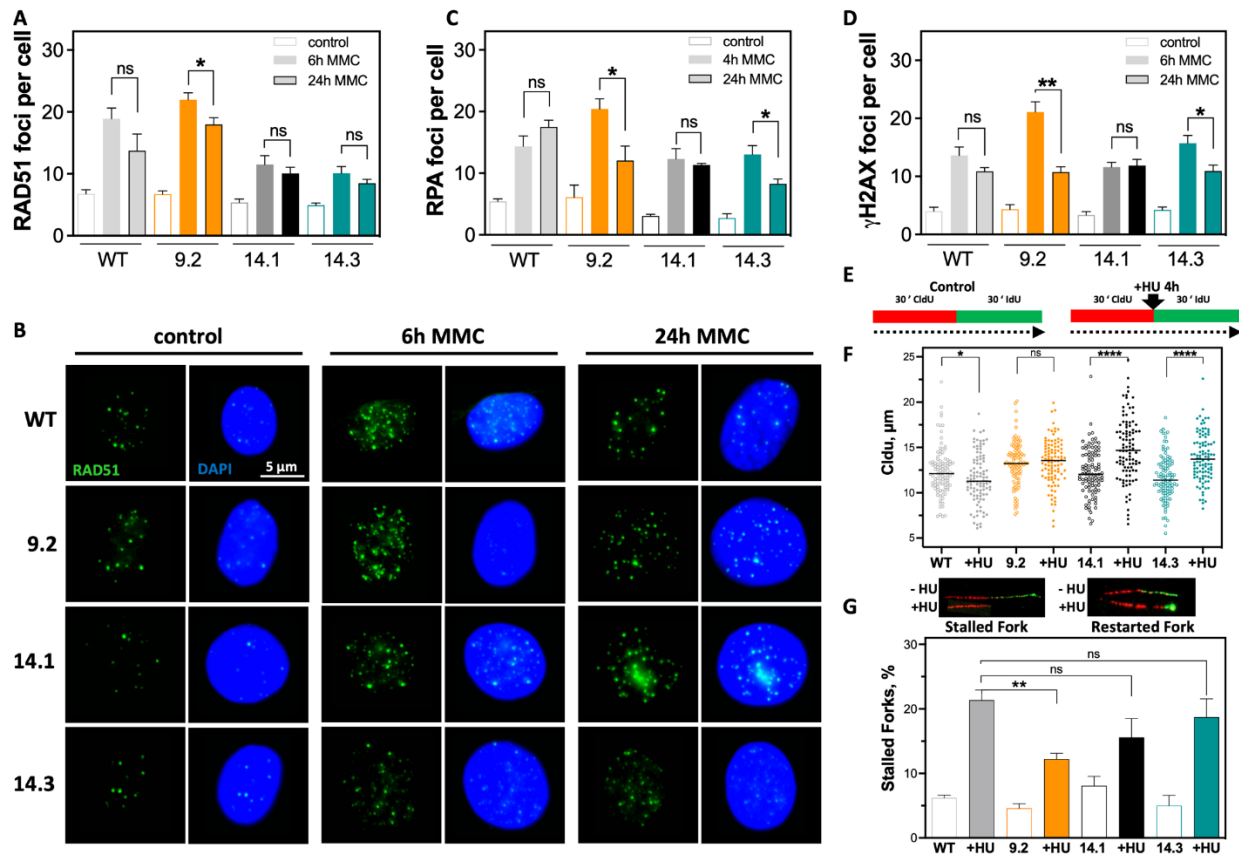

Figure 3. Resistance indicates more efficient DSB repair and avoidance of replication-associated DNA damage. (**A–D**) Formation of DNA repair foci after MMC treatment. (**A,B**) RAD51 foci (green) 6 h and 24 h after treatment with 0.5 μg/mL MMC for 1 h, (**C**) quantification of RPA foci 4 h and 24 h after MMC, and (**D**) γH2AX foci 6 h and 24 h after using the same protocol. Nuclei were counterstained with DAPI. γH2AX foci were quantified manually; RAD51 and RPA foci were quantified using the Aklides® NUK system (MediPan). Scale bar represents 5 μm (40× magnification). At least 100 cells were analyzed in each biological replicate. (**E–G**) DNA fiber assay after treatment with HU for 4 h, in MCF7 WT and *BRCA1* mutated clones. (**E**) Treatment scheme shows sequential labeling with CldU and IdU for 30 min each and addition of HU for 4 h between CldU and IdU. Incorporated nucleotides were detected by immunofluorescence. The length of the DNA fibers was measured with the ImageJ 1.52n software. (**F**) DNA fiber length of DNA strands already synthesized before HU administration and (**G**) number of replication forks halted within the next 30 min after HU removal. Shown are the mean values of three independent experiments ± SEM. Asterisks (*) indicate significant differences (* $p < 0.05$; ** $p < 0.01$, **** $p < 0.0001$; ns = not significant Student's *t*-test).

This suggests that in the resistant *BRCA1* exon-9.2 clone, induction of DNA cross-links led to increased DSBs, which, nevertheless, can be repaired most efficiently. Since the resolution of DSBs 24 h after MMC treatment reached a roughly comparable level in all cell lines, differences in DSB repair alone do not seem to reflect sensitivity to MMC. This could be due to differences in BRCA1-dependent stabilization of active DNA replication forks, which prevents nucleolytic degradation of newly synthesized DNA [14,24]. To test this hypothesis, the stability of replication forks after treatment with Hydroxy urea (HU) was examined by a DNA fiber assay (Figure 3E,F). A significant degradation of newly

synthesized DNA after HU treatment was observed in MCF7 WT, with 11.6 ± 0.3 μm compared with the untreated control with 12.4 ± 0.4 μm ($p = 0.045$). In contrast, neither the *BRCA1* exon-9.2 nor the two *BRCA1* exon 14 clones showed degradation of previously synthesized DNA. The *BRCA1* exon-9.2 showed no significant effect of HU treatment. The two *BRCA1* exon-14 clones even showed a significant increase in DNA fiber length compared with untreated controls, with 14.9 ± 0.4 vs. 12.3 ± 0.3 μm and 13.9 ± 0.3 vs. 11.7 ± 0.3 μm. It is possible that an increased dNTP level is present in the exon 14 clones. Analysis of replication fork restart after removal of HU represents another feature of functional HR [22]. It was observed that the resistant *BRCA1* exon-9.2 clone had the least difficulty in replication fork restart, visible by the lowest proportion of stalled replication forks, with only 12%, while the two *BRCA1* exon 14 clones showed significantly higher proportions of 15% and 18%, and the MCF7 WT the highest level of about 22% (Figure 3G).

2.4. Resistance to Irradiation Emerges from Low Level of DNA Replication Stress

As MMC treatment and PARP1i are mainly causing DNA damage during the S phase; the response to irradiation (IR), inducing various types of DNA damage in all cell cycle phases was analyzed. Cells were irradiated, and cellular survival was determined (Figure 4A). The *BRCA1* exon-9.2 clone was found to be resistant to IR. The *BRCA1* exon-14.3 clone showed significantly increased radiosensitivity, consistent with its sensitivity against MMC treatment and PARPi. The survival of the *BRCA1* exon-14.1 clone after IR was comparable to the MCF7 WT in 2D (Figure 4A). The same distribution of radiosensitivity of the *BRCA1* clones was observed under 3D culture conditions (Figure 4B). However, all cell lines showed lower radiosensitivity in 3D, with significantly smaller differences between cell lines (Figure 4B).

It was tested whether the differences in radiosensitivity affected DNA replication processes. Cells were irradiated with 6 Gy and examined by the DNA fiber assay (Figure 4B,C). Strikingly, the resistant *BRCA1* exon-9.2 clone replicated significantly faster than the MCF7 WT, with a length of 10.1 ± 0.25 μm vs. only 8.7 ± 0.23 μm (Figure 4B and Figure S5C). The *BRCA1* exon-14.1 clone also replicated slightly faster than the MCF7 WT with 9.3 ± 0.24 μm. Only the *BRCA1* exon-14.3 clone showed a slowing of replication to 8.4 ± 0.21 μm, already in the untreated situation. Thus, there appears to be endogenously less RS in the resistant *BRCA1* exon-9.2 clone. IR resulted in minimal shortening to 8.1 ± 0.22 μm in the resistant *BRCA1* exon-9.2 clone (Figure 4C). In the clones with mutant exon 14, IdU length was reduced to 6.9 ± 0.24 μm (14.1) and 6.3 ± 0.21 μm (14.3), and the MCF7 WT showed the greatest reduction to 4.9 ± 0.14 μm. This suggests that the resistant *BRCA1* exon-9.2 clone is capable of handling RS induced by IR most effectively. Confirming this, a faster restart of DNA replication, represented by a high value for the IdU/CldU (I/C) ratio, was observed in the resistant *BRCA1* exon-9.2 clone with a value of 0.63 ± 0.02 (Figure 4D). The *BRCA1* exon-14.1 clone showed an I/C ratio of 0.55 ± 0.02, comparable to MCF7 WT with 0.53 ± 0.01, whereas the sensitive *BRCA1* exon-14.3 clone showed the lowest value of 0.48 ± 0.01.

The cellular mechanism triggering these differences could be the activation of the S phase-specific DDR mediated by ATR and CHK1 (Figure 4E,F). No significant differences were seen in the activation of ATR (Figure 4E), with only MCF7 WT showing an increase in phosphorylation of ATR 6 h after IR, whereas the *BRCA1* clones showed no difference compared to the untreated situation. In contrast, activation of CHK1 showed marked differences (n.s.), with the strongest activation in *BRCA1* exon-9.2 clone, slightly lower activation in the two *BRCA1* exon-14 clones, and the lowest activation in MCF7 WT cells (Figure 4F). FANCD2 expression was examined after IR (Figure 4G) to further analyze a replication conflict due to decreased activation of FANCD2 by monoubiquitination, as described for *BRCA1*-deficient cells [32]. It was apparent that the *BRCA1* exon-14.3 and MCF7 WT showed significantly greater activation after IR compared with the *BRCA1* exon-14.1 and the *BRCA1* exon-9.2 clones. No change in the PARP1 expression was observed after irradiation (Supplementary Figure S7). Activation of the ATR kinase is mediated by RPA-coated single-stranded DNA (ssDNA) [33]. The effect of inhibition of ATR on RPA

foci formation after irradiation was investigated (Figure 4H). The most significant increase in RPA foci in the resistant *BRCA1* exon-9.2 clone ($p = 0.0066$) compared with the other cell lines was observed. Thus, the data presented here indicate that both sensitivity and resistance can be caused by mutations in *BRCA1* and, in sum, are attributable to differences in the management of replication conflicts.
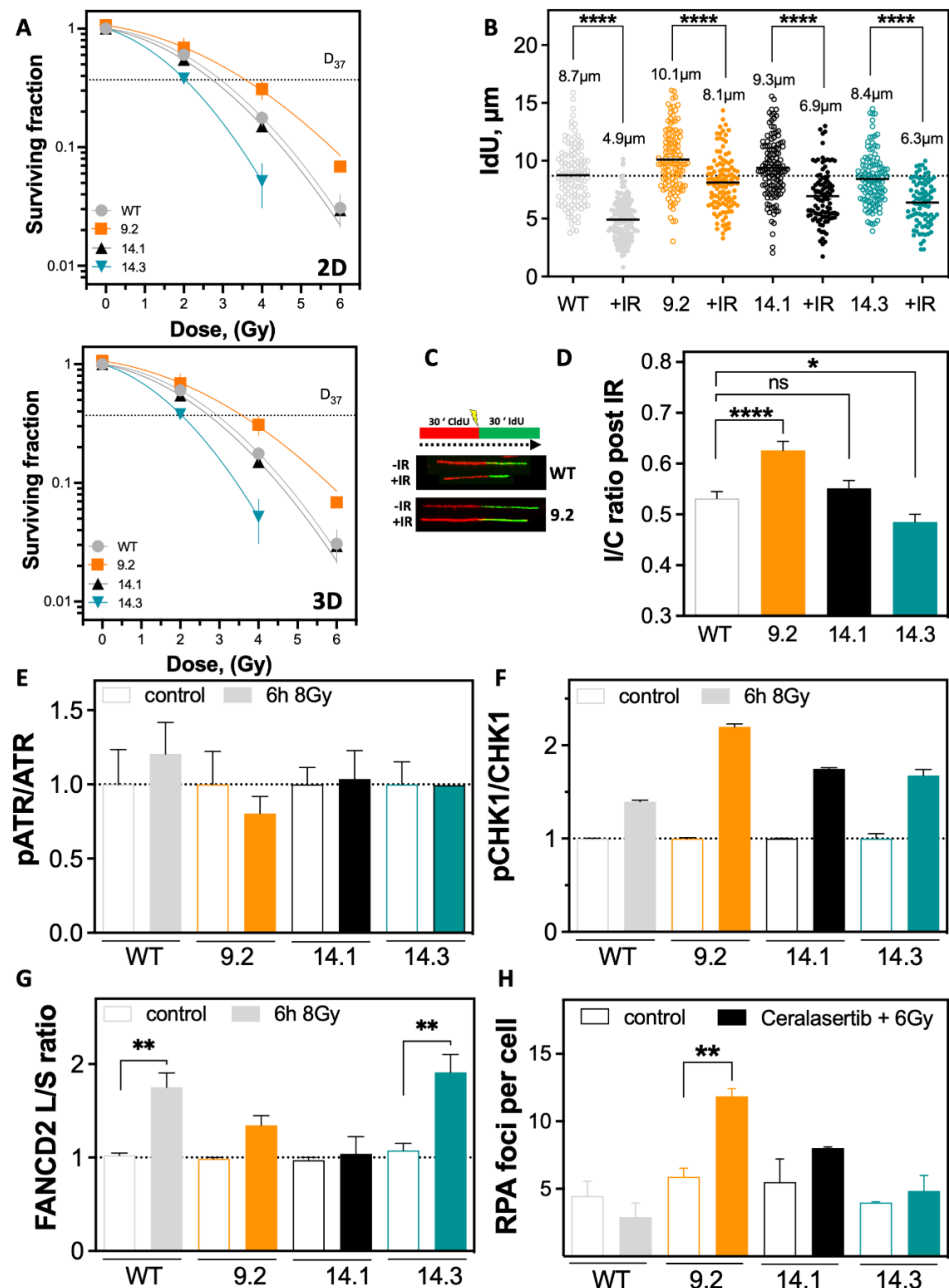

Figure 4. Less DNA replication stress is associated with resistance to irradiation. (**A,B**) Differences in cellular survival after irradiation in 2D and 3D cultures. Cells were seeded 12 h before IR, fixed after 14 days, and the number of colonies with >50 cells was determined. (**B–D**) DNA fiber assay after irradiation with 6 Gy, in MCF7 WT and *BRCA1* mutated clones. (**B**) Treatment scheme shows sequential labeling with CldU and IdU for 30 min each and IR between both labels. Incorporated nucleotides were detected by immunofluorescence. The length of the DNA fibers was measured with the Image J 1.52n software. (**C**) DNA fiber length of DNA strands after IR (IdU) and (**D**) the ratio of DNA fiber length pre to post irradiation (I/C ratio) was calculated. (**E–G**) Activation of ATR, CHK1,

and FANCD2 6 h after IR were detected in total cell extracts of exponentially growing cells, analyzed by Western blot and calculated as the ratio of pATR to ATR, pCHK1 to CHK1 or FANCD2L/FAND2S. (**H**) RPA foci after IR and treatment with the ATR inhibitor Ceralasertib were quantified using the Aklides® NUK system (MediPan) at a magnification of $40\times$. At least 100 cells were analyzed in each biological replicate. Shown are the mean values of three independent experiments $\pm$ SEM. Asterisks (*) indicate significant differences; (* $p < 0.05$; ** $p < 0.01$; **** $p < 0.0001$, ns = not significant Student's *t*-test).

3. Discussion

This study showed that a combination of efficient DNA repair and avoidance of RS results in resistance to different DNA-damaging sources in a *BRCA1* mutated clones of the MCF7 cell line, which carries a *BRCA1* gene amplification, confirming data shown by ref. [26]. The amplification of DDR genes such as *BRCA1* and the possible resulting elevated protein expression, present in about 20% of breast cancer tumors, were associated with therapy resistance [1]. BRCA1 has important functions in HR and DNA replication fork protection [24,34]. Though many studies investigate how *BRCA1* gene amplification or mutations contribute to therapy resistance, many questions remain unanswered. Mutations in *BRCA1* exon 9 and 14, in a *BRCA1* gene-amplified setting, are not yet well characterized, as most investigations focus on the functional domains exclusively.

All *BRCA1* mutated clones analyzed in our study had impaired HR capacity, but RAD51 foci formation was only reduced in clones mutated in exon 14 (Figures 1 and 2). The interaction of BRCA1 with PALB2 promotes RAD51 loading [35], which seems to be impaired in *BRCA1* exon 14 mutated clones. This might be due to the location of the introduced mutation which is behind the coiled-coil (CC) domain, interacting with PALB2 [36] and the S/T-Q cluster domain (SCD), which harbors the ATR/ATM phosphorylation sites [37]. However, the *BRCA1* exon-9.2 mutated clone can efficiently form RAD51 foci, despite a reduced HR capacity. This mutation is located in between the RING domain, required for BARD1-BRCA1 heterodimerization to perform the E3 ubiquitin ligase activity [38] and the nuclear localization signal (NLS). It was previously shown that mutations in the *BRCA1* gene can generate truncated versions of the BRCA1 protein influencing the resistance to different DNA-damaging agents [39–42]. It is possible that a truncated protein variant in the *BRCA1* exon 14 mutated clones may contribute to the observed reduced formation of RAD51 foci, as the NLS would still be present on a truncated protein version, but the function of the CC-domain might be affected. This would not be the case for the resistant *BRCA1* exon-9.2 clone. It is well-established that BRCA1 signaling at DSB sites is not restricted to promotion of HR via PALB2–BRCA2–Rad51. The BRCA1-A complex formed on the scaffold protein ABRAXAS1 at the damage site is important for pathway choice for the repair of DSBs [43]. Subsequently, it is the recruitment of CtIP to form the BRCA1-C complex that promotes end resection and HR. Alternatively, recruitment of the helicase BRIP1 (a.k.a. BACH1, FANCJ) is required to form the BRCA1-B complex that is involved in DNA damage response in S phase [44]. The interactions of BRCA1 with ABRAXAS1, BRIP1, and CtIP are all mediated by the BRCA1 carboxyterminal (BRCT) domain binding a phosphorylated by S phase cyclin-dependent kinases. Truncations in exon 14 would thus prevent formation of any of the BRCA1-A, -B, and -C complexes.

HR capacity was determined by a transient transfection of the DR-GFP plasmid since it was shown that a transient or stable transfection does not influence the outcome of the observed HR capacity [45]. It is likely, though, as the introduction of a single or very few DSBs is not sufficient to activate a global DNA damage response [46]. Therefore, analyzing RAD51 foci formation as a readout for the functionality of HR was conducted. The ability of the *BRCA1* exon-9.2 clone to efficiently form RAD51 foci contributes to the observed resistances to PARP1i and MMC treatment as both agents induce DSBs that are repaired by HR [47]. Thus, no complete defect of HR was observed in any of the *BRCA1* mutated clones, though the exon 9.2 mutated clone seemed to be more proficient in HR than the exon 14 mutated clones.

Mechanisms contributing to resistance to PARPi in *BRCA1* mutated cells are (I) increase in drug efflux, (II) restoration of HR, (III) decreased PARP1 trapping, and (IV) stabilization of stalled DNA replication forks [9,48]. All *BRCA1* mutated clones still show residual HR activity, most strongly in the MMC- and PAPR1i-resistant *BRCA1* exon-9.2 clone, contributing to the observed resistance. However, the rather small differences in HR performance strongly suggest that a second mechanism partly responsible for the observed resistance is involved. It is unlikely that a decrease of PARP1 trapping occurred since the resistance was also visible after MMC treatment. Therefore, the most obvious mechanism responsible for resistance seems to be the stabilization of the DNA fork [49], since BRCA1 is also known to play a role in this process. The resistant *BRCA1* exon-9.2 clone indeed showed the most efficient DNA replication fork restart after HU treatment and no degradation of newly synthesized DNA, which suggests that this clone has the most stable replication forks compared with the *BRCA1* exon 14 mutated clones and the MCF7 WT (Figure 3).

DNA damage induced by MMC treatment and PARP1i occurs predominantly in the S phase of the cell cycle, disrupting the DNA synthesis and leading to DSBs, which are then repaired by HR [50]. Ionizing radiation (IR) was used to test the DNA-damaging source, inducing several DNA damages. IR causes the same results as after MMC treatment and PARP1i. The *BRCA1* exon-9.2 clone was radioresistant, while the *BRCA1* exon-14.3 clone was radiosensitive and the *BRCA1* exon-14.1 clone showed comparable survival to the MCF7 WT (Figure 4). Since the previous results indicated a lower RS in the resistant exon-9.2 clone, the data after IR confirmed these observations. The *BRCA1* exon-9.2 clone showed the highest replication speed, while the 14.3 clone showed the lowest. Since the main feature of replication stress is defined as transient slowing or stalling of DNA replication forks [16], this strongly indicates that the resistant 9.2 clone exhibits the least RS in the untreated state, while the sensitive 14.3 clone exhibits the highest. The same could be observed after IR, as again the *BRCA1* exon-9.2 showed the lowest RS, and the exon-14.3 clone the highest. A high level of RS leads to genomic instability [51] and ultimately increased cell death, which correlates with the survival outcome determined in the colony formation assay.

The differences in RS were not manifested by differences in the ATR activation after IR, whereas significant differences in the CHK1 phosphorylation were observed, indicating the described ATR-independent activation of CHK1 in the *BRCA1* mutated clones (Figure 4) [52]. CHK1 can counteract RS by inhibiting firing of dormant origins to allow the cell to restart of the stalled forks instead of opening dormant origins [20–22,53]. Since the highest activation of CHK1 is observed in the resistant *BRCA1* exon-9.2 clone, this further supports the observation that it has the lowest level of RS. CHK1 phosphorylation is not as high in the *BRCA1* exon 14 mutated clones, not rescuing the already high RS. Supporting this, the strongest accumulation of RPA after inhibition of ATR was seen in the resistant BRCA1-9.2 clone after irradiation (Figure 4).

Overexpression of remaining DDR genes was shown to compensate the loss of some DDR genes such as *BRCA1* [45,54]. However, this seems not to be the case in the present *BRCA1* mutated clones. In the untreated state no elevated expression of RAD51, ATR, or CHK1 could be observed. FANCD2 was even significantly downregulated in all *BRCA1* mutated clones, which is surprising since it has been shown that depletion of *BRCA1* together with *FANCD2* is synthetically lethal [32]. Upon DNA damage induction, FANCD2/FANCI are increasingly ubiquitinated and co-localize with DNA damage foci in the nucleus [55,56], which also happens in response to RS [57]. They protect stalled replication forks together with BRCA1/BRCA2/RAD51 from MRE11 or DNA2 degradation [14,24]. FANCD2 can, however, also act independently of FANCI. It was shown, that FANCD2 can regulate BLM functions to promote the recovery of stalled replication forks [25]. All *BRCA1* mutated clones showed functional FANCD2 ubiquitination after IR, except for the *BRCA1* exon-14.1 clone. This was quite unexpected, as it has a medium level of RS, comparable to the MCF WT, but basically no increase in FANCD2 ubiquitination. The failure of activating FANCD2 in this clone must be further investigated. In the sensitive *BRCA1* exon-14.3 clone, the L/S ratio of FANCD2 (Large/Small FANCD2) was the highest, strongly suggesting that this

clone tries to compensate for the high level of RS by high ubiquitination of FANCD2. In the resistant *BRCA1* exon-9.2 clone, a lower L/S ratio was observed, which was expected as this clone has low RS.

In summary, this study showed that *BRCA1* indels in exons 9 and 14 can result in increased therapy resistance or sensitivity. In addition, it seems that a dominant negative effect of the truncating exon 14 mutations is present. All results taken together strongly indicate that a combination of efficient DNA repair and avoidance or rather enhanced counteraction against RS by increased CHK1 activation is responsible for the observed therapy resistance. The analysis of how to overcome this resistance might enable new strategies for treatment of tumors with similar features.

4. Materials and Methods

4.1. Cell Lines, Culture and Treatment

The MCF7 and HCC1937 cell lines were purchased from the American Type Culture Collection (ATCC, Manassas, VA, USA). All cell lines were cultivated in DMEM medium with 10% FCS and 1% penicillin streptomycin in incubators at 37 °C, 5% CO_2 atmosphere, and 100% humidity in cell culture flasks. For the 3D growth 10,000 cells were seeded in 25 µL drops of Basement Membrane Extract (Cultrex®, growth factor reduced) in 24-well plates, covered with 750 µL culture medium. For mitomycin C (MMC; medac GmbH) treatment concentrations ranging from 1.5 µM to 3.0 µM were used for a maximum of 1 h incubation time. Talazoparib (Selleckchem #S7048) treatment was carried out for 24 h with concentrations of 1 to 10 nM. Ceralasertib (Biozol, Eching, Germany) treatment was carried out for 4 h before and 24 h after irradiation at a concentration of 1 µM.

4.2. CRISPR/Cas9-Mediated Modifications of BRCA1

The CRISPR/Cas9 system was used for genome editing of the *BRCA1* gene essentially as described [58]. Two different exons (9 and 14) were targeted with one single-guide RNA (sgRNA) each, designed with the help of crispr.mit.edu (Table 2). An additional guide targeting intron 1 was found to be inefficient and was not followed up further.

Table 2. Oligonucleotides used for expression of sgRNA sequences targeting BRCA1. Target sequence is underlined.

Exon	Direction	Sequence (5′ to 3′)
9	forward	CACCG<u>TTGTTACAAATCACCCCTCA</u>
	reverse	AAAC<u>TGAGGGGTGATTTGTAACAA</u>C
14	forward	CACCG<u>CCCATCATTAGATGATAGG</u>
	reverse	AAAC<u>CCTATCATCTAATGATGGG</u>C

The oligonucleotides were hybridized and ligated into vector PX458 (Addgene #48138, kindly provided by I. Vetterlein), digested with *Bbs*I, and amplified in *E.coli* (DH5α). The correct insert with the sgRNAs was confirmed by Sanger sequencing. The sgRNA-expressing plasmids were transiently transfected into MCF7 cells using electroporation. Successfully transfected cells (GFP-positive) were sorted after 48 h via flow cytometry as single cells and expanded in 96-well plates.

4.3. PCR Screening

Genomic DNA was isolated using DNeasy Blood & Tissue (Qiagen, Hilden, Germany) and DNA concentrations were measured using a NanoDrop™ One/OneC Microvolume UV-Vis Spectrophotometer (ThermoFisher Scientific, Waltham, MA, USA). Primers were designed to anneal around the Cas9 cutting site within the *BRCA1* gene. To detect small indel variations, a short sequence around the Cas9 cutting site was amplified, while to detect larger variations a longer fragment was amplified (Table 3)

Table 3. Primer sequences used to amplify the CRISPR/Cas9 targeted regions of the *BRCA1* gene.

Exon	Length and Direction	Tm (°C)	Sequence (5′ to 3′)	Amplicon Size (bp)
9	short forward	58.9	TTCCCTATAGTGTGGGAGATCA	101
	short reverse	54.7	CAAACTTTGCCATTACCCTTTT	
	long forward	55.3	CCACACCCAGCTACTGACCT	494
	long reverse	55.3	CTCTTCCAGCTGTTGCTCCT	
14	short forward	55.9	CGATGGTTTTCTCCTTCCATT	169
	short reverse	55.3	TTGCTCCTCCACATCAACAA	
	long forward	61.4	CCACACCCAGCTACTGACCT	419
	long reverse	59.4	CTCTTCCAGCTGTTGCTCCT	

For PCR, GoTaq® Flexi Polymerase (Promega, Walldorf, Germany) with the Green GoTaq® Flexi Reaction Buffer supplemented with 5 mM MgCl$_2$, 200 µM dNTPs, 100 pmol/µL forward and reverse primer, and 100 ng genomic DNA as template was used. PCR was performed using a Primus 25 advanced® Thermocycler with the following conditions: Initial denaturation (95 °C for 2 min) followed by 35 cycles of denaturation (95 °C for 30 s), annealing (54 °C for 30 s) and extension (72 °C for 50 s), ending with a final extension (72 °C for 10 min). Fragments were then loaded on to a 2% agarose gel, run for 30 min at 120 V, and stained with ethidium bromide, or analyzed by BioAnalyzer 2100 Expert (B.02.08.SI648) using DNA 7500 chips (Agilent Technologies, Santa Clara, CA, USA).

4.4. Amplicon Sequencing and Clone Characterization

Sequencing of amplicons was performed using Illumina's next-generation sequencing methodology [59]. Amplicons per clone (Table 3) were pooled, while each pool contained long and short fragments of exon under consideration plus additional fragments for (either) *POLD* (Primers: 5′-CCTGTGCAATTAGGCTTGAG and 5′- CTTCAGGCCGAC-CTTGAATG; amplicon size 500 bp) or *POLE* (Primers: 5′-GGTGTTCAGGGAGGCCTAAT and 5′-TACTTCCCAGAAGCCACCTG; amplicon size 195 bp) serving as controls. Amplicons were quality checked and quantified using the 2100 Bioanalyzer instrument in combination with a high-sensitivity DNA kit (both Agilent Technologies). Prior to library preparation, amplicons per clone were pooled as described above. Libraries were prepared from 50 ng of pooled amplicons (per clone) using NEBNext Ultra II Directional RNA Library Preparation Kit in combination with NEBNext Multiplex Oligos for Illumina Set 1 (96 Unique Dual Index Primer Pairs) following the manufacturer's instructions in general (New England Biolabs, Frankfurt am Main, Germany). Deviating from the protocol, the amplicons were not fragmented but inserted directly into the library preparation. Quantification and quality checking of libraries was conducted using a 2100 Bioanalyzer instrument and DNA 7500 kit (Agilent Technologies). Libraries were pooled and sequenced on a MiSeq (Illumina, San Diego, CA, USA). System runs in 301 cycle/paired-end mode using SBS 600 cycles v3 sequencing reagents. Sequence information was converted to FASTQ format using bcl2fastq v2.20.0.422.

Both adapter clipping and quality trimming were applied to the raw reads using Cutadapt 2.8 [60] (parameters: -q 15 -m 1 -a AGATCGGAAGAGCACACGTCTGAACTCCAGTCA -A AGATCGGAAGAGCGTCGTGTAGGGAAAGAGTGT). The resulting paired-end reads were merged with the tool fastq_mergepairs from USEARCH v8.0.1517 [61]. Amplicon sequences were identified in the merged reads based on their primer sequences with the Python script identifyAmplicons.py (parameter: –primers primers.fa) (https: //github.com/PhKoch/amplicon/releases/tag/0.3, accessed on 28 September 2022). For each clone, the abundance of the amplicons was determined to characterize its type of mutation. To this end, sequences of amplicons with high abundance were aligned to the genomic *BRCA1* sequence. Only two different amplicons with comparable abundance were identified in all clones analyzed (Table 1 and Supplemental Figure S1); despite the expected

presence of three genomic copies of *BRCA1* in MCF7, the clones were further characterized by FISH.

4.5. FISH Analysis

FISH was used according to standard procedures and previously described [62]. Two commercially available probes were combined with a homemade one: a BRCA1-specific probe (Abnova, Heidelberg, Germany; SpectrumOrange), a centromere-specific one for chromosome 17 (D17Z1–Abbott/Vysis, Chicago, IL, USA; SpectrumGreen), and a whole chromosome paint for chromosome 17 (wcp 17; SpectrumAqua) [62]. Then, 10 to 20 metaphases per cell line were acquired and analyzed for each probe set on a Zeiss Axioplan microscope, equipped with ISIS v2.86 software (MetaSystems, Altlussheim, Germany).

4.6. Western Blot and Immunostaining

Total protein was extracted from exponentially growing cells and 25 µg protein was resolved by SDS-PAGE using 4%–15% gradient gel (Bio-Rad Laboratories, Feldkirchen, Germany). After transfer and blocking in 5% BSA for at least 1 h, proteins were detected by primary antibodies against ATR [C-1] (Santa Cruz Biotechnology, Heidelberg, Germany 1:750), p-ATR S428 (Cell Signaling Technology, Leiden, The Netherlands, #2853, 1:500), BRCA1 [MS110] (Calbiochem/Merck Chemicals, Darmstadt, Germany, 1:1000), CHK1 [2G1D5] (Cell Signaling, 1:750), p-CHK1 S296 (Cell Signaling #2349, 1:750), FANCD2 [FI17] (Santa Cruz, 1:2000), PARP1 [C210] (BD, 1:1000), HSC70 [B6] (Santa Cruz, 1:10.000), RAD51 [PC130] (Calbiochem, 1:1000), and β-Actin [AC-74] (Sigma-Aldrich, Taufkirchen, Germany, 1:20.000). Primary antibodies were detected with IRDYE 680 conjugated anti-mouse IgG, IRDYE 800 conjugated anti-mouse IgG, IRDYE 680 conjugated anti-rabbit IgG, or IRDYE 800 conjugated anti-rabbit IgG (LiCor, 1:7500).

For immunofluorescence staining, cells were seeded on culture slides. After treatment, cells were permeabilized, fixed with 4% paraformaldehyde, and blocked overnight in 3% BSA. Foci were detected using primary antibodies against RAD51 [AB-1] (Calbiochem, 1:500), γH2AX [Ser139] (Millipore/Merck Chemicals, Darmstadt, Germany, 1:250) or RPA [MA-34] (Santa Cruz, 1:400), followed by secondary antibodies Alexa Fluor 488 goat anti-rabbit IgG (Cell signaling, 1:600), Alexa Fluor 488 goat anti-mouse IgG (Cell signaling, 1:600), or Alexa Flour 594 goat anti-mouse IgG (Cell signaling, 1:500). Nuclei were stained with DAPI and samples were mounted (Vector Laboratories, Newark, CA, USA). The γH2AX foci were quantified manually by capturing fluorescence images using a Zeiss Axioplan 2 fluorescence microscope equipped with a charge-coupled device camera and Axiovision software (Carl Zeiss Microscopy, Oberkochen, Germany), followed by quantification using Image J software. RPA and RAD51 foci were quantified automatically by the Aklides®-system (MediPan, Blankenfelde-Mahlow, Germany). A minimum of 100 cells per dose and slide were quantified.

4.7. Homologous Recombination Assay

The homologous recombination (HR) capacity was measured by transient transfection of I-Sce-1 linearized pDR-GFP plasmid (Addgene #264752, kindly provided by M. Jasin). First, 1 µg of the linearized plasmid was transfected into cells using FuGENE (Roche, Mannheim, Germany) in a 1:3 µg/µL ratio according to the manufacturer's instructions. To measure transfection efficiency, cells were transfected with 1 µg pEGFP-N1 (Addgene #6085-1) in a parallel approach. After 48 h, cells were harvested and the fraction of GFP-positive cells was determined by flow cytometry. HR capacity was calculated according to GFP-positive cells (pDR-GFP) and transfection efficiency (pEGFP-N1).

4.8. Cell Cycle

For cell cycle analysis, cells were harvested, fixed with ice-cold 80% ethanol, and stored at −20 °C. Cells were washed in PBS + 0.1% Tween20 and stained with propidium iodide (10 µg/mL with 1% RNase and 0.1% Triton X-100) for 30 min in the dark. Flow cy-

tometry analysis was performed using a MACSQuant10 with MACSQuantify Software 2.11 (Miltenyi Biotec, Bergisch Gladbach, Germany). The proportion of cells in the respective cell cycle phases was calculated using ModFit LT™ 3.2 software (Verity Software House, Topsham, ME, USA).

4.9. 2D and 3D Clonogenic Survival

For the 2D colony formation assay, 250 cells per well were seeded in a 6-well plate 12 h before treatment with MMC or irradiation and were cultured for 14 days. Cells were fixed with 70% ethanol and stained with 1% crystal violet (Sigma-Aldrich). Colonies with more than 50 cells were counted and normalized to untreated samples.

The 3D soft agar colony formation assay was performed as described before [63,64] with slight variations. For the assay, 96-well plates were used, containing 60 μL 0.6% agarose as bottom layer and 50 μL 0.3% agarose cell-containing top layer with 1500 cells per well. Instead of a feeding layer, 10 μL of medium was additionally added on top of the cell-containing layer. Cells were irradiated 12 h after plating and cultured for 10 days. Colonies with a diameter greater than 50 μm were counted and normalized to untreated controls. Each survival curve represents the mean of at least three independent experiments.

4.10. DNA Fiber Assay

Classical DNA Fiber Assay: Exponentially growing cells were pulse labeled with 25 μM CldU (Sigma-Aldrich) followed by 250 μM IdU (Sigma-Aldrich) for 30 min each. HU (2 mM) was given for 4 h in between the labels. The cells were harvested and DNA fiber spreads were prepared and stained as described previously [65]. Fibers were examined using Axioplan 2 fluorescence microscope (Carl Zeiss Microscopy). CldU and IdU tracts were measured using ImageJ software. At least 100 fibers per sample and independent experiment were analyzed.

Coming DNA Fiber Assay: Exponentially growing spheroids at day 3 post seeding were pulse labeled with 25 μM CldU (Sigma-Aldrich), followed by 250 μM IdU (Sigma-Aldrich) for 30 min each. Irradiation with 6 Gy was performed between the first and second label. Spheroids were harvested and DNA fiber was prepared using the DNA combing system of Genomic Vision. Fibers were examined using an Axioplan 2 fluorescence microscope (Carl Zeiss Microscopy). CldU and IdU tracts were measured using Image J software. At least 100 fibers per sample and independent experiment were analyzed.

4.11. Statistical Analysis

Statistical analysis, curve fitting, and graph creation were performed using GraphPad Prism (Version 6.02) software (Graph Pad Software, San Diego, CA, USA). Data are given as mean (+SEM) of at least three replicate experiments. Unless stated otherwise, significance was tested by Student's *t*-test.

Author Contributions: Conceptualization and experiment design, K.B., S.C. and H.P., Writing—Original draft preparation, K.B., S.C. and H.P., Writing—Review and editing, all authors, Investigation, and analysis S.C., E.R., J.J., N.A., L.P.H., A.Z., L.P., T.L., S.K., P.K., M.G., H.P. and K.B. Verification and supervision K.B., H.P., C.P., T.L., N.C. and K.R. All authors have read and agreed to the published version of the manuscript.

References

1. Wu, Z.; Li, S.; Tang, X.; Wang, Y.; Guo, W.; Cao, G.; Chen, K.; Zhang, M.; Guan, M.; Yang, D. Copy Number Amplification of DNA Damage Repair Pathways Potentiates Therapeutic Resistance in Cancer. *Theranostics* **2020**, *10*, 3939–3951. [CrossRef] [PubMed]
2. Tung, N.; Lin, N.U.; Kidd, J.; Allen, B.A.; Singh, N.; Wenstrup, R.J.; Hartman, A.R.; Winer, E.P.; Garber, J.E. Frequency of Germline Mutations in 25 Cancer Susceptibility Genes in a Sequential Series of Patients With Breast Cancer. *J. Clin. Oncol.* **2016**, *34*, 1460–1468. [CrossRef] [PubMed]
3. Jin, T.Y.; Park, K.S.; Nam, S.E.; Yoo, Y.B.; Park, W.S.; Yun, I.J. BRCA1/2 Serves as a Biomarker for Poor Prognosis in Breast Carcinoma. *Int. J. Mol. Sci.* **2022**, *23*, 3754. [CrossRef] [PubMed]
4. Wang, C.; Feng, H.; Cheng, X.; Liu, K.; Cai, D.; Zhao, R. Potential Therapeutic Targets of B7 Family in Colorectal Cancer. *Front. Immunol.* **2020**, *11*, 681. [CrossRef]
5. Zhong, Q.; Peng, H.L.; Zhao, X.; Zhang, L.; Hwang, W.T. Effects of BRCA1- and BRCA2-related mutations on ovarian and breast cancer survival: A meta-analysis. *Clin. Cancer Res.* **2015**, *21*, 211–220. [CrossRef]
6. Liu, J.; Doty, T.; Gibson, B.; Heyer, W.D. Human BRCA2 protein promotes RAD51 filament formation on RPA-covered single-stranded DNA. *Nat. Struct Mol. Biol.* **2010**, *17*, 1260–1262. [CrossRef]
7. Lord, C.J.; Ashworth, A. The DNA damage response and cancer therapy. *Nature* **2012**, *481*, 287–294. [CrossRef]
8. Davies, H.; Glodzik, D.; Morganella, S.; Yates, L.R.; Staaf, J.; Zou, X.; Ramakrishna, M.; Martin, S.; Boyault, S.; Sieuwerts, A.M.; et al. HRDetect is a predictor of BRCA1 and BRCA2 deficiency based on mutational signatures. *Nat. Med.* **2017**, *23*, 517–525. [CrossRef]
9. Wang, N.; Yang, Y.; Jin, D.; Zhang, Z.; Shen, K.; Yang, J.; Chen, H.; Zhao, X.; Yang, L.; Lu, H. PARP inhibitor resistance in breast and gynecological cancer: Resistance mechanisms and combination therapy strategies. *Front. Pharmacol.* **2022**, *13*, 967633. [CrossRef]
10. Tutt, A.; Tovey, H.; Cheang, M.C.U.; Kernaghan, S.; Kilburn, L.; Gazinska, P.; Owen, J.; Abraham, J.; Barrett, S.; Barrett-Lee, P.; et al. Carboplatin in BRCA1/2-mutated and triple-negative breast cancer BRCAness subgroups: The TNT Trial. *Nat. Med.* **2018**, *24*, 628–637. [CrossRef]
11. Telli, M.L.; Timms, K.M.; Reid, J.; Hennessy, B.; Mills, G.B.; Jensen, K.C.; Szallasi, Z.; Barry, W.T.; Winer, E.P.; Tung, N.M.; et al. Homologous Recombination Deficiency (HRD) Score Predicts Response to Platinum-Containing Neoadjuvant Chemotherapy in Patients with Triple-Negative Breast Cancer. *Clin. Cancer Res.* **2016**, *22*, 3764–3773. [CrossRef] [PubMed]
12. Hoppe, M.M.; Sundar, R.; Tan, D.S.P.; Jeyasekharan, A.D. Biomarkers for Homologous Recombination Deficiency in Cancer. *J. Natl Cancer Inst.* **2018**, *110*, 704–713. [CrossRef] [PubMed]
13. Miller, R.E.; Leary, A.; Scott, C.L.; Serra, V.; Lord, C.J.; Bowtell, D.; Chang, D.K.; Garsed, D.W.; Jonkers, J.; Ledermann, J.A.; et al. ESMO recommendations on predictive biomarker testing for homologous recombination deficiency and PARP inhibitor benefit in ovarian cancer. *Ann. Oncol* **2020**, *31*, 1606–1622. [CrossRef] [PubMed]
14. Schlacher, K.; Christ, N.; Siaud, N.; Egashira, A.; Wu, H.; Jasin, M. Double-strand break repair-independent role for BRCA2 in blocking stalled replication fork degradation by MRE11. *Cell* **2011**, *145*, 529–542. [CrossRef]
15. Taglialatela, A.; Alvarez, S.; Leuzzi, G.; Sannino, V.; Ranjha, L.; Huang, J.W.; Madubata, C.; Anand, R.; Levy, B.; Rabadan, R.; et al. Restoration of Replication Fork Stability in BRCA1- and BRCA2-Deficient Cells by Inactivation of SNF2-Family Fork Remodelers. *Mol. Cell* **2017**, *68*, 414–430.e8. [CrossRef]
16. Mutreja, K.; Krietsch, J.; Hess, J.; Ursich, S.; Berti, M.; Roessler, F.K.; Zellweger, R.; Patra, M.; Gasser, G.; Lopes, M. ATR-Mediated Global Fork Slowing and Reversal Assist Fork Traverse and Prevent Chromosomal Breakage at DNA Interstrand Cross-Links. *Cell Rep.* **2018**, *24*, 2629–2642.e5. [CrossRef]
17. Rickman, K.; Smogorzewska, A. Advances in understanding DNA processing and protection at stalled replication forks. *J. Cell Biol.* **2019**, *218*, 1096–1107. [CrossRef]
18. Pathania, S.; Bade, S.; Le Guillou, M.; Burke, K.; Reed, R.; Bowman-Colin, C.; Su, Y.; Ting, D.T.; Polyak, K.; Richardson, A.L.; et al. BRCA1 haploinsufficiency for replication stress suppression in primary cells. *Nat. Commun.* **2014**, *5*, 5496. [CrossRef]

19. Couch, F.B.; Bansbach, C.E.; Driscoll, R.; Luzwick, J.W.; Glick, G.G.; Betous, R.; Carroll, C.M.; Jung, S.Y.; Qin, J.; Cimprich, K.A.; et al. ATR phosphorylates SMARCAL1 to prevent replication fork collapse. *Genes Dev.* **2013**, *27*, 1610–1623. [CrossRef]

20. Eykelenboom, J.K.; Harte, E.C.; Canavan, L.; Pastor-Peidro, A.; Calvo-Asensio, I.; Llorens-Agost, M.; Lowndes, N.F. ATR activates the S-M checkpoint during unperturbed growth to ensure sufficient replication prior to mitotic onset. *Cell Rep.* **2013**, *5*, 1095–1107. [CrossRef]

21. Maya-Mendoza, A.; Petermann, E.; Gillespie, D.A.; Caldecott, K.W.; Jackson, D.A. Chk1 regulates the density of active replication origins during the vertebrate S phase. *EMBO J.* **2007**, *26*, 2719–2731. [CrossRef] [PubMed]

22. Petermann, E.; Woodcock, M.; Helleday, T. Chk1 promotes replication fork progression by controlling replication initiation. *Proc. Natl. Acad. Sci. USA* **2010**, *107*, 16090–16095. [CrossRef] [PubMed]

23. Federico, M.B.; Campodonico, P.; Paviolo, N.S.; Gottifredi, V. Beyond interstrand crosslinks repair: Contribution of FANCD2 and other Fanconi Anemia proteins to the replication of DNA. *Mutat Res.* **2018**, *808*, 83–92. [CrossRef]

24. Schlacher, K.; Wu, H.; Jasin, M. A distinct replication fork protection pathway connects Fanconi anemia tumor suppressors to RAD51-BRCA1/2. *Cancer Cell* **2012**, *22*, 106–116. [CrossRef] [PubMed]

25. Chaudhury, I.; Sareen, A.; Raghunandan, M.; Sobeck, A. FANCD2 regulates BLM complex functions independently of FANCI to promote replication fork recovery. *Nucleic Acids Res.* **2013**, *41*, 6444–6459. [CrossRef] [PubMed]

26. Karnan, S.; Mohseni, M.; Konishi, Y.; Tamaki, A.; Hosokawa, Y.; Park, B.H.; Konishi, H. Controversial BRCA1 allelotypes in commonly used breast cancer cell lines. *Breast Cancer Res. Treat* **2010**, *119*, 249–251. [CrossRef]

27. Chen, J.; Silver, D.P.; Walpita, D.; Cantor, S.B.; Gazdar, A.F.; Tomlinson, G.; Couch, F.J.; Weber, B.L.; Ashley, T.; Livingston, D.M.; et al. Stable interaction between the products of the BRCA1 and BRCA2 tumor suppressor genes in mitotic and meiotic cells. *Mol. Cell* **1998**, *2*, 317–328. [CrossRef]

28. Scully, R.; Ganesan, S.; Vlasakova, K.; Chen, J.; Socolovsky, M.; Livingston, D.M. Genetic analysis of BRCA1 function in a defined tumor cell line. *Mol. Cell* **1999**, *4*, 1093–1099. [CrossRef]

29. Naipal, K.A.; Verkaik, N.S.; Ameziane, N.; van Deurzen, C.H.; Ter Brugge, P.; Meijers, M.; Sieuwerts, A.M.; Martens, J.W.; O'Connor, M.J.; Vrieling, H.; et al. Functional ex vivo assay to select homologous recombination-deficient breast tumors for PARP inhibitor treatment. *Clin. Cancer Res.* **2014**, *20*, 4816–4826. [CrossRef]

30. Cruz, C.; Castroviejo-Bermejo, M.; Gutierrez-Enriquez, S.; Llop-Guevara, A.; Ibrahim, Y.H.; Gris-Oliver, A.; Bonache, S.; Morancho, B.; Bruna, A.; Rueda, O.M.; et al. RAD51 foci as a functional biomarker of homologous recombination repair and PARP inhibitor resistance in germline BRCA-mutated breast cancer. *Ann. Oncol.* **2018**, *29*, 1203–1210. [CrossRef]

31. Dueva, R.; Iliakis, G. Replication protein A: A multifunctional protein with roles in DNA replication, repair and beyond. *NAR Cancer* **2020**, *2*, zcaa022. [CrossRef] [PubMed]

32. Kais, Z.; Rondinelli, B.; Holmes, A.; O'Leary, C.; Kozono, D.; D'Andrea, A.D.; Ceccaldi, R. FANCD2 Maintains Fork Stability in BRCA1/2-Deficient Tumors and Promotes Alternative End-Joining DNA Repair. *Cell Rep.* **2016**, *15*, 2488–2499. [CrossRef] [PubMed]

33. Menolfi, D.; Jiang, W.; Lee, B.J.; Moiseeva, T.; Shao, Z.; Estes, V.; Frattini, M.G.; Bakkenist, C.J.; Zha, S. Kinase-dead ATR differs from ATR loss by limiting the dynamic exchange of ATR and RPA. *Nat. Commun.* **2018**, *9*, 5351. [CrossRef] [PubMed]

34. Moynahan, M.E.; Chiu, J.W.; Koller, B.H.; Jasin, M. Brca1 controls homology-directed DNA repair. *Mol. Cell* **1999**, *4*, 511–518. [CrossRef]

35. Foo, T.K.; Xia, B. BRCA1-Dependent and Independent Recruitment of PALB2-BRCA2-RAD51 in the DNA Damage Response and Cancer. *Cancer Res.* **2022**, *82*, 3191–3197. [CrossRef]

36. Sy, S.M.; Huen, M.S.; Chen, J. PALB2 is an integral component of the BRCA complex required for homologous recombination repair. *Proc. Natl. Acad. Sci. USA* **2009**, *106*, 7155–7160. [CrossRef]

37. Traven, A.; Heierhorst, J. SQ/TQ cluster domains: Concentrated ATM/ATR kinase phosphorylation site regions in DNA-damage-response proteins. *Bioessays* **2005**, *27*, 397–407. [CrossRef]

38. Baer, R.; Ludwig, T. The BRCA1/BARD1 heterodimer, a tumor suppressor complex with ubiquitin E3 ligase activity. *Curr. Opin. Genet. Dev.* **2002**, *12*, 86–91. [CrossRef]

39. Johnson, N.; Johnson, S.F.; Yao, W.; Li, Y.C.; Choi, Y.E.; Bernhardy, A.J.; Wang, Y.; Capelletti, M.; Sarosiek, K.A.; Moreau, L.A.; et al. Stabilization of mutant BRCA1 protein confers PARP inhibitor and platinum resistance. *Proc. Natl. Acad. Sci. USA* **2013**, *110*, 17041–17046. [CrossRef]

40. Krais, J.J.; Wang, Y.; Patel, P.; Basu, J.; Bernhardy, A.J.; Johnson, N. RNF168-mediated localization of BARD1 recruits the BRCA1-PALB2 complex to DNA damage. *Nat. Commun.* **2021**, *12*, 5016. [CrossRef]

41. Nacson, J.; Krais, J.J.; Bernhardy, A.J.; Clausen, E.; Feng, W.; Wang, Y.; Nicolas, E.; Cai, K.Q.; Tricarico, R.; Hua, X.; et al. BRCA1 Mutation-Specific Responses to 53BP1 Loss-Induced Homologous Recombination and PARP Inhibitor Resistance. *Cell Rep.* **2018**, *25*, 1384. [CrossRef] [PubMed]

42. Wang, Y.; Bernhardy, A.J.; Cruz, C.; Krais, J.J.; Nacson, J.; Nicolas, E.; Peri, S.; van der Gulden, H.; van der Heijden, I.; O'Brien, S.W.; et al. The BRCA1-Delta11q Alternative Splice Isoform Bypasses Germline Mutations and Promotes Therapeutic Resistance to PARP Inhibition and Cisplatin. *Cancer Res.* **2016**, *76*, 2778–2790. [CrossRef] [PubMed]

43. Wang, B.; Matsuoka, S.; Ballif, B.A.; Zhang, D.; Smogorzewska, A.; Gygi, S.P.; Elledge, S.J. Abraxas and RAP80 form a BRCA1 protein complex required for the DNA damage response. *Science* **2007**, *316*, 1194–1198. [CrossRef] [PubMed]

44. Roy, R.; Chun, J.; Powell, S.N. BRCA1 and BRCA2: Different roles in a common pathway of genome protection. *Nat. Rev. Cancer* **2011**, *12*, 68–78. [CrossRef]

45. Parplys, A.C.; Seelbach, J.I.; Becker, S.; Behr, M.; Wrona, A.; Jend, C.; Mansour, W.Y.; Joosse, S.A.; Stuerzbecher, H.W.; Pospiech, H.; et al. High levels of RAD51 perturb DNA replication elongation and cause unscheduled origin firing due to impaired CHK1 activation. *Cell Cycle* **2015**, *14*, 3190–3202. [CrossRef]

46. Saleh-Gohari, N.; Bryant, H.E.; Schultz, N.; Parker, K.M.; Cassel, T.N.; Helleday, T. Spontaneous homologous recombination is induced by collapsed replication forks that are caused by endogenous DNA single-strand breaks. *Mol. Cell Biol.* **2005**, *25*, 7158–7169. [CrossRef]

47. Meyer, F.; Becker, S.; Classen, S.; Parplys, A.C.; Mansour, W.Y.; Riepen, B.; Timm, S.; Ruebe, C.; Jasin, M.; Wikman, H.; et al. Prevention of DNA Replication Stress by CHK1 Leads to Chemoresistance Despite a DNA Repair Defect in Homologous Recombination in Breast Cancer. *Cells* **2020**, *9*, 238. [CrossRef]

48. Noordermeer, S.M.; van Attikum, H. PARP Inhibitor Resistance: A Tug-of-War in BRCA-Mutated Cells. *Trends Cell Biol.* **2019**, *29*, 820–834. [CrossRef]

49. Ray Chaudhuri, A.; Callen, E.; Ding, X.; Gogola, E.; Duarte, A.A.; Lee, J.E.; Wong, N.; Lafarga, V.; Calvo, J.A.; Panzarino, N.J.; et al. Replication fork stability confers chemoresistance in BRCA-deficient cells. *Nature* **2016**, *535*, 382–387. [CrossRef]

50. De Silva, I.U.; McHugh, P.J.; Clingen, P.H.; Hartley, J.A. Defining the roles of nucleotide excision repair and recombination in the repair of DNA interstrand cross-links in mammalian cells. *Mol. Cell Biol.* **2000**, *20*, 7980–7990. [CrossRef]

51. Burrell, R.A.; McClelland, S.E.; Endesfelder, D.; Groth, P.; Weller, M.C.; Shaikh, N.; Domingo, E.; Kanu, N.; Dewhurst, S.M.; Gronroos, E.; et al. Replication stress links structural and numerical cancer chromosomal instability. *Nature* **2013**, *494*, 492–496. [CrossRef] [PubMed]

52. Buisson, R.; Boisvert, J.L.; Benes, C.H.; Zou, L. Distinct but Concerted Roles of ATR, DNA-PK, and Chk1 in Countering Replication Stress during S Phase. *Mol. Cell* **2015**, *59*, 1011–1024. [CrossRef] [PubMed]

53. Ang, M.K.; Patel, M.R.; Yin, X.Y.; Sundaram, S.; Fritchie, K.; Zhao, N.; Liu, Y.; Freemerman, A.J.; Wilkerson, M.D.; Walter, V.; et al. High XRCC1 protein expression is associated with poorer survival in patients with head and neck squamous cell carcinoma. *Clin. Cancer Res.* **2011**, *17*, 6542–6552. [CrossRef] [PubMed]

54. Martin, R.W.; Orelli, B.J.; Yamazoe, M.; Minn, A.J.; Takeda, S.; Bishop, D.K. RAD51 up-regulation bypasses BRCA1 function and is a common feature of BRCA1-deficient breast tumors. *Cancer Res.* **2007**, *67*, 9658–9665. [CrossRef]

55. Smogorzewska, A.; Matsuoka, S.; Vinciguerra, P.; McDonald, E.R., 3rd; Hurov, K.E.; Luo, J.; Ballif, B.A.; Gygi, S.P.; Hofmann, K.; D'Andrea, A.D.; et al. Identification of the FANCI protein, a monoubiquitinated FANCD2 paralog required for DNA repair. *Cell* **2007**, *129*, 289–301. [CrossRef]

56. Sims, A.E.; Spiteri, E.; Sims, R.J., 3rd; Arita, A.G.; Lach, F.P.; Landers, T.; Wurm, M.; Freund, M.; Neveling, K.; Hanenberg, H.; et al. FANCI is a second monoubiquitinated member of the Fanconi anemia pathway. *Nat. Struct Mol. Biol.* **2007**, *14*, 564–567. [CrossRef] [PubMed]

57. Howlett, N.G.; Taniguchi, T.; Durkin, S.G.; D'Andrea, A.D.; Glover, T.W. The Fanconi anemia pathway is required for the DNA replication stress response and for the regulation of common fragile site stability. *Hum. Mol. Genet.* **2005**, *14*, 693–701. [CrossRef]

58. Ran, F.A.; Hsu, P.D.; Wright, J.; Agarwala, V.; Scott, D.A.; Zhang, F. Genome engineering using the CRISPR-Cas9 system. *Nat. Protoc.* **2013**, *8*, 2281–2308. [CrossRef]

59. Bentley, D.R.; Balasubramanian, S.; Swerdlow, H.P.; Smith, G.P.; Milton, J.; Brown, C.G.; Hall, K.P.; Evers, D.J.; Barnes, C.L.; Bignell, H.R.; et al. Accurate whole human genome sequencing using reversible terminator chemistry. *Nature* **2008**, *456*, 53–59. [CrossRef]

60. Martin, M. Cutadapt removes adapter sequences from high-throughput sequencing reads. *EmbNet.J.* **2011**, *17*, 10–12. [CrossRef]

61. Edgar, R.C. Search and clustering orders of magnitude faster than BLAST. *Bioinformatics* **2010**, *26*, 2460–2461. [CrossRef] [PubMed]

62. Liehr, T. Molecular Cytogenetics in the Era of Chromosomics and Cytogenomic Approaches. *Front. Genet.* **2021**, *12*, 720507. [CrossRef] [PubMed]

63. Horibata, S.; Vo, T.V.; Subramanian, V.; Thompson, P.R.; Coonrod, S.A. Utilization of the Soft Agar Colony Formation Assay to Identify Inhibitors of Tumorigenicity in Breast Cancer Cells. *J. Vis. Exp.* **2015**, *99*, e52727. [CrossRef] [PubMed]

64. Meerz, A.; Deville, S.S.; Muller, J.; Cordes, N. Comparative Therapeutic Exploitability of Acute Adaptation Mechanisms to Photon and Proton Irradiation in 3D Head and Neck Squamous Cell Carcinoma Cell Cultures. *Cancers (Basel)* **2021**, *13*, 1190. [CrossRef] [PubMed]

65. Parplys, A.C.; Petermann, E.; Petersen, C.; Dikomey, E.; Borgmann, K. DNA damage by X-rays and their impact on replication processes. *Radiother. Oncol.* **2012**, *102*, 466–471. [CrossRef]

Article

Prevention of DNA Replication Stress by CHK1 Leads to Chemoresistance Despite a DNA Repair Defect in Homologous Recombination in Breast Cancer

Felix Meyer [1,†], Saskia Becker [1,†], Sandra Classen [1], Ann Christin Parplys [1], Wael Yassin Mansour [1,2], Britta Riepen [1], Sara Timm [3], Claudia Ruebe [3], Maria Jasin [4], Harriet Wikman [5], Cordula Petersen [6], Kai Rothkamm [1] and Kerstin Borgmann [1,*]

1   Laboratory of Radiobiology and Experimental Radiooncology, Center of Oncology, University Medical
     Center Hamburg-Eppendorf, 20246 Hamburg, Germany; fe.meyer@uke.de (F.M.);
     saskiaalexandra.becker@uke.de (S.B.); sandra.classen@uke.de (S.C.); a.parplys@uke.de (A.C.P.);
     w.mansour@uke.de (W.Y.M.); riepen@uke.de (B.R.); k.rothkamm@uke.de (K.R.)
2   Tumor Biology Department, National Cancer Institute, Cairo University, Cairo 11796, Egypt
3   Department of Radiation Oncology, Saarland University, 66421 Hamburg/Saar, Germany;
     sara.timm@uks.eu (S.T.); claudia.ruebe@uks.eu (C.R.)
4   Developmental Biology Program, Memorial Sloan Kettering Cancer Center, New York, NY 10065, USA;
     m-jasin@ski.mskcc.org
5   Department of Tumor Biology, University Center Hamburg-Eppendorf, 20246 Hamburg, Germany;
     h.wikman@uke.de
6   Department of Radiotherapy and Radiooncology, University Medical Center Hamburg-Eppendorf,
     20246 Hamburg, Germany; cor.petersen@uke.de
*   Correspondence: borgmann@uke.de; Tel.: +49-40-74105-3596
†   These authors contributed equally to the manuscript.

Abstract: Chromosomal instability not only has a negative effect on survival in triple-negative breast cancer, but also on the well treatable subgroup of luminal A tumors. This suggests a general mechanism independent of subtypes. Increased chromosomal instability (CIN) in triple-negative breast cancer (TNBC) is attributed to a defect in the DNA repair pathway homologous recombination. Homologous recombination (HR) prevents genomic instability by repair and protection of replication. It is unclear whether genetic alterations actually lead to a repair defect or whether superior signaling pathways are of greater importance. Previous studies focused exclusively on the repair function of HR. Here, we show that the regulation of HR by the intra-S-phase damage response at the replication is of overriding importance. A damage response activated by Ataxia telangiectasia and Rad3 related-checkpoint kinase 1 (ATR-CHK1) can prevent replication stress and leads to resistance formation. CHK1 thus has a preferred role over HR in preventing replication stress in TNBC. The signaling cascade ATR-CHK1 can compensate for a double-strand break repair error and lead to resistance of HR-deficient tumors. Established methods for the identification of HR-deficient tumors for Poly(ADP-Ribose)-Polymerase 1 (PARP1) inhibitor therapies should be extended to include analysis of candidates for intra-S phase damage response.

Keywords: triple-negative breast cancer (TNBC); chromosomal instability (CIN); CIN70 score; homologous recombination (HR); DNA-damage response (DDR); CHK1

1. Introduction

Breast cancer is a very heterogeneous disease whose prognosis is determined by the molecular subtype. Tumors of the triple-negative breast cancer (TNBC) subtype show the worst prognosis [1],

which could be attributed to increased chromosomal instability (CIN) [2]. Using the CIN, a gene expression profile consisting of 70 genes associated with a functional aneuploidy (CIN70 score) was extracted. The CIN70 score is the highest for TNBCs compared to other subtypes and a correlation of high/intermediate CIN70 score with prognosis has been observed in numerous studies and tumor entities [3]. A high CIN70 value may be caused by defects in DNA repair, as all BRCA1/2 deficient tumors and one in four sporadically occurring TNBCs show a defect in homologous recombination-mediated (HR-mediated) DNA double-strand break (DSB) repair. HR represents the main DSB repair pathway in the S-phase [4]. It processes DSBs with two open ends, one-ended replication-associated DSB and stalled DNA replication forks.

Two-ended DSBs are repaired by synthesis-dependent strand annealing (SDSA) [5]. As first step DNA end resection is initiated via the nucleases CtIP and MRE11 and is completed by DNA2, EXO1 and BLM helicase [6]. RPA binds the single-stranded DNA overhangs and activates ATR/ATRIP, Claspin and CHK1, thereby initiating HR [7]. RPA is then replaced by RAD51 with the involvement of several HR proteins [5]. One-ended DSBs arise when a replication fork collides with a single-strand DNA break (SSB) or when a replication fork collapses [8]. They are repaired by break-induced replication (BIR). Stalled replication forks are usually protected from nucleolytic degradation by numerous HR factors [9] or SMARCAL1 and ZRANB3 [10]. However, insufficient stabilization leads to collapse or breakage of the replication fork. Cellular replication stress, dNTP depletion, or collision of replication forks with DNA lesions results in fork reversal or fork regression and chicken foot formation [11]. SMARCAL1 is recruited by RPA-bound ssDNA to the replication fork [12], while Poly(ADP-Ribose)-Polymerase 1 (PARP1) is involved in fork reversal [11]. The RPA-bound ssDNA segments at the paused replication fork lead to the activation of ATR, which phosphorylates CHK1. ATR is the most important DNA damage-related kinase in S-phase, where it has a major impact on DNA repair and the regulation of DNA replication [13]. ATR phosphorylates the intra-S phase kinase CHK1, whereupon CHK1 translocates into the nucleus and undergoes autophosphorylation [14]. Under replication stress, CHK1 is associated with phosphorylated Claspin, which enhances ATR-dependent phosphorylation and supports recruitment of CHK1 to the replication fork [15]. Thus, ATR-mediated phosphorylation of CHK1 activates DNA repair and the intra-S phase checkpoint. CHK1 regulates elongation [16] and activation of replication origins, stabilizes replication forks [17], and delays S-phase progression [14,18]. The stalling of replication forks at DNA lesions can be avoided by CHK1-mediated activation of translesion synthesis (TLS) [19]. Besides the stabilization of replication forks, CHK1 is essential for the activation of DNA repair by HR through phosphorylation of RAD51 and BRCA2 [7].

It is unclear to what extent the activation of CHK1 influences the sensitivity of HR deficient tumors. Previous methods to identify these tumors focused on the HR defects that result from a BRCA1/2 mutation and a high HR deficiency score (HRD-score). For both a significantly better response to platinum-based chemotherapy was observed [20–24]. In addition to genetic analysis, it is also possible to characterize HR-deficient tumors functionally. The ex vivo tissue slice culture assay analyzes primary tumor samples for their ability to perform HR. This is assessed by the formation of RAD51 foci after DNA damage, where absence of foci formation indicates HR deficiency [25,26]. It remains unclear in both approaches: (i) whether the observed genetic alteration leads to a functional repair defect, (ii) whether the loss of the RAD51 foci formation provides sufficient information about the functionality of HR, and (iii) how overexpression of RAD51 in interaction with CHK1, in its multiple functions, impacts on these processes. This study investigated the latter point, especially with regard to replication stress, in sporadic non-BRCA1/2-mutated TNBC cells.

2. Materials and Methods

2.1. Clinical in Silico Analysis

Clinical- and mRNA expression data were extracted from the TCGA database from the cBioportal data (http://www.cbioportal.org). For each tumor, the CIN70 score was calculated according to Birbak

et al. [3] by adding the expression values of all CIN70 genes from 1400 patients. For the calculation of disease-specific survival (DSS), the survival data of the patients according to CIN70 score, CHK1 or RAD51 mRNA expression were used and the extreme quartiles were plotted and analyzed using a log-rank test. The mRNA expression of RAD51 and CHK1 of the extreme CIN70 score quartiles were plotted depending on the molecular subtype.

2.2. Cell Culture and Treatments

All cell lines used in the study were either purchased from the American Type Culture Collection (ATCC, Manassas, VA, USA) or kindly provided by Prof. Dr. H. Wikman. The cell lines were cultivated in DMEM medium with 10% FCS, 2% glutamine, and 1% penicillin streptomycin in incubators at 37 °C, 5% CO_2 atmosphere and 100% humidity in cell culture flasks. To inhibit PARP1, olaparib was used in increasing concentrations up to 50 μM and incubated for 5 days. For the treatment with mitomycin C (MMC) concentrations up to 1.5 μg/mL for maximum 1 h were used. The inhibition of CHK1 was achieved by using the small molecule inhibitor MK8776 at 2 μM for 2 h.

2.3. Homologous Recombination Assay

HR frequency was measured by stable or transient transfection of I-Sce-1-linearized pDR-GFP (Addgene #26475) and DR-oriP-GFP (kindly provided by M. Jasin) plasmids. Briefly, 1 μg linearized plasmid (pDR-GFP) or 0.5 μg (DR-oriP-GFP) linearized plasmid plus 0.5 μg MSCV-N-EBNA1 (Addgene #37954) was transfected into cells using FuGENE (Roche, Basel, Switzerland) in a 1:3 μg/μL ratio according to the manufacturer's instruction. After 24 h cells were harvested, and the fraction of GFP-positive cells was determined by flow cytometry.

2.4. Western Blot and Immunostaining

Total protein was extracted from exponentially growing cells and 40 μg/ml were resolved by SDS-PAGE using a 4%–15% gradient gel (Bio-Rad Laboratories). After transfer and blocking overnight at 4 °C in Odyssey Blocking Buffer (Li-Cor, Lincoln, NE, USA) proteins were detected by primary antibodies against BRCA2 [2A-9] (1:500, kindly provided by Stephen Smith, Leibnitz Institute, Jena, Germany), FANCD2 [FI17] (Santa Cruz, 1:2000), ATR [N-19] (Santa Cruz, 1:1000), CHK1 [2G1D5] (Cell Signaling, 1:750), RAD51 [14B4] (1:2.000, GeneTex, Irvine, CA, USA), PARP1 [C210] (BD, 1:1000), RPA [9H8] (Santa Cruz, 1:1000), pCHK1 [Ser296] (Cell Signaling, 1:1000), pATR [Ser428] (Cell Signaling, 1:1000), pRPA [S4/S8], (Bethyl, Montgomery, TX, USA, 1:1000), β-actin [AC-74] (1:50.000, Sigma, St. Louis, MO, USA) or HSC70 [B6] (Santa Cruz, 1:1000). Primary antibodies were detected with IRDYE 680 conjugated anti-mouse IgG, IRDYE 800 conjugated anti-rabbit IgG (Licor, 1:7500), IRDYE 680 conjugated anti-rabbit IgG (Licor, 1:7.500 or 15.000) or IRDYE 800 conjugated anti-mouse IgG (Licor 1:7.500 or 15.000). For immunofluorescence staining, cells were seeded on culture slides. After treatment cells were fixed, permeabilized and blocked overnight in 3%BSA. Foci were detected using primary antibodies against RAD51 [AB-1] (Calbiochem, 1:500), γH2AX [Ser139] (Millipore, Burlington, MA, USA, 1:250) or RPA [MA34] (Santa Cruz, 1:400), followed by secondary antibodies Alexa Fluor 488 goat anti rabbit IgG (Cell signaling, 1:600), Alexa Fluor 488 goat anti mouse IgG (Cell signaling, 1:600) or Alexa Fluor 594 goat anti-mouse IgG (Cell signaling, 1:500). EdU was stained with Alexa Fluor Azide 594 or 647(Life Technologies, Carlsbad, CA, USA, 1:500), nuclei were stained with DAPI and the samples were mounted (Vector Laboratories). Fluorescence images were captured using a Zeiss Axioplan 2 epifluorescence microscope equipped with a charge-coupled device camera and Axiovision software. For quantitative analysis, foci were counted by fluorescence microscopy using a 1000-fold magnification. There were 100 cells per dose per slide and experiment were evaluated blindly.

2.5. Transmission Electron Microscopy

Treated cells were fixed with 2% paraformaldehyde and 0.05% glutaraldehyde in PBS. Fixed samples were dehydrated using increasing concentrations of ethanol and infiltrated with

LR White resin overnight (Plano, Wetzlar, Germany). Subsequently, samples were embedded in fresh resin with accelerator at 37 °C until the resin was polymerized. Ultrathin sections (70 nm) were cut on a Microtome Ultracut UCT (Leica, Wetzlar, Germany) with diamond knives (Diatome, Biel, Switzerland), gathered up on pioloform-coated nickel grids and processed for immunogold-labeling. To block nonspecific staining sections were placed on drops of blocking solution (Aurion, Wageningen, The Netherlands). Afterwards sections were rinsed and incubated with primary antibodies against yH2AX (Millipore, 1:250) and RPA (Santa Cruz, 1:400). After rinsing, secondary antibodies conjugated with 6-nm or 10-nm gold particles (Aurion, Wageningen, The Netherlands) were applied to the grids for 1.5 h. Sections were then rinsed and fixed with 2% glutaraldehyde in PBS. All sections were stained with 3% uranyl acetate and examined using Tecnai BiotwinTM transmission electron microscope (FEI, Eindhoven, The Netherlands). Detection, localization and counting of gold beads and clusters were performed at the electron microscope by eye.

2.6. DNA Fiber Assay

Exponentially growing cells were pulse labeled with 25 μM CldU (Sigma) followed by 250 μM IdU (Sigma) for 30 min each. HU was given for 2 h between both labels, Inhibitors 2 h before labelling, MMC was given at the beginning of the 2nd pulse labelling time. Labeled cells were harvested, DNA fiber spreads prepared and stained as described [27]. Fibers were examined using an Axioplan 2 fluorescence microscope (Zeiss, Oberkochen, Germany). CldU and IdU tracks were measured using ImageJ (version 1.48, Company, City, State abbrev. If USA, Country) [27,28]. At least 300 forks were analyzed.

2.7. Clonogenic Survival

For survival assays 250 cells were seeded in a 6-well plate 6 h before treatment and cells were cultured for 14 days. Cells were fixed and stained with 1% crystal violet (Sigma-Aldrich, St. Louis, MO, USA). Colonies with more than 50 cells were determined microscopically and normalized to untreated samples. Each survival curve represents the mean of at least three independent experiments.

2.8. Statistical Analysis

Statistical analysis, curve fitting and graphs were performed using Prism 6.02 (GraphPad Software, San Diego, CA, USA). Data are given as mean (+SEM) of 3–5 replicate experiments. Unless stated otherwise, significance was tested by Student's *t*-test.

3. Results

3.1. Long-Term Disease Specific Survival in Luminal and Triple-Negative Breast Cancer Tumors Depends On RAD51 and CHK1 mRNA Expression

The relationship between CIN and prognosis has already been investigated in a large number of tumors, whereby a high CIN70 value was often associated with a worse prognosis [3]. However, it is unclear whether CIN70 affects both good and poorly treatable subgroups of breast cancer. To clarify this, the effect of the CIN70 score on disease-specific survival (DSS) was analyzed in all subgroups, as well as only in LumA and TNBC using the two extreme quartiles (Figure 1A–C and Supplementary Figure S1A). Irrespective of the subtype, tumors with high CIN70 showed significantly worse 5- and 10-year DSS compared to patients with tumors harboring a low CIN70.
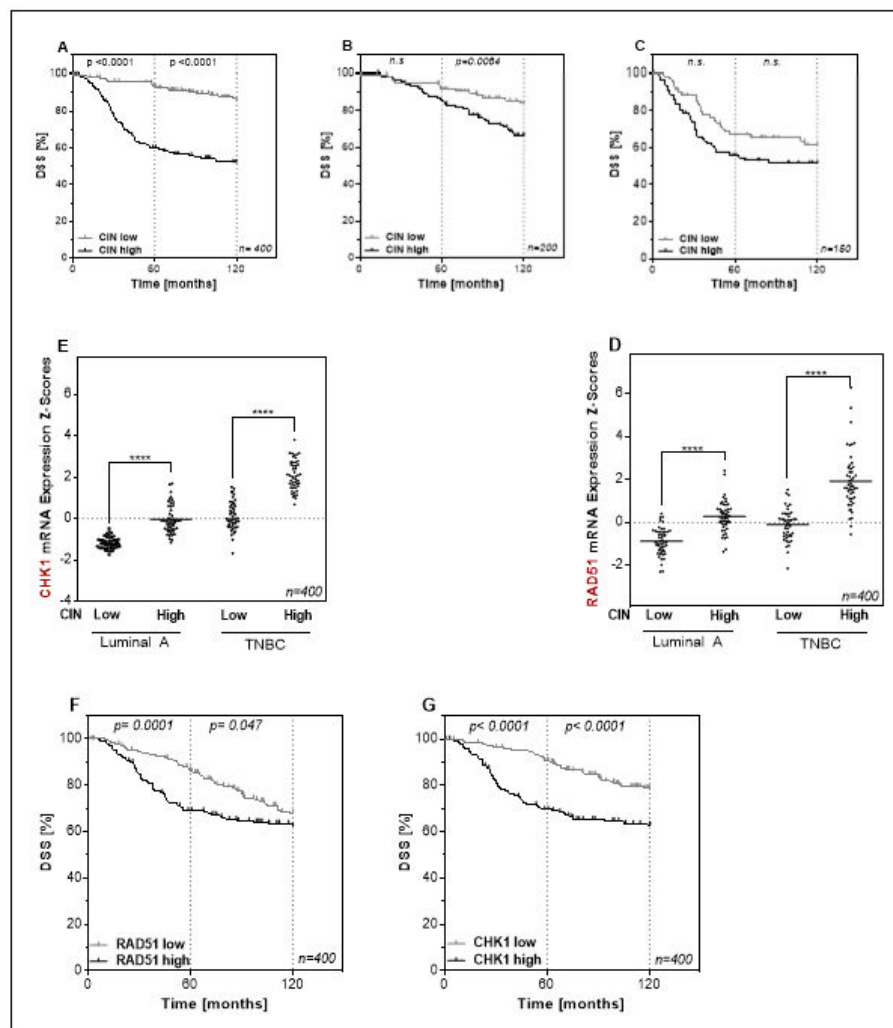
Figure 1. A high gene expression profile consisting of 70 genes associated with a functional aneuploidy (CIN70) score is negatively associated with disease-specific survival in luminal A (LumA) and triple-negative breast cancer (TNBC) subtypes and correlates with the expression of RAD51 and CHK1. (**A–C**). Kaplan–Meier analysis of the CIN70 score as prognostic factor for disease-specific survival (DSS) in breast cancer patients (**A**) ($n = 400$) patients with LumA (**B**) ($n = 200$) and TNBCs (**C**) ($n = 150$) using the two extreme quartiles. The CIN70 score defines the differential mRNA expression of 70 genes in tumors classified as stable and unstable based on their structural and numerical chromosomal alterations [3]. DSS is plotted against time after therapy. All, LumA and TNBC tumors with CIN high showed significantly worse 5- and 10-year DSS compared to tumors with CIN low, with 52% vs. 86% after 10 years for all, 84% vs. 67% after 10 years (n.s/$p = 0.0084$) for LumA and 52% vs. 62% after 10 years (n.s/n.s) for TNBC tumors. p-values were calculated on the basis of the log-rank test. (**D,E**). mRNA expression of RAD51 (**D**) and CHK1 (**E**) for LumA and TNBC tumors of the Metabric data set sorted by CIN70 score using the two extreme quartiles. RAD51 is expressed significantly higher in CIN high than in CIN low tumors, both in LumA, with -0.88 ± 0.09 vs. 0.27 ± 0.1 and -0.11 ± 0.01 vs. 1.92 ± 0.19, respectively. A significantly increased expression in CIN high compared to CIN low was also found for CHK1, with 1.17 ± 0.04 and -0.03 ± 0.096 for LumA and 0.13 ± 0.1 vs. 2.08 ± 0.1 for TNBC. (**F,G**). Kaplan–Meier analysis of DSS of 400 patients according to the RAD51 (**F**) or CHK1 (**G**) expression using the two extreme quartiles. DSS is plotted against time after therapy. Patients whose tumor had a high expression of RAD51 showed significantly lower DSS compared to low RAD51 expression (68% vs. 62%). For the expression of CHK1, the negative effect of a high expression on survival was even more evident (62% vs. 80%). p-values were calculated on the basis of the log-rank test (**** $p < 0.0001$; Student's *t*-test).

The cause for an increased CIN70 could be a defect in the DNA repair pathway homologous recombination or the DNA damage response. To test this, the role of mRNA expression of RAD51 and CHK1 in respect to CIN70 was analyzed. It was noticeable that the RAD51 expression is significantly higher in CIN high (Figure 1D and Supplementary Figure S1B,D) than in CIN low tumors. This effect was especially pronounced in the TNBC subtype. A significantly increased expression in CIN high compared to CIN low was also found for CHK1 (Figure 1E and Supplementary Figure S1C,D) in both subtypes. Consequently, increased expression of RAD51 and CHK1 in CIN high tumors had a negative effect on survival (Figure 1F,G). Patients whose tumor had a high expression of RAD51 showed significantly lower DSS after both 5 and 10 years compared to low RAD51 expression. For the expression of CHK1, the negative effect of a high expression on survival was even more evident. These data suggest that both increased expression of RAD51 and CHK1 may lead to a decreased DNA repair or DNA damage response resulting in tumors with increased chromosomal instability [27].

3.2. No Correlation of HR Capacity, Replication Fork Protection, and Sensitivity to PARP1 Inhibition and MMC Treatment

Numerous publications have shown that contrary to the assumption that the more protein present, the more DNA repair capacity can be expected—high expression of RAD51 does not lead to improved HR capacity [27–31]. However, the effect of a high CHK1 expression in tumors has not yet been investigated. It is possible that differences in genetic background or individual cellular adaptation strategies such as tolerance to replication stress are responsible for this phenomenon. To test these aspects, a genetically related system of TNBC was chosen consisting of three MDA-MB-231-derived cell lines, which differ only in their metastatic pattern. While MDA-MB-231 metastasizes to all organs, BR is exclusively colonized in the brain [32] and SA in the bone marrow [33]. For comparison, the luminal cell line MCF7 was used. With this system we first investigated the influence of the expression of DNA repair proteins on the various functions of HR, such as double-strand break (DSB) repair, replication fork protection and cellular survival after treatment with PARP1 inhibitor or MMC. A comparable upregulation of CHK1 and RAD51 on the protein level was detected in TNBC cell lines, showing a TNBC-associable expression pattern (Figure 2A, Supplementary Figure S2A–D). The MDA-MB-231 showed a slightly increased expression of CHK1 and a further increase in BR and SA compared to the luminal cell line MCF7. The same pattern is observed for the expression of RAD51 with a significant increase in MDA-MB-231, BR, and SA compared to MCF7 cells. Differences in HR based on a higher S/G2 phase fraction can be excluded. (Supplementary Figure S3).
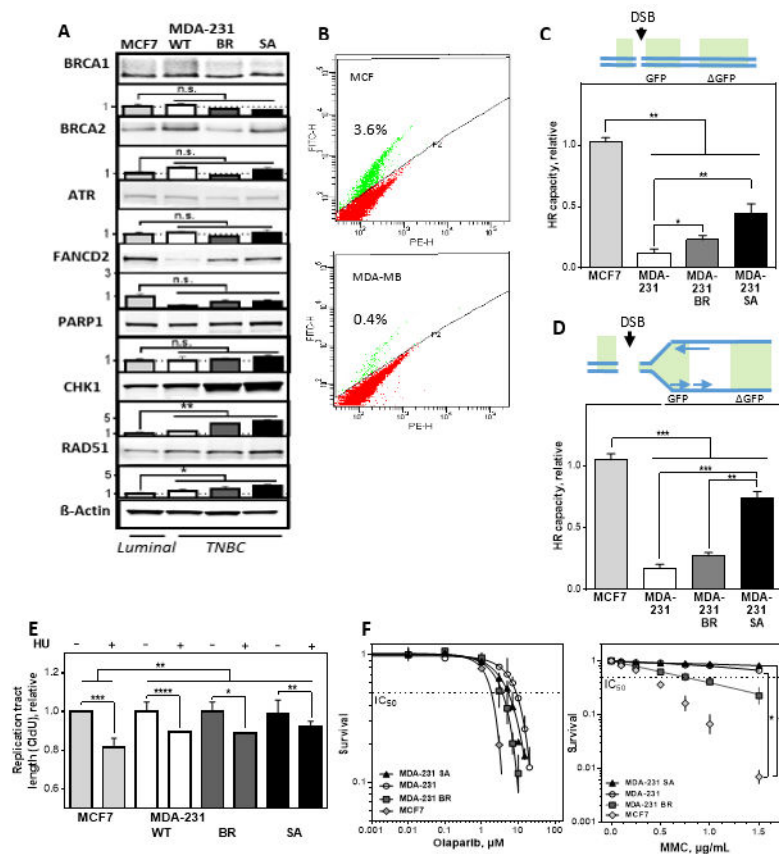
Figure 2. Low homologous recombination (HR) capacity is compatible with efficient replication fork protection and resistance to PARP1 inhibition and mitomycin C (MMC) in TNBCs. (**A**) Immunoblot detection of BRCA1, BRCA2, ATR, FANCD2, PARP1, CHK1 and RAD51 derived from total cell extracts of exponentially growing MCF7 and MDA-MB-231/BR/SA cells. The MDA-MB-231 showed a slightly increased expression of CHK1 (1.49 ± 0.1) and a further increase in BR (3.7 ± 0.1) and SA (4.3 ± 0.3) compared to MCF7 cells. The same pattern is observed for the expression of RAD51 with a significant increase of 1.64 ± 0.3 in MDA-MB-231, 2.4 ± 0.5 and 2.6 ± 0.3 in BR and SA compared to MCF7 cells. ß-Actin was used as the loading control. Data are presented as mean ± SEM. Immunoblot signals were detected and quantified by a LiCor system. (**B**–**D**) Repair of open and replication-associated DNA double-strand break (DSB) as a measure of HR capacity, determined by plasmid-reconstruction assay and analyzed by FACS. Cells were transiently transfected with the pDRGFP construct (**C**) or DR-ori-GFP plus the ori-activating MSCV-N EBNA1 construct (**D**) for 24 h. The number of GFP-expressing cells was normalized to the absolute HR capacity of MCF7. A significantly lower HR capacity for frank DSB was found in all TNBCs compared to MCF7 cells, with 0.12 ± 0.008 for MDA-MB-231, 0.23 ± 0.04 for BR, and 0.45 ± 0.07 for SA. The same pattern was observed for DSBs adjacent to a DNA replication origin, with 0.17 ± 0.03 for MDA-MB-231, 0.27 ± 0.03 for BR, and 0.75 ± 0.05 for SA compared to MCF7 cells. (**E**) Mean length of DNA fibers in MCF7 and MDA-MB-231/BR/SA cells. The cells were sequentially labelled with CldU and IdU for 30 min and treated with HU between both labels for 4 h. DNA was spread on slides, fixed and incorporated nucleotides were detected by immunofluorescence. Although all cell lines showed a shortening of the CldU tract, MCF7 showed the most pronounced shortening with 0.8 ± 0.004, followed by MDA-MB-231 and BR with 0.89 ± 0.003 and 0.89 ± 0.001. SA showed only a minimal shortening of the CldU tract with 0.93 ± 0.006. The length of the DNA fibers was measured with the Image J software and calculated relative to the absolute length of the untreated controls. (**F**) Cellular survival after treatment with olaparib (left) or MMC (right) in MCF7 and MDA-MB-231/BR/SA cells. The cells were seeded 24-h prior treatment with olaparib or MMC for 5 days or 1 h, fixed after 14 days, and the number of colonies was counted. Shown are means from three independent experiments ± SEM. Asterisks represent significant differences (* $p < 0.05$; ** $p < 0.01$; *** $p < 0.001$; **** $p < 0.0001$, n.s. not significant; Student's *t*-test).

Due to the different DNA structure represented by a DSB somewhere in the genome and a DSB adjacent to an active replication fork, we used two DNA repair constructs that allow both situations to be simulated. For this purpose, two repair constructs were used to investigate the DNA repair capacity by HR of a single DNA double-strand break (DR-GFP) (Figure 2B,C) or a DNA double-strand break adjacent to an origin of replication (DR-ori-GFP) (Figure 2D), transfected and analyzed by flow cytometry [34]. Significantly lower HR capacities for frank DSBs and DSBs adjacent to a DNA replication origin were found in all TNBCs compared to MCF7 cells. It is striking that the original cell line had the lowest HR capacity in both constructs, BR a slightly higher and SA the highest HR capacity. Thus, increased expression of RAD51 and CHK1 is not associated with increased DNA DSB repair capacity in TNBC.

In addition to DSB repair, HR proteins are required for the stabilization of replication forks, protecting them from nucleolytic degradation, with RAD51 and CHK1 being critical factors [9,35]. To test their protective function, the DNA fiber assay was performed after depletion of the nucleotide pool by addition of hydroxyurea (HU) (Figure 2E). Although all cell lines showed a shortening of the CldU tract, MCF7 with the highest HR capacity showed the most pronounced shortening, followed by MDA-MB-231 and BR. SA showed the strongest protection and only a minimal shortening of the CldU tract.

Next, we tested whether the difference in HR capacity is reflected by sensitivity to PARP1 inhibition by olaparib or MMC treatment in the colony formation assay. Figure 2F shows cellular survival after increasing concentrations of olaparib (left) and MMC (right) for the four cell lines studied. Although the HR capacity showed clear differences, this was not reflected by the sensitivity against PARP1 inhibition since all cell lines showed comparable IC50 values between 1.9 ± 0.2 µM for the cell lines with the highest and 8.5 ± 0.2 µM for the cell line with the lowest HR capacity. The same effect, but to a greater extent, was observed after treatment with MMC. Again, the cell line with the lowest HR capacity showed a 10-fold higher resistance. Thus, there was no correlation between HR capacity, and cellular sensitivity to chemotherapeutic agents exhibiting their toxic effect at the replication fork.

3.3. MMC Sensitivity Is Associated with DNA Damage Foci Formation in the S-Phase

Functional HR is characterized by the formation of RAD51 foci after damage followed by their removal after successful DNA repair in S- and G2-phase. Figure 3A shows the formation of RAD51 foci after treatment with MMC in pulse-labeled EdU-positive cells. All cell lines were able to form RAD51 foci; however, MMC-resistant TNBCs showed only a weak induction compared to the sensitive lines. A comparable pattern was also observed for the number of γH2AX foci, with a significantly stronger fold increase in sensitive compared to resistant cell lines. These results indicate that HR is the preferred DNA repair pathway in the two resistant cell lines in the S-phase.
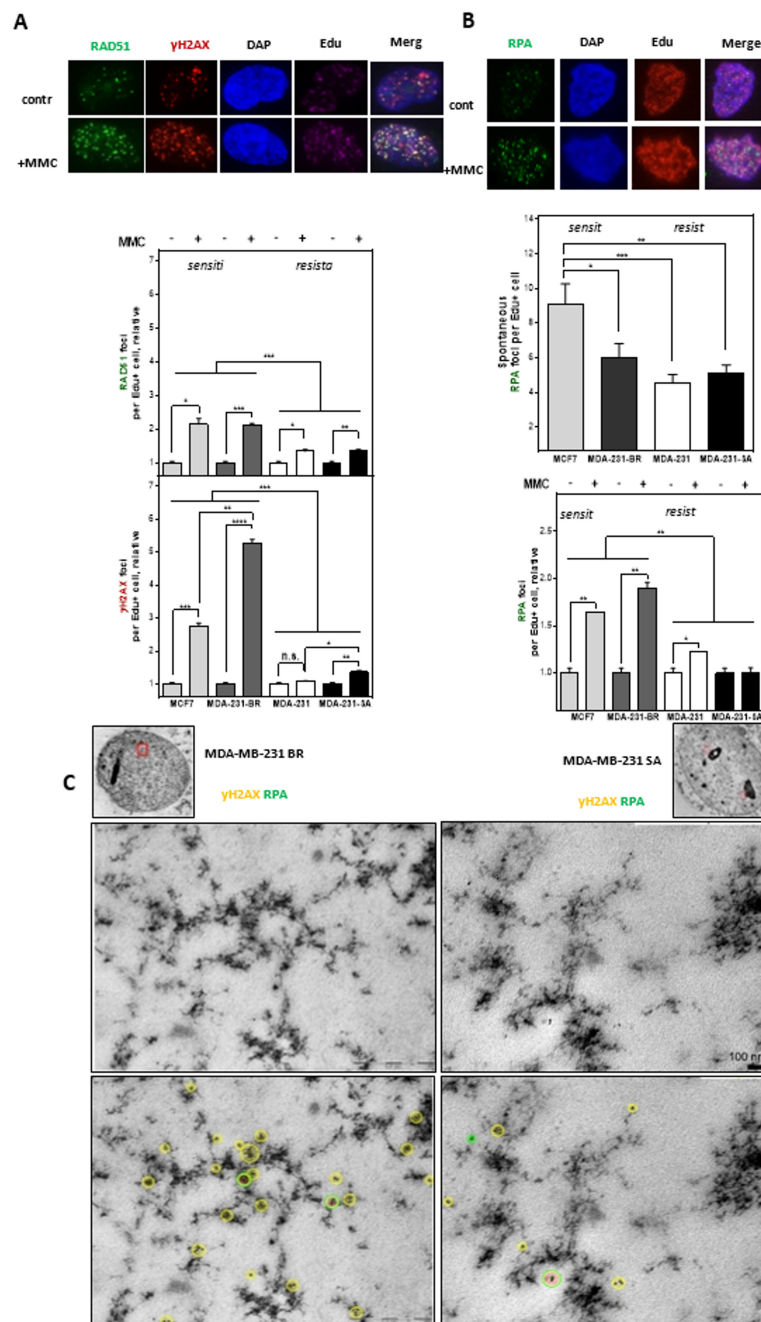
Figure 3. Resistance to MMC is due to the improved repair of DNA damage at DNA replication forks. (**A**) RAD51(green) and γH2AX foci (red) as well as (**B**) RPA foci (green) in S-Phase (Edu+) cells arising spontaneously or after treatment with MMC. Cells were treated with 0.5 μg/mL MMC for 1 h after pulse labeling with 10 μM Edu for 20 min. Immunofluorescent staining was performed 24 h after treatment with γH2AX or RPA and fluorescent second antibodies. Replicating cells were discriminated by incorporated Edu stained with the "click-it" reaction. Foci analysis was done with the Image J Software. Foci were only counted in Edu-positive nuclei (*n* = 100). DNA was counterstained by DAPI. The number of Foci was calculated relatively to the number of Foci in untreated control. Shown are means of three independent experiments ± SEM. Asterisks represent significant differences (* *p* < 0.05; ** *p* < 0.01; *** *p* < 0.001; **** *p* < 0.0001, n.s. not significant; Student's t-test). (**C**) Transmission electron microscopy shows colocalization of gold-labeled γH2AX (yellow) and RPA (green) for MDA-MB-231 BR and MDA-MB-231 SA cells in untreated and MMC treated cells (0.5 μg/mL) 24 h after treatment within nuclear ultrastructure mainly associated to heterochromatic regions.

In order to analyze whether the high amounts of RAD51 and γH2AX-foci in the MMC-sensitive cells arise from increased replication stress RPA-foci after MMC treatment were quantified in EdU-positive cells (Figure 3B). The two sensitive cell lines clearly showed 1.5 to 2 times higher amounts of RPA foci than the resistant cell lines without exogenous damage. This increased replication stress in the sensitive cell lines also occurred after treatment with MMC, with on average significantly more RPA foci compared to the resistant cell lines.

To further localize the occurrence of DNA damage in the S-phase, replication-associated DSBs were visualized by electron microscopy by parallel labeling of γH2AX and RPA after mitomycin C in one of the sensitive and resistant cell lines. (Figure 3C, Supplementary Figure S4). In the sensitive cell line, an accumulation of γH2AX adjacent to isolated RPA foci in heterochromatic areas (dark staining) was already observed in the untreated state, while the resistant line showed both RPA and γH2AX rather sporadically and broadly distributed and less frequent.

This trend intensified further after treatment with MMC and reveals the accumulation of several γH2AX signals in the sensitive cell line around a single RPA signal, whereas in the resistant cell line both markers remained scattered in the nucleus (Supplementary Figure S4). This suggests that the sensitive cell line shows increased DSBs at stalled replication forks, generally also referred to as replication stress. The data very clearly indicate that MMC sensitivity is most likely due to increased replication stress in the two sensitive cell lines.

3.4. Activation of DNA Damage Response Leads to Resistance to MMC by Avoiding Replication Stress

The potential mechanism underlying the differential cellular sensitivity to MMC was investigated by visualization of replication processes [36]. Figure 4A shows the frequency distribution of DNA strand lengths, i.e., before actual damage by MMC or after MMC treatment (Supplementary Figure S5A), compared to untreated control. The sensitive cell lines MCF7 and BR showed significantly shorter DNA strands after damage with MMC than in the untreated control, while the two resistant cell lines showed moderate or no shortening. These observations demonstrate that the differential HR capacity shown in Figure 2B–D cannot explain the observed differences in cellular sensitivity to MMC, which instead appear to be linked to the protection of replication tracts, and therefore to the DNA damage response at the replication fork. To verify this, the activation of ATR, CHK1, and RPA was investigated.

Figure 4B shows the phosphorylation of ATR, CHK1, and RPA after MMC (Supplementary Figure S6A,B). The phosphorylation of CHK1 was clearly associated with resistance to MMC, and showed a more than two-fold activation in the two resistant cell lines compared to the two sensitive. This activation, which can be clearly assigned to resistance, is also reflected in the reduced phosphorylation of RPA showing a 7.0 ± 0.4 and 6.0 ± 0.02 fold increase in the two sensitive cell lines but not in the two resistant ones. The activation of ATR, on the other hand, showed no consistent response in the sensitive and resistant cell linesThese activation patterns suggest that CHK1 plays a crucial role in MMC resistance. To test this hypothesis, we treated the cells with MMC in the presence of a CHK1 inhibitor and determined the length of the DNA strands with the DNA fiber assay. Figure 4C shows the frequency distribution of CldU or IdU (Supplementary Figure S5B) labeled DNA fibers, i.e., before MMC damage, but in the presence of the CHK1 inhibitor MK8776. As expected, the two resistant cell lines showed a significant effect in response to the CHK1 inhibitor, while there were only minor effects present in the sensitive ones. This confirms the assumption that the observed resistance is due to an increased activation of CHK1.
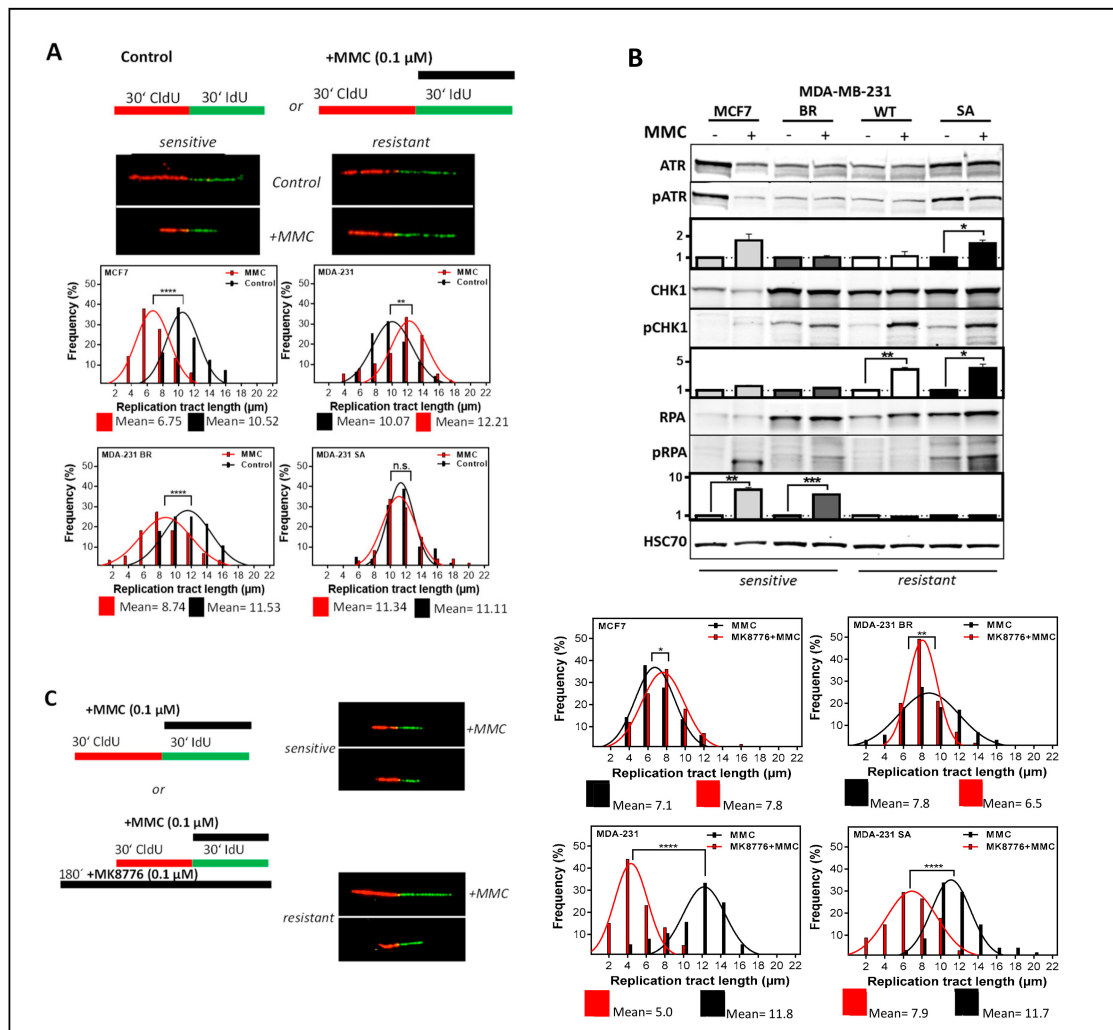
Figure 4. CHK1 inhibition leads to increased replication stress only in MMC-resistant TNBC. (**A**) Examples and frequency distribution of DNA fiber lengths (CldU) in untreated and MMC treated cells. Exponentially growing cells were sequentially labeled with CldU and IdU in the absence or presence of MMC (0.1 μM). DNA was spread and incorporated CldU and IdU was detected with appropriate antibodies. Shown are means ± SEM of DNA fiber length (CldU) frequency distributions of three independent experiments. Asterisks represent significant differences (** $p < 0.01$; *** $p < 0.0001$, Student's *t*-test). (**B**) Immunodetection of activated intra-S phase checkpoint proteins. Cells were treated with 1.5 μg/mL MMC for 1 h and proteins were extracted 24 h later. Proteins were separated and transferred by Western blotting. Detection of proteins was performed with appropriate antibodies. HSC70 served as the loading control. Phosphorylation of the untreated control was used for standardization and ratios of phosphorylated to non-phosphorylated protein are shown. Data from three independent experiments were used for quantification. Errors are mean values + SEM. (**C**) DNA fiber lengths of CldU labeled tracts after treatment with MMC in the presence of the CHK1 inhibitor MK8776 (1 μM). Exponentially growing cells were incubated for 2 h with MK8776 and sequentially labeled with CldU and IdU (plus 0.1 μM MMC), DNA was spread and incorporated nucleotides were detected with the appropriate antibodies. The frequency distribution of DNA fiber lengths in the first label (CldU) of three independent experiments is shown. Asterisks represent significant differences (* $p < 0.05$; ** $p < 0.01$; *** $p < 0.001$; **** $p < 0.0001$, n.s. not significant; Student's t-test).

3.5. Activation of CHK1 Protects against DNA Damage in the S-Phase and Mediates Resistance to MMC in HR-Deficient Cell Lines

Next, it was investigated whether the observed replication stress after inhibition of CHK1 in the two resistant cell lines had a more pronounced effect on DNA damage and cellular survival. Figure 5A shows the occurrence of a pan-nuclear γH2AX signal as a marker of the replicative catastrophe [37] after MMC damage. While in the two sensitive cell lines a large proportion of cells with pan-nuclear γH2AX signal could be observed following MMC treatment, the two resistant lines showed a 3–4 times lower percentage of pan-nuclear γH2AX positive cells. Conversely, after combined treatment with MMC and CHK1 inhibitor, the percentage of pan-nuclear γH2AX positive cells increased 6- and 2.5-fold respectively in the two resistant cell lines, whereas the two sensitive lines showed only a 1.2-fold increase relative to MMC mono treatment. These results suggest that MMC treatment alone was already sufficient to induce the replicative catastrophe in sensitive cells. In the resistant cells, this effect was only achieved to a comparable extent when MMC was combined with CHK1 inhibition.
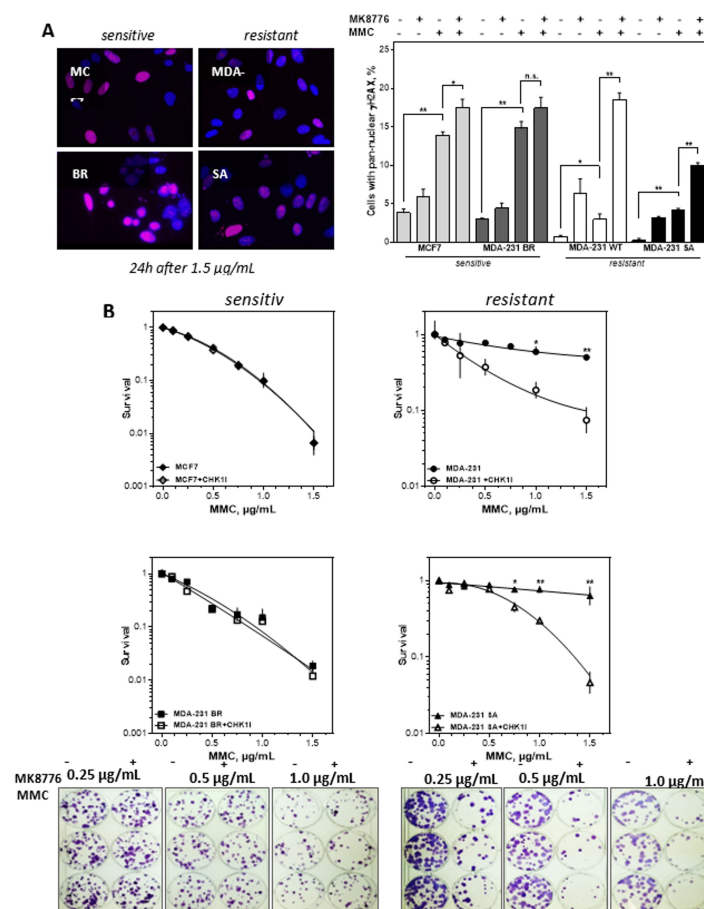
Figure 5. CHK1 inhibition sensitizes only cells with resistance towards MMC.

(**A**) Percentage and representative examples of cells with pan-nuclear yH2AX signal (red) after treatment with MMC alone or combined with CHK1 (MK8776) inhibition. Exponentially growing cells were treated with 0.5 μg MMC for 1 h after being incubated with 2 μM MK8776 for 2 h. The 24 h after treatment immunofluorescence staining for γH2AX was performed and nuclei were counterstained with DAPI. Cells with pan-nuclear γH2AX signal indicating replication stress were microscopically evaluated. Means + SEM of three independent experiments are shown. Asterisks represent significant differences (* $p < 0.05$, ** $p < 0.001$, *** $p < 0.0001$, Student's *t*-test). (**B**) Cellular survival after treatment with MMC alone or in combination with the CHK1 inhibitor MK8776. Cells were plated, treated with MK8776 (2 μM) for 2 h and/or MMC for 1 h, fixed and stained after 14 days and the number of colonies was counted. Adding MK8776 sensitized the two resistant cell lines to MMC ($p = 0.003$ and 0.007 at 1.5μg/mL MMC). For the two MMC sensitive cells there was no sensitizing effect by the CHK1 inhibitor. Shown are means of three independent experiments ± SEM. Asterisks represent significant differences (* $p < 0.05$; ** $p < 0.01$, Student's *t*-test). Induction of the replicative catastrophe should result in cell death, which was investigated by the colony formation assay. Figure 5B shows that adding the CHK1 inhibitor MK8776 sensitized the two resistant cell lines to MMC. The IC50 values for the two cell lines were reduced by an enhancement factor of 4.3 and 2.9. For the two MMC sensitive cells there was no sensitizing effect by the CHK1 inhibitor. Thus, only cell lines resistant to MMC could be sensitized by inhibition of CHK1 (* $p < 0.05$; ** $p < 0.01$; *** $p < 0.001$; **** $p < 0.0001$, n.s. not significant; Student's t-test).

4. Discussion

In this study, we showed a negative association of a high CIN70 score with DSS in breast cancer and confirmed data from previous studies [2,3]. Furthermore, we observed that a high CIN 70 score determines survival in both good and poorly curable subgroups of breast cancer. The high CIN70 score in LumA corresponds to the low CIN70 score of the TNBC. This implies that the use of a more aggressive therapy for LumA with a high CIN70 score could possibly lead to significantly higher survival rates. An increased DNA repair capacity to compensate the higher CIN with a resulting therapy resistance as the cause of the poor prognosis for breast as well as other tumors [3]. We confirm here that this assumption applies not only to TNBCs but also to LumA, with a significantly increased mRNA expression of RAD51 and CHK1 in tumors with high CIN scores. Accordingly, DSS was negatively associated with increased expression of both genes. This confirms data from us and others showing an association of high expression and poor prognosis for RAD51 [38–41], as well as CHK1 [41–43] at the protein and mRNA levels, respectively. However, there is also a highly significant increase in mRNA expression with CIN, both for RAD51 and even stronger for CHK1. This observation clearly shows that more DNA repair protein does not lead to increased DNA repair. It seems more likely that the superior DNA damage response with cell cycle checkpoints or increased tolerance to DNA damage is causal. Both options would lead to decreased response and poorer survival of treated patients. In the present study, the general DNA damage response appears to be the decisive factor for the observed therapy resistance in TNBCs.

In addition, we showed that TNBC cells display no degradation of replication forks and no increased olaparib sensitivity despite a reduced HR capacity. Rather, resistance was observed after MMC with adequate RAD51 focus formation and correspondingly low levels of the DNA damage marker γH2AX in the S-phase. This was due to a pronounced activation of the DNA damage response by CHK1, which ensured unimpaired replication and could be reversed by CHK1 inhibition. Thus, this study demonstrates an important role of CHK1 which can compensate for a reduced HR capacity by preventing replication stress in TNBC.

A correlation of increased RAD51 and CHK1 expression was observed in several studies and was significantly associated with TNBC status [44]. The low HR capacity in TNBC cells observed here also confirms the described limited HR functionality in TNBCs in the clinical setting [21]. Despite high RAD51 expression and functional BRCA1 a low HR capacity was observed by the plasmid reconstruction assay. This could be attributed to a lack of activation of CHK2 via ATM [45]. It is more

likely that the induction of a single DSB activates neither ATM, nor ATR [8]. The limited validity of the detection of a single DSB is strongly supported by the observation that cells without BRCA1 expression show a high HR capacity for a replication-independent DSB and virtually no HR capacity for a replication-associated DSB (Supplementary Figure S7).

One of the further functions of HR is the protection of replication forks. Cells with the highest HR capacity showed the highest instability of replication forks. Reduced protection of replication forks has already been observed in tumor cells despite functional HR [9]. This distinguishes tumor from non-tumor cells for which stabilization of replication forks by HR factors is essential [46].

Despite their low HR capacity, MDA-MB-231 were resistant to olaparib and MMC. Both agents lead to one-ended DSB, which occur when a replication fork hits a single strand break and collapses [47,48]. A replication run-off occurs, the replication machinery dissociates and a DNA end is released [49] which is the substrate for the third function of HR [47]. The one-ended DSB resulting from MMC treatment represents a more complex repair situation for the cell and activates both nucleotide excision and Fanconi repair factors [50]. Only after successful activation of FANCD2 a substrate for HR is provided in the further repair process [51,52]. All cell lines could successfully form RAD51 foci according to their cellular survival after MMC. Thus, no HR defect was observed.

The processes of HR at the replication fork, such as fork protection and repair of one-ended DSB, are controlled by the intra-S phase damage response kinase ATR and its downstream kinase CHK1 [45]. The replication fork stabilizing function of CHK1 can be observed after PARP1 inhibition and MMC treatment and is independent of ATR, RAD51, and BRCA1 [35,45,53,54]. The resistance mechanism may involve avoidance of one-ended DBSs or activation of alternative DNA repair pathways [14,55]. More obvious is the direct negative effect of CHK1. The inhibition of CHK1 leads to the increased initiation of replication and increased phosphorylation of further ATR targets. This results in production of more DSBs, reduced MRE11 activity [17] and an affected HR function due to the phosphorylation of RAD51 [56]. Thus, efficient utilization of the ATR-CHK1 signaling cascade can compensate for reduced HR function. This is confirmed by studies in ovarian carcinoma [57]. Thus, the activation of CHK1 could influence the sensitivity of HR deficient tumors. Therefore, the established methods to successfully identify HR deficient tumors should be extended by the detection of CHK1 activation. This could be made possible by extending BRCA1/2 testing by genes of the intra S-phase damage response or the combined detection of RAD51 with RPA in S-phase cells [25,26,58].

References

1. Bianchini, G.; Balko, J.M.; Mayer, I.A.; Sanders, M.E.; Gianni, L. Triple-negative breast cancer: Challenges and opportunities of a heterogeneous disease. *Nat. Rev. Clin. Oncol.* **2016**, *13*, 674–690. [CrossRef]
2. Carter, S.L.; Eklund, A.C.; Kohane, I.S.; Harris, L.N.; Szallasi, Z. A signature of chromosomal instability inferred from gene expression profiles predicts clinical outcome in multiple human cancers. *Nat. Genet.* **2006**, *38*, 1043–1048. [CrossRef]
3. Birkbak, N.J.; Eklund, A.C.; Li, Q.; McClelland, S.E.; Endesfelder, D.; Tan, P.; Tan, I.B.; Richardson, A.L.; Szallasi, Z.; Swanton, C. Paradoxical relationship between chromosomal instability and survival outcome in cancer. *Cancer Res.* **2011**, *71*, 3447–3452. [CrossRef] [PubMed]

4. Karanam, K.; Kafri, R.; Loewer, A.; Lahav, G. Quantitative live cell imaging reveals a gradual shift between DNA repair mechanisms and a maximal use of HR in mid S phase. *Mol. Cell* **2012**, *47*, 320–329. [CrossRef] [PubMed]

5. Heyer, W.D.; Ehmsen, K.T.; Liu, J. Regulation of homologous recombination in eukaryotes. *Annu. Rev. Genet.* **2010**, *44*, 113–139. [CrossRef] [PubMed]

6. Symington, L.S.; Gautier, J. Double-strand break end resection and repair pathway choice. *Annu. Rev. Genet.* **2011**, *45*, 247–271. [CrossRef] [PubMed]

7. Sorensen, C.S.; Syljuasen, R.G.; Falck, J.; Schroeder, T.; Ronnstrand, L.; Khanna, K.K.; Zhou, B.B.; Bartek, J.; Lukas, J. Chk1 regulates the S phase checkpoint by coupling the physiological turnover and ionizing radiation-induced accelerated proteolysis of Cdc25A. *Cancer Cell* **2003**, *3*, 247–258. [CrossRef]

8. Saleh-Gohari, N.; Bryant, H.E.; Schultz, N.; Parker, K.M.; Cassel, T.N.; Helleday, T. Spontaneous homologous recombination is induced by collapsed replication forks that are caused by endogenous DNA single-strand breaks. *Mol. Cell. Biol.* **2005**, *25*, 7158–7169. [CrossRef]

9. Schlacher, K.; Wu, H.; Jasin, M. A distinct replication fork protection pathway connects Fanconi anemia tumor suppressors to RAD51-BRCA1/2. *Cancer Cell* **2012**, *22*, 106–116. [CrossRef]

10. Poole, L.A.; Cortez, D. Functions of SMARCAL1, ZRANB3, and HLTF in maintaining genome stability. *Crit. Rev. Biochem. Mol. Biol.* **2017**, *52*, 696–714. [CrossRef]

11. Liao, H.; Ji, F.; Helleday, T.; Ying, S. Mechanisms for stalled replication fork stabilization: New targets for synthetic lethality strategies in cancer treatments. *EMBO Rep.* **2018**, *19*. [CrossRef] [PubMed]

12. Puccetti, M.V.; Adams, C.M.; Kushinsky, S.; Eischen, C.M. Smarcal1 and Zranb3 Protect Replication Forks from Myc-Induced DNA Replication Stress. *Cancer Res.* **2019**, *79*, 1612–1623. [CrossRef] [PubMed]

13. Ciccia, A.; Elledge, S.J. The DNA damage response: Making it safe to play with knives. *Mol. Cell* **2010**, *40*, 179–204. [CrossRef] [PubMed]

14. Gonzalez Besteiro, M.A.; Gottifredi, V. The fork and the kinase: A DNA replication tale from a CHK1 perspective. *Mutat. Res. Rev. Mutat. Res.* **2015**, *763*, 168–180. [CrossRef]

15. Saldivar, J.C.; Cortez, D.; Cimprich, K.A. The essential kinase ATR: Ensuring faithful duplication of a challenging genome. *Nat. Rev. Mol. Cell Biol.* **2017**, *18*, 622–636. [CrossRef]

16. Petermann, E.; Maya-Mendoza, A.; Zachos, G.; Gillespie, D.A.; Jackson, D.A.; Caldecott, K.W. Chk1 requirement for high global rates of replication fork progression during normal vertebrate S phase. *Mol. Cell. Biol.* **2006**, *26*, 3319–3326. [CrossRef]

17. Thompson, R.; Montano, R.; Eastman, A. The Mre11 nuclease is critical for the sensitivity of cells to Chk1 inhibition. *PLoS ONE* **2012**, *7*, e44021. [CrossRef]

18. Petermann, E.; Woodcock, M.; Helleday, T. Chk1 promotes replication fork progression by controlling replication initiation. *Proc. Natl. Acad. Sci. USA* **2010**, *107*, 16090–16095. [CrossRef]

19. Yamada, M.; Watanabe, K.; Mistrik, M.; Vesela, E.; Protivankova, I.; Mailand, N.; Lee, M.; Masai, H.; Lukas, J.; Bartek, J. ATR-Chk1-APC/CCdh1-dependent stabilization of Cdc7-ASK (Dbf4) kinase is required for DNA lesion bypass under replication stress. *Genes Dev.* **2013**, *27*, 2459–2472. [CrossRef]

20. Tung, N.M.; Garber, J.E. BRCA1/2 testing: Therapeutic implications for breast cancer management. *Br. J. Cancer* **2018**, *119*, 141–152. [CrossRef]

21. Telli, M.L.; Timms, K.M.; Reid, J.; Hennessy, B.; Mills, G.B.; Jensen, K.C.; Szallasi, Z.; Barry, W.T.; Winer, E.P.; Tung, N.M.; et al. Homologous Recombination Deficiency (HRD) Score Predicts Response to Platinum-Containing Neoadjuvant Chemotherapy in Patients with Triple-Negative Breast Cancer. *Clin. Cancer Res.* **2016**, *22*, 3764–3773. [CrossRef] [PubMed]

22. Watkins, J.; Weekes, D.; Shah, V.; Gazinska, P.; Joshi, S.; Sidhu, B.; Gillett, C.; Pinder, S.; Vanoli, F.; Jasin, M.; et al. Genomic Complexity Profiling Reveals that HORMAD1 Overexpression Contributes to Homologous Recombination Deficiency in Triple-Negative Breast Cancers. *Cancer Discov.* **2015**, *5*, 488–505. [CrossRef] [PubMed]

23. Zhao, E.Y.; Shen, Y.; Pleasance, E.; Kasaian, K.; Leelakumari, S.; Jones, M.; Bose, P.; Ch'ng, C.; Reisle, C.; Eirew, P.; et al. Homologous Recombination Deficiency and Platinum-Based Therapy Outcomes in Advanced Breast Cancer. *Clin. Cancer Res.* **2017**, *23*, 7521–7530. [CrossRef] [PubMed]

24. Gulhan, D.C.; Lee, J.J.; Melloni, G.E.M.; Cortes-Ciriano, I.; Park, P.J. Detecting the mutational signature of homologous recombination deficiency in clinical samples. *Nat. Genet.* **2019**, *51*, 912–919. [CrossRef]

25. Meijer, T.G.; Verkaik, N.S.; Sieuwerts, A.M.; Van Riet, J.; Naipal, K.A.T.; Van Deurzen, C.H.M.; Den Bakker, M.A.; Sleddens, H.; Dubbink, H.J.; Den Toom, T.D.; et al. Functional Ex Vivo Assay Reveals Homologous Recombination Deficiency in Breast Cancer Beyond BRCA Gene Defects. *Clin. Cancer Res.* **2018**, *24*, 6277–6287. [CrossRef]

26. Naipal, K.A.; Verkaik, N.S.; Ameziane, N.; van Deurzen, C.H.; Ter Brugge, P.; Meijers, M.; Sieuwerts, A.M.; Martens, J.W.; O'Connor, M.J.; Vrieling, H.; et al. Functional ex vivo assay to select homologous recombination-deficient breast tumors for PARP inhibitor treatment. *Clin. Cancer Res.* **2014**, *20*, 4816–4826. [CrossRef]

27. Parplys, A.C.; Seelbach, J.I.; Becker, S.; Behr, M.; Wrona, A.; Jend, C.; Mansour, W.Y.; Joosse, S.A.; Stuerzbecher, H.W.; Pospiech, H.; et al. High levels of RAD51 perturb DNA replication elongation and cause unscheduled origin firing due to impaired CHK1 activation. *Cell Cycle* **2015**, *14*, 3190–3202. [CrossRef]

28. Magwood, A.C.; Mundia, M.M.; Baker, M.D. High levels of wild-type BRCA2 suppress homologous recombination. *J. Mol. Biol.* **2012**, *421*, 38–53. [CrossRef]

29. Wurster, S.; Hennes, F.; Parplys, A.C.; Seelbach, J.I.; Mansour, W.Y.; Zielinski, A.; Petersen, C.; Clauditz, T.S.; Munscher, A.; Friedl, A.A.; et al. PARP1 inhibition radiosensitizes HNSCC cells deficient in homologous recombination by disabling the DNA replication fork elongation response. *Oncotarget* **2016**, *7*, 9732–9741. [CrossRef]

30. Paffett, K.S.; Clikeman, J.A.; Palmer, S.; Nickoloff, J.A. Overexpression of Rad51 inhibits double-strand break-induced homologous recombination but does not affect gene conversion tract lengths. *DNA Repair* **2005**, *4*, 687–698. [CrossRef]

31. Kim, P.M.; Allen, C.; Wagener, B.M.; Shen, Z.; Nickoloff, J.A. Overexpression of human RAD51 and RAD52 reduces double-strand break-induced homologous recombination in mammalian cells. *Nucleic Acids Res.* **2001**, *29*, 4352–4360. [CrossRef] [PubMed]

32. Yoneda, T.; Williams, P.J.; Hiraga, T.; Niewolna, M.; Nishimura, R. A bone-seeking clone exhibits different biological properties from the MDA-MB-231 parental human breast cancer cells and a brain-seeking clone in vivo and in vitro. *J. Bone Miner. Res.* **2001**, *16*, 1486–1495. [CrossRef] [PubMed]

33. Pollari, S.; Kakonen, S.M.; Edgren, H.; Wolf, M.; Kohonen, P.; Sara, H.; Guise, T.; Nees, M.; Kallioniemi, O. Enhanced serine production by bone metastatic breast cancer cells stimulates osteoclastogenesis. *Breast Cancer Res. Treat.* **2011**, *125*, 421–430. [CrossRef] [PubMed]

34. Moynahan, M.E.; Cui, T.Y.; Jasin, M. Homology-directed dna repair, mitomycin-c resistance, and chromosome stability is restored with correction of a Brca1 mutation. *Cancer Res.* **2001**, *61*, 4842–4850.

35. Min, W.; Bruhn, C.; Grigaravicius, P.; Zhou, Z.W.; Li, F.; Kruger, A.; Siddeek, B.; Greulich, K.O.; Popp, O.; Meisezahl, C.; et al. Poly(ADP-ribose) binding to Chk1 at stalled replication forks is required for S-phase checkpoint activation. *Nat. Commun.* **2013**, *4*, 2993. [CrossRef]

36. Parplys, A.C.; Petermann, E.; Petersen, C.; Dikomey, E.; Borgmann, K. DNA damage by X-rays and their impact on replication processes. *Radiother. Oncol.* **2012**, *102*, 466–471. [CrossRef]

37. Toledo, L.; Neelsen, K.J.; Lukas, J. Replication Catastrophe: When a Checkpoint Fails because of Exhaustion. *Mol. Cell* **2017**, *66*, 735–749. [CrossRef]

38. Tennstedt, P.; Fresow, R.; Simon, R.; Marx, A.; Terracciano, L.; Petersen, C.; Sauter, G.; Dikomey, E.; Borgmann, K. RAD51 overexpression is a negative prognostic marker for colorectal adenocarcinoma. *Int. J. Cancer* **2013**, *132*, 2118–2126. [CrossRef]

39. Wiegmans, A.P.; Al-Ejeh, F.; Chee, N.; Yap, P.Y.; Gorski, J.J.; Da Silva, L.; Bolderson, E.; Chenevix-Trench, G.; Anderson, R.; Simpson, P.T.; et al. Rad51 supports triple negative breast cancer metastasis. *Oncotarget* **2014**, *5*, 3261–3272. [CrossRef]

40. Alshareeda, A.T.; Negm, O.H.; Aleskandarany, M.A.; Green, A.R.; Nolan, C.; TigHhe, P.J.; Madhusudan, S.; Ellis, I.O.; Rakha, E.A. Clinical and biological significance of RAD51 expression in breast cancer: A key DNA damage response protein. *Breast Cancer Res. Treat.* **2016**, *159*, 41–53. [CrossRef]

41. Rodriguez, A.A.; Makris, A.; Wu, M.F.; Rimawi, M.; Froehlich, A.; Dave, B.; Hilsenbeck, S.G.; Chamness, G.C.; Lewis, M.T.; Dobrolecki, L.E.; et al. DNA repair signature is associated with anthracycline response in triple negative breast cancer patients. *Breast Cancer Res. Treat.* **2010**, *123*, 189–196. [CrossRef] [PubMed]

42. Grabauskiene, S.; Bergeron, E.J.; Chen, G.; Chang, A.C.; Lin, J.; Thomas, D.G.; Giordano, T.J.; Beer, D.G.; Morgan, M.A.; Reddy, R.M. CHK1 levels correlate with sensitization to pemetrexed by CHK1 inhibitors in non-small cell lung cancer cells. *Lung Cancer* **2013**, *82*, 477–484. [CrossRef] [PubMed]

43. Albiges, L.; Goubar, A.; Scott, V.; Vicier, C.; Lefebvre, C.; Alsafadi, S.; Commo, F.; Saghatchian, M.; Lazar, V.; Dessen, P.; et al. Chk1 as a new therapeutic target in triple-negative breast cancer. *Breast* **2014**, *23*, 250–258. [CrossRef] [PubMed]

44. Woditschka, S.; Evans, L.; Duchnowska, R.; Reed, L.T.; Palmieri, D.; Qian, Y.; Badve, S.; Sledge, G., Jr.; Gril, B.; Aladjem, M.I.; et al. DNA double-strand break repair genes and oxidative damage in brain metastasis of breast cancer. *J. Natl. Cancer Inst.* **2014**, *106*. [CrossRef]

45. Jazayeri, A.; Falck, J.; Lukas, C.; Bartek, J.; Smith, G.C.; Lukas, J.; Jackson, S.P. ATM- and cell cycle-dependent regulation of ATR in response to DNA double-strand breaks. *Nat. Cell Biol.* **2006**, *8*, 37–45. [CrossRef]

46. Zadorozhny, K.; Sannino, V.; Belan, O.; Mlcouskova, J.; Spirek, M.; Costanzo, V.; Krejci, L. Fanconi-Anemia-Associated Mutations Destabilize RAD51 Filaments and Impair Replication Fork Protection. *Cell Rep.* **2017**, *21*, 333–340. [CrossRef]

47. Llorente, B.; Smith, C.E.; Symington, L.S. Break-induced replication: What is it and what is it for? *Cell Cycle* **2008**, *7*, 859–864. [CrossRef]

48. Saleh-Gohari, N.; Helleday, T. Conservative homologous recombination preferentially repairs DNA double-strand breaks in the S phase of the cell cycle in human cells. *Nucleic Acids Res.* **2004**, *32*, 3683–3688. [CrossRef]

49. Strumberg, D.; Pilon, A.A.; Smith, M.; Hickey, R.; Malkas, L.; Pommier, Y. Conversion of topoisomerase I cleavage complexes on the leading strand of ribosomal DNA into 5′-phosphorylated DNA double-strand breaks by replication runoff. *Mol. Cell. Biol.* **2000**, *20*, 3977–3987. [CrossRef]

50. Deans, A.J.; West, S.C. DNA interstrand crosslink repair and cancer. *Nat. Rev. Cancer* **2011**, *11*, 467–480. [CrossRef]

51. Huang, J.; Liu, S.; Bellani, M.A.; Thazhathveetil, A.K.; Ling, C.; de Winter, J.P.; Wang, Y.; Wang, W.; Seidman, M.M. The DNA translocase FANCM/MHF promotes replication traverse of DNA interstrand crosslinks. *Mol. Cell* **2013**, *52*, 434–446. [CrossRef] [PubMed]

52. Akkari, Y.M.; Bateman, R.L.; Reifsteck, C.A.; Olson, S.B.; Grompe, M. DNA replication is required To elicit cellular responses to psoralen-induced DNA interstrand cross-links. *Mol. Cell. Biol.* **2000**, *20*, 8283–8289. [CrossRef] [PubMed]

53. Kim, H.; George, E.; Ragland, R.; Rafail, S.; Zhang, R.; Krepler, C.; Morgan, M.; Herlyn, M.; Brown, E.; Simpkins, F. Targeting the ATR/CHK1 Axis with PARP Inhibition Results in Tumor Regression in BRCA-Mutant Ovarian Cancer Models. *Clin. Cancer Res.* **2017**, *23*, 3097–3108. [CrossRef] [PubMed]

54. Yarden, R.I.; Metsuyanim, S.; Pickholtz, I.; Shabbeer, S.; Tellio, H.; Papa, M.Z. BRCA1-dependent Chk1 phosphorylation triggers partial chromatin disassociation of phosphorylated Chk1 and facilitates S-phase cell cycle arrest. *Int. J. Biochem. Cell Biol.* **2012**, *44*, 1761–1769. [CrossRef]

55. Mijic, S.; Zellweger, R.; Chappidi, N.; Berti, M.; Jacobs, K.; Mutreja, K.; Ursich, S.; Ray Chaudhuri, A.; Nussenzweig, A.; Janscak, P.; et al. Replication fork reversal triggers fork degradation in BRCA2-defective cells. *Nat. Commun.* **2017**, *8*, 859. [CrossRef]

56. Sorensen, C.S.; Hansen, L.T.; Dziegielewski, J.; Syljuasen, R.G.; Lundin, C.; Bartek, J.; Helleday, T. The cell-cycle checkpoint kinase Chk1 is required for mammalian homologous recombination repair. *Nat. Cell Biol.* **2005**, *7*, 195–201. [CrossRef]

57. Huntoon, C.J.; Flatten, K.S.; Wahner Hendrickson, A.E.; Huehls, A.M.; Sutor, S.L.; Kaufmann, S.H.; Karnitz, L.M. ATR inhibition broadly sensitizes ovarian cancer cells to chemotherapy independent of BRCA status. *Cancer Res.* **2013**, *73*, 3683–3691. [CrossRef]

58. Telli, M.L.; Stover, D.G.; Loi, S.; Aparicio, S.; Carey, L.A.; Domchek, S.M.; Newman, L.; Sledge, G.W.; Winer, E.P. Homologous recombination deficiency and host anti-tumor immunity in triple-negative breast cancer. *Breast Cancer Res. Treat.* **2018**, *171*, 21–31. [CrossRef]

Exploiting Chromosomal Instability of PTEN-Deficient Triple-Negative Breast Cancer Cell Lines for the Sensitization Against PARP1 Inhibition in a Replication-Dependent Manner

Johanna Rieckhoff [1], Felix Meyer [1], Sandra Classen [1], Alexandra Zielinski [1], Britta Riepen [1], Harriet Wikman [2], Cordula Petersen [3], Kai Rothkamm [1], Kerstin Borgmann [1] and Ann Christin Parplys [1,*]

[1] Laboratory of Radiobiology & Experimental Radio Oncology, Centre of Oncology, University Medical Center Hamburg-Eppendorf, 20246 Hamburg, Germany; j.rieckhoff@uke.de (J.R.); fe.meyer@uke.de (F.M.); s.classen@uke.de (S.C.); a.zielinski@uke.de (A.Z.); riepen@uke.de (B.R.); k.rothkamm@uke.de (K.R.); borgmann@uke.de (K.B.)

[2] Department of Tumor Biology, Center of Experimental Medicine, University Medical Center, Hamburg-Eppendorf, 20246 Hamburg, Germany; h.wikman@uke.de

[3] Department of Radiotherapy and Radio Oncology, University Medical Center Hamburg-Eppendorf, 20246 Hamburg, Germany; cor.petersen@uke.de

* Correspondence: a.parplys@uke.de

Simple Summary: The poor prognosis of patients with TNBC have fostered a major effort to identify more patients who would benefit from targeted therapies. Here we recognize *PTEN* as a potential CIN-causing gene in TNBC and consider PTEN-deficient TNBC for the treatment with PARP1 inhibitors due to the protective role of PTEN during DNA replication.

Abstract: Chromosomal instability (CIN) is an emerging hallmark of cancer and its role in therapeutic responses has been increasingly attracting the attention of the research community. To target the vulnerability of tumors with high CIN, it is important to identify the genes and mechanisms involved in the maintenance of CIN. In our work, we recognize the tumor suppressor gene Phosphatase and Tensin homolog (*PTEN*) as a potential gene causing CIN in triple-negative breast cancer (TNBC) and show that TNBC with low expression levels of PTEN can be sensitized for the treatment with poly-(ADP-ribose)-polymerase 1 (PARP1) inhibitors, independent of Breast Cancer (BRCA) mutations or a BRCA-like phenotype. In silico analysis of mRNA expression data from 200 TNBC patients revealed low expression of PTEN in tumors with a high CIN70 score. Western blot analysis of TNBC cell lines confirm lower protein expression of PTEN compared to non TNBC cell lines. Further, PTEN-deficient cell lines showed cellular sensitivity towards PARP1 inhibition treatment. DNA fiber assays and examination of chromatin bound protein fractions indicate a protective role of PTEN at stalled replication forks. In this study, we recognize *PTEN* as a potential CIN-causing gene in TNBC and identify its important role in the replication processes.

Keywords: CIN; TNBC; PTEN; PARP1 inhibition; replication stress; replication fork instability

---

1. Introduction

Chromosomal instability (CIN) is a type of genomic instability that is defined by the loss or rearrangement of chromosomes that classifies numerical CIN or structural CIN [1]. Defects in several cellular processes, including cell-cycle checkpoint controls, chromosome segregation, DNA repair and

DNA replication are known to cause CIN [2–4]. The spectrum of gene alterations and mutations that cause CIN is only partially known, but insights would be beneficial for the treatment of tumors with high CIN (CIN[+]).

Phosphatase and Tensin homolog (*PTEN*) is an important tumor-suppressor gene frequently mutated or deleted in human cancer. Loss of PTEN has been associated with aneuploidy and poor prognosis in cancer patients [5]. PTEN is known to play an important role in antagonizing the PI3K-AKT pathway in the cytoplasm [6]. Nuclear PTEN is involved in genome maintenance pathways [5]. Several reports indicated, however, that reduced levels or deletion of PTEN also are associated with decreased homologous recombination (HR) efficiency [6–9]. Furthermore, PTEN deficiency induces DNA replication stress, disrupts mitotic spindle architecture and leads to the accumulation of structural and numerical CIN. PTEN is a well-known guardian of the genome due to its control of multiple processes maintaining CIN [5].

PTEN is also often found to be mutated in triple-negative breast cancer (TNBC) [10], the most aggressive subtype of breast carcinoma. It has been reported that loss of PTEN is frequent in TNBC [11] and is associated with an especially aggressive behavior [12] and advanced stage of cancer such as brain metastases [13]. The lack of estrogen, progesterone and human epidermal growth factor receptor 2 (HER-2) of TNBC leaves little scope for targeted therapies [14]. The inhibition of poly-(ADP-ribose)-polymerase 1 (PARP1) is a promising approach for TNBC with a defined defect in the HR repair pathway based on the concept of "synthetic lethality" [15].

Although PARP1 inhibitor therapy has predominantly targeted Breast Cancer (BRCA)-mutated cancers, there is growing evidence that PARP1 inhibitor treatment for non-BRCA-mutant tumors might be beneficial for CIN[+] tumors [16,17].

We aimed to determine the role of PTEN in causing CIN in TNBC. First, we performed an in silico analysis of PTEN messenger RNA expression (mRNA) in TNBC and analyzed PTEN expression in different breast cancer cell lines by Western blot. To further explore the mechanism of PTEN in TNBC, we analyzed DNA replication processes by DNA fiber assays and examined the role of PTEN at the chromatin. To measure the sensitivity towards PARP1 inhibition treatment, we performed a cell survival assay.

2. Results

2.1. Low PTEN Expression Levels Correlate with CIN

To investigate whether PTEN plays a role in the maintenance of CIN in TNBC, an in silico analysis of mRNA expression data from TNBC tumors, previously determined in the Metabric study, was performed [18]. The CIN70 expression signature was derived from a surrogate measure of CIN and is defined as the average expression of 70 genes that correlate with "total functional aneuploidy" in solid tumors [19]. Strikingly, the analysis revealed a significantly lower mRNA expression of PTEN in TNBC with high CIN70 scores (-1.9 ± 0.2) in comparison with TNBC with low CIN70 scores (-0.9 ± 0.13) (Figure 1a), indicating CIN[+] in TNBC with a low PTEN expression. To further investigate the role of PTEN in vitro, we selected five TNBC cell lines (MDA231, BT549, HS578, BT20, GI101) with no mutation in BRCA1-, BRCA2- or BRCA-like phenotypes and four non-TNBC cell lines (SKBR3, MCF7, T47D, BT474) to analyze PTEN expression. Western blot data showed no expression of PTEN in BT549, intermediate expression in MDA231 and low expression among the three other TNBC cell lines (Figure 1b). On average, TNBC cell lines showed a 1.85-fold lower expression of PTEN with 1.6 ± 0.4 compared to 2.9 ± 0.2 in non-TNBC (Figure 1c).
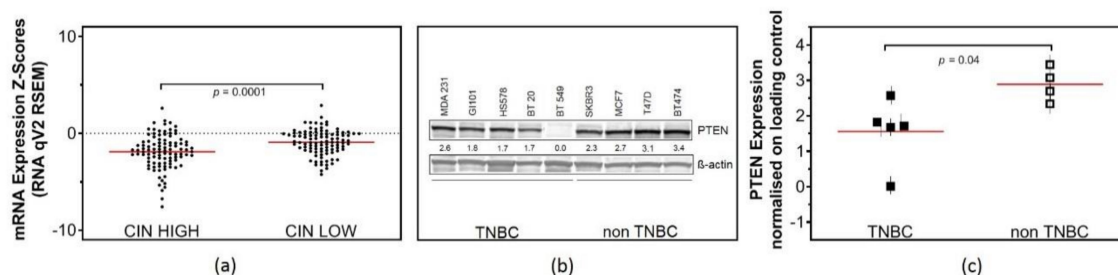
Figure 1. High chromosomal instability (CIN) scores and low phosphatase and tensin homolog (PTEN) expression in triple-negative breast cancer (TNBC). (**a**) In silico analysis of PTEN mRNA expression data, comparing 100 TNBC patients with a high CIN70 score to 100 TNBC patients with a low CIN70 score. (Student's *t*-test $p = 0.0001$) (**b**) Western Blot analysis of PTEN expression in TNBC (MDA231, BT549, BT20, GI101 and HS578T) and non-TNBC breast cancer cell lines (MCF7, T47D, SKBR3, BT474) in relation to ß-actin as loading control. (**c**) Grouped analysis of quantitative PTEN expression normalized on ß-actin, comparing TNBC and non-TNBC breast cancer cell lines. (Student's t-test $p = 0. 0416$). Each value represents the mean of the quantitative analysis of three independent experiments with the SEM indicated.

2.2. Low Expression of PTEN Causes Replication Stress in TNBC Cell Lines

Recently, we determined the HR competence of the cell lines investigated here and we could show that HR was reduced in TNBC cell lines [20]. Since CIN often occurs as a result of defective DNA repair and replication stress [21,22], we performed the DNA fiber assay to analyze the performance of PTEN-deficient cells in DNA replication. Exponentially growing breast cancer cell lines were sequentially pulse-labeled for 30 min each with 5-Chloro-2'-deoxyuridine (CldU) and Iododeoxyuridine (IdU). For replication fork progression, the lengths of DNA fibers were measured in untreated controls (CldU- and IdU-labeled fibers) and active replication origins were counted by quantification of IdU-labeled, CldU-negative fibers. While replication fork progression did not differ between TNBC and non-TNBC cell lines (Figure 2a), the firing of second pulse origins was significantly higher in TNBC, with 23.12% ± 3.2, compared to 13.17% ± 2.6 in non-TNBC cell lines (Figure 2b).
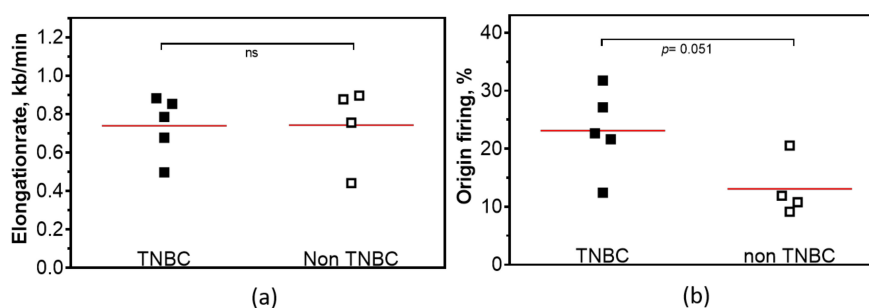

Figure 2. Replication stress in TNBC compared to non-TNBC. (**a**) Replication fork progression and (**b**) activation of replication origins in untreated cell lines of TNBC in comparison to untreated non-TNBC breast cancer cell lines. (Student's *t*-test $p = 0.98$ (**a**) and $p = 0.051$ (**b**). Each value represents the mean of three independent experiments.

2.3. Replication-Dependent Sensitization by PARP1 Inhibition Due to Reduced Replication Fork Elongation and Fork Stalling

Inhibition of PARP1 is an emerging strategy that can be used to selectively target genomic unstable tumors [17]. To investigate the effect of PARP1 inhibition on the replication processes of TNBC, we used the DNA fiber assay to analyze the impact of PARP1 inhibition on the elongation processes, replication fork stalling and the activation of second pulse origins (Figure 3a–g). Exponentially growing TNBC cell lines were sequentially pulse-labeled for 30 min each with CldU and IdU. To analyze

the effect of PARP1 inhibition on replication processes, 1 µM Olaparib was added 120 min before pulse labelling. For fork progression, the lengths of DNA fibers were measured in treated samples and compared to untreated controls (CldU- and IdU-labeled fibers) (Figure 3b). Fork stalling was analyzed by counting CldU-labeled, IdU-negative fibers (Figure 3c). Newly activated replication origins were counted by the quantification of IdU-labeled, CldU-negative fibers (Figure 3d). As shown in Figure 3e, single treatment with 1 µM Olaparib provoked shorter replication tracts in all TNBC cell lines. Furthermore, replication fork stalling was observed for almost all cell lines, albeit to a lesser degree (Figure 3f). The analysis of replication origins showed that origin firing was downregulated in almost all cell lines after PARP1 inhibition (Figure 3g). However, in contrast to the other cell lines, we could observe that the BT549 cell line with no expression of PTEN showed a strong activation of second pulse origin firing. This may be due to the high extent of replication fork stalling.
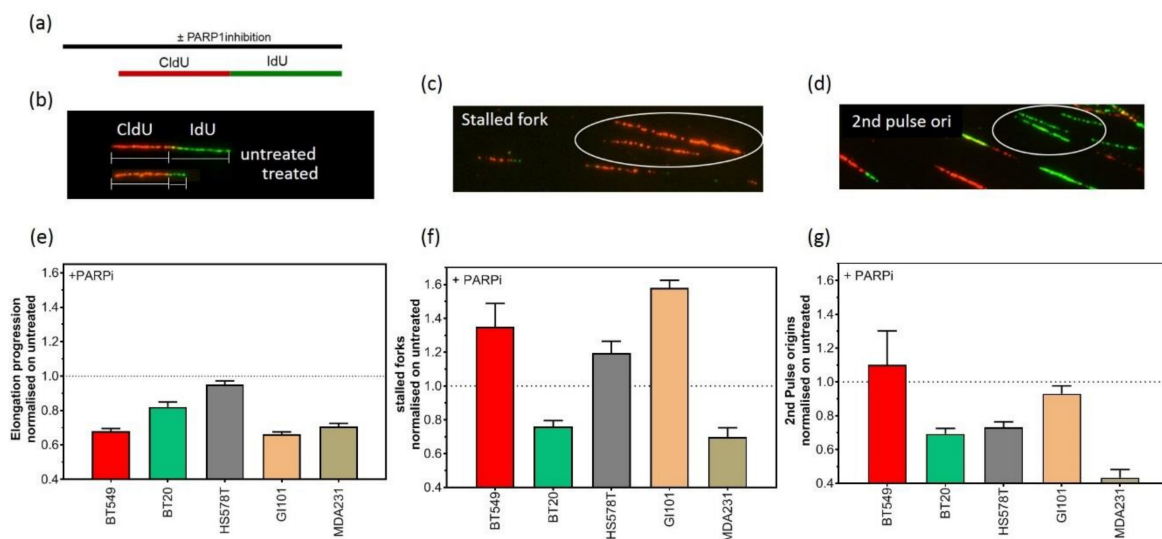
Figure 3. Replication fork elongation, stalling and new origin firing after PARP1 inhibition. (**a**) Overview of DNA fiber assay labelling protocol. Representative picture of reduced IdU-fiber length after treatment, in comparison to full-length IdU fiber in untreated sample (**b**), of CldU labelled, IdU-negative fiber indicating stalled replication fork (**c**) and representative picture of IdU labelled, CldU negative fiber, indicating second pulse origin firing (**d**). Quantitative analysis of elongation tract length (**e**), replication fork stalling (**f**) and second pulse origin firing (**g**) after PARP1 inhibition normalized on untreated controls. Each value represents the mean of at least three independent experiments with SEM indicated.

Given the HR repair defect and the replication-dependent sensitivity of PTEN-deficient cells, we tested the cellular sensitivity of these cells to Olaparib. For three out of five TNBC cell lines, the IC50 was at or below 1 µM Olaparib and only 10% or fewer of the cells survived the treatment with 10 µM Olaparib (Figure 4).

2.4. Lack of PTEN Leads to Replication Fork Instability in TNBC Cell Lines

To further analyze the high amount of replication fork stalling after PARP1 inhibition, we examined the stability of replication forks after treatment with Hydroxyurea (HU) for the TNBC cell lines. Earlier works had shown that the nascent DNA strands of HU-induced stalled replication forks undergo extensive nucleolytic degradation in HR-deficient cells [23]. Exponentially growing TNBC cell lines were pulse-labeled with CldU. CldU was washed out and cells were treated for four hours with 2 mM HU. After HU treatment, cells were washed with phosphate-buffered saline (PBS) and labeled with IdU (Figure 5a). We assessed the stability of replication forks after HU treatment by measuring the length of CldU tracks. TNBC cell lines showed a shortening of the CldU tracks after HU treatment compared to untreated controls, indicating replication fork instability (Figure 5b). BT549 cells with

no expression of PTEN showed the strongest reduction in CldU track length (Figure 5c). In addition, we could demonstrate that the amount of degraded DNA negatively correlated with the amount of PTEN (Figure 5d). These data support the idea that PTEN could be a protective factor at replication forks. By further analyzing SKBR3, MCF7, T47D and BT474 with a high amount of PTEN, we could show that PTEN is a general protective factor at stalled replication forks. No change or increase in CldU track length was observed in three out of four cell lines with a high amount of PTEN (Figure S5).
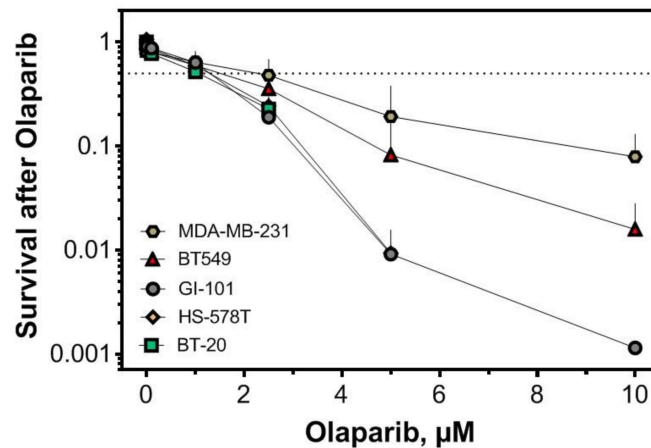
Figure 4. Cellular sensitivity of TNBC to PARP1 inhibition. Colony-forming assays were performed after treatment, with increasing concentrations of the PARP1 inhibitor Olaparib for 90 min. Each value represents the mean of at least three independent experiments, with SEM indicated.
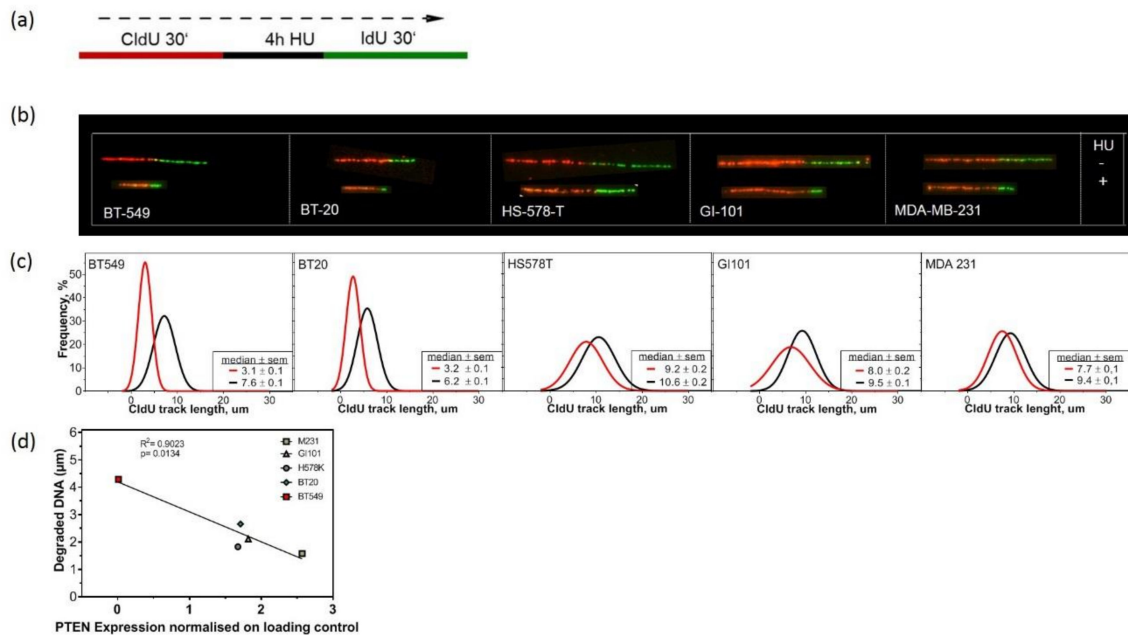
Figure 5. Fork instability after Hydroxyurea (HU) treatment in TNBC, dependent on PTEN expression. (**a**) Overview of DNA fiber assay labelling protocol. (**b**) Representative images of DNA fibers of 5 TNBC cell lines after treatment with 2 mM HU for four hours and untreated cells. Unstable replication fork indicated by shortening in CldU-labelled tract length in comparison to untreated controls. (**c**) Quantitative analysis of CldU elongation track length after treatment with 2 mM HU in comparison to untreated controls. (red: HU treatment, black: untreated) (**d**) CldU elongation length correlates negatively with PTEN expression measured at protein level (see Figure 1). Each value represents the mean of three independent experiments with the SEM indicated.

2.5. PTEN Protects Replication Forks by Supporting the Recruitment of Repair Proteins to the Chromatin

To study the effects of different protein amounts of PTEN, we selected MDA-MB-231 BR (Brain-seeking) cells to analyze the effects of PTEN overexpression compared to BT549 and MDA231. The MDA-MB-231 BR cell line was established from the parental MDA-MD-231 cell line following serial in vivo passaging to the brain [24] and expresses a lower amount of PTEN compared to MDA231 [25]. MDA-MB-231 BR cells were transduced by lentiviral particles containing the PTEN coding sequence (pPTENiZs2puro++tTR+) under the control of doxycycline response element (MDA231/PTEN). MDA 231/PTEN shows the highest expression of PTEN with 5.4 ± 0.2 (normalised on loading control) compared to 2.6 ± 0.3 for MDA231 with an intermediate expression and no expression of PTEN in BT549 (Figure 6a,b and S6). For MDA231/PTEN and MDA231, we could show that PTEN was located at the chromatin with a 2.2-fold higher expression of PTEN for MDA231/PTEN. Additionally, we observed that BT549 had lower amounts of Partner and localiser of BRCA2 (PALB2), PARP1 and Checkpoint kinase 1 (CHK1) at the chromatin compared with MDA231/PTEN and MDA231 (PALB2: 1.1 vs. 3.4 and 1.8, PARP1 3.0 vs. 16.4 and 8.0 and CHK1 1.1 vs. 4.3 and 4.1) (Figure 6a and S6). These data lead us to analyze the phosphorylation of Chk1, an important activator of the Intra-S-phase checkpoint after induced replication stress. After HU treatment, we found that there was an almost two-fold lower phosphorylation of CHK1 in BT549 compared to MDA231/PTEN and MDA231 (Figure 6b). Interestingly, the recruitment and activation of the upstream Kinase Ataxia teleangiectasia and Rad3 related (ATR) of the Intra-S-Phase was not affected after HU treatment. Rather, the data show the strongest activation of ATR in BT549 compared to the other cell lines. Finally, we elucidated the effect of different amounts of PTEN on replication stress. We compared the effect of low PTEN expression in TNBC cell lines with TNBC cell line MDA231/PTEN. MDA231/PTEN displayed a faster replication fork progression, with 1.04 kb/min compared to 0.74 kb/min, and, with 19% compared to 24%, a lower amount of origin firing compared to TNBC with low amounts of PTEN in the unperturbed state (Figure S8a,b). HU treatment had a mild effect on CldU track length (Figure S8c). After PARP1 inhibition, the elongation rate (0.94) and origin firing (1) did not change compared to the untreated state (Figure S8d,f). Only a slight increase in fork stalling could be detected (Figure S8e).
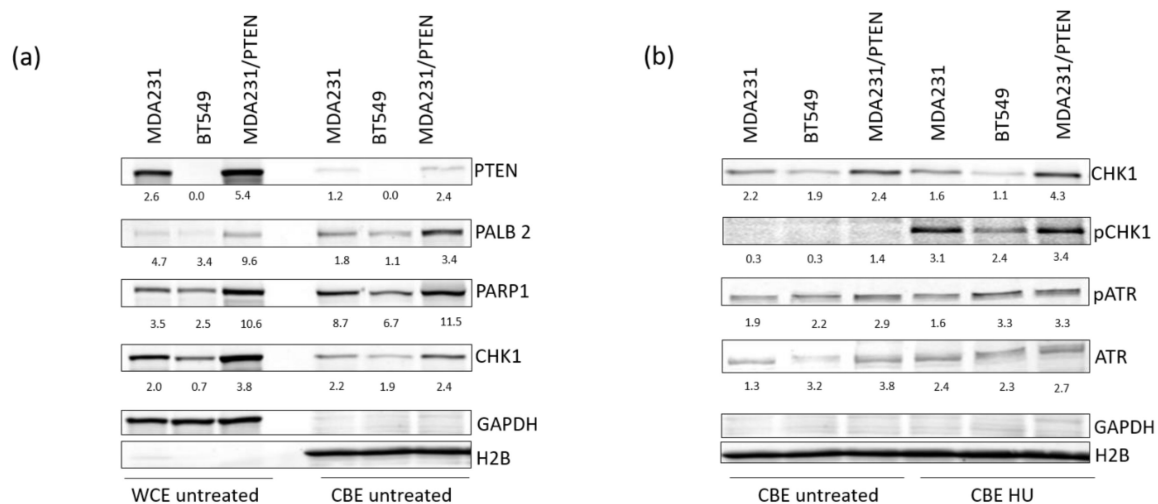

Figure 6. PTEN expression and recruitment of DNA repair proteins to the chromatin in TNBC. (**a**) Western blot analysis of PTEN, PALB2, PARP1 and CHK1 expression in whole cell extracts (WCE) and chromatin-bound extracts (CBE) of untreated TNBC cell lines. GAPDH and H2B served as a loading control for the WCE and CBE, respectively. (**b**) Western blot analysis of CHK1, pCHK1, ATR and pATR expression at the chromatin after treatment with 2 mM HU for 4 h in comparison to untreated controls. H2B served as a loading control.

3. Discussion

The poor prognosis and molecular heterogeneity of patients with TNBC have fostered a major effort to identify more patients who would benefit from targeted therapies. The aim of our work was to investigate the underlying mechanism of PTEN in the maintenance of CIN and to evaluate the potential of PARP1 inhibitor treatment in TNBC with high CIN.

PTEN is mutated in a wide variety of solid tumors. It was reported earlier that disruption of *PTEN* in Mouse Embryonic Fibroblasts (MEFs) leads to extensive centromere breakage and chromosomal translocations due to physical interaction with centromeres and its role in DNA repair [6]. Here, we show that low mRNA expression levels of *PTEN* in tumors from TNBC patients are significantly associated with high CIN (Figure 1a). In vitro analysis aggregates these findings. TNBC cell lines express lower protein levels of PTEN compared to non-TNBC cell lines (Figure 1b). In line with the observation in Prostate cancer cell lines [9], our data provide strong evidence for the involvement of PTEN in double-strand breaks (DSB) repair via HR in TNBC, based on experiments with the reporter plasmid assay [20].

The relationships between HR and DNA replication are well documented [26]. Cells that lack efficient DNA repair systems, particularly HR, show replication stress in the unperturbed state, which is defined as the slowing or stalling of replication fork progression [27]. With this in mind, we were further interested to see if TNBC cell lines with low protein expression of PTEN exhibit replication stress. We demonstrate that all analyzed breast cancer cell lines show slow fork progression (Figure 2a). Moreover, in TNBC cell lines the activation of replication origins was much higher compared to non-TNBC cell lines (Figure 2b). Earlier, we reported that HR-deficiency due to *PALB2*-haploinsufficiency, Rad51AP1-, NUCKS- knockdown and Rad51 overexpression resulted in replication stress due to compromised replication fork progression and high activation of dormant origins [20,28–30]. We reveal from our data that PTEN-deficient TNBC cell lines display endogenous replication stress due to uncontrolled origin firing.

We assume that consecutive rounds of replication stress are a strong driver of CIN and not only do they repair deficiency, but endogenous replication stress could make TNBC cell lines eligible for PARP1 treatment. The sensitization of HR-deficient tumors to PARP1 inhibitors was primarily explained by the concept of synthetic lethality [31]. However, the molecular mechanisms that drive this synthetic lethality remain unclear. PARP1 and HR proteins intersect at DSB repair and replication forks [32]. We reported that PARP1 inhibitors enhance the therapeutic ratio achieved by radiotherapy by interfering with the replication elongation for the HR-deficient head and neck squamous cell carcinoma (HNSCC) cell lines [33]. Here, we demonstrate that replication stress in PTEN-deficient TNBC is increased during the inhibition of PARP1, as evidenced by a further reduction in replication fork progression and a high number of stalled replication forks (Figure 3d,e). We observed that BT549 with no expression of PTEN displayed the strongest effects in replication fork progression and fork stalling. In addition, BT549 showed a strong activation of second pulse origin firing upon PARP1 inhibition (Figure 3g). PARP1 inhibitors cause an increase in DNA single-strand breaks (SSBs), which are converted during replication to DSBs in BRCA1/2-defective cells. However, researchers previously primarily studied DNA damage induction, repair capacity and cell cycle progression upon PARP1 inhibition [34,35]. Recent findings have suggested that the slowing, stalling or collapse of DNA replication forks is the prevalent source of DNA damage, which may contribute to genome instability and lead to the generation of structural and numerical CIN [3]. Our work provides evidence that PTEN plays an important role during replication processes. Although previous studies have focused exclusively on replication fork progression and linked slower fork progression with structural and numerical CIN in cancer, we could show that not only replication fork progression is affected, but also fork stalling and origin firing. ATR safeguards stalled replication forks from collapse and prevents replication catastrophe [36]. ATR kinase activity slows down replication forks and prevents origin firing in damaged cells. By suppressing the excessive firing of replication origins, this prevents the exhaustion of the rate-limiting pool of RPA and the conversion of ssDNA to DSBs in the S phase, a serious threat

to genome stability. Our results demonstrate that considerable effort needs to be expended to identify additional synthetic lethal interactions with genes of the replication stress response.

PARP1 inhibitors have emerged as promising cancer therapeutics, especially for BRCA-mutated tumors that display a deficiency in HR [15]. An ongoing phase II trial of the PARP1 inhibitor Talazoparib is testing patients with pathologic mutations in a somatic or germline non-BRCA1/2 HR pathway gene, such as *PTEN* (NCT02401347). However, further data on the use of PARP1 inhibitors in non-BRCA HR deficiencies are still missing [16]. Previously, we reported that PTEN contributes to HR in prostate cancer and proposed the treatment of agents targeted against defects in HR such as PARP1 inhibitors to PTEN-deficient tumors [9]. Here, we show for the first time that TNBC cell lines with low PTEN protein levels can be sensitized for treatment with PARP1 inhibitors, independent of BRCA mutations or a BRCA-like phenotype. Only 10% or less of the cells survived the treatment with 10 μM Olaparib, which is comparable with the survival rate found in BRCA2 knock out cells or BRCA deficient cell lines [37].

Cells have acquired a multitude of fork protection mechanisms to minimize the genotoxic effects during replication stress [38]. The regulation of replication stress in response to DNA damage involves the reduction in fork progression, the regulation of origin firing [39] and the stabilization of stalled forks [40]. There is evidence that PTEN is an important factor for the stabilization of replication forks, and thus maintains genome stability under replication stress [41]. Wang et al. showed that PTEN is located at replication sites, and physically interacts with replication protein A 1 (RPA1) as well as Ubiquitin Thioesterase OTUB1, which regulates RPA1 stability. After HU-treatment, the length of nascent replication tracts was decreased in PTEN -/- HCT116. Our data support the observation that PTEN also plays an important role in protecting replication forks in TNBC by showing a reduction in CldU track length after HU treatment in cells with lower amounts of PTEN (Figure 5). Here, the amount of degraded DNA negatively correlated with the amount of PTEN. This implies that the amount of PTEN could be essential for fork protection. By analyzing SKBR-3, MCF7, T47D and BT474 we could show that PTEN is a general protective factor at stalled replication forks (Figure S4). There is also evidence that loss of PTEN induces uncontrolled origin firing (Figure 3g). Replication fork stalling and degradation of newly replicated DNA results in regions of ssDNA. ssDNA is protected by RPA coating, followed by the recruitment and activation of ATR and phosphorylation of its main downstream effector CHK1 [42]. The phosphorylation of CHK1 stabilizes the forks and downregulates origin firing, thus delaying the cell cycle progression and allowing to repair DNA damage. Dysregulation in this process may give rise to uncontrolled initiation of origin firing and fork collapse, thus causing genomic instability.

Latterly, we analyzed the effect of different amounts of PTEN at the chromatin using MDA-MB-231 BR to overexpress PTEN, and compared it to moderate expression of PTEN (MDA-MB-231) and no expression of PTEN (BT549) (Figure 6). We could show that PTEN is localized to the chromatin in untreated cells. Further, the amount of PALB2, PARP1 and CHK1 at the chromatin was dependent on the amount of PTEN (Figure 6a). It has been reported for many HR proteins, like BRCA1 and BRCA2, that they might have a repair independent role of protecting stalled replication forks [43,44]. PARP1 has also been implicated in the restart of stalled replication forks through a mechanism that is dependent on Meiotic Recombination 11 Homolog A (Mre11), suggesting that DNA end resection is a critical control point regulated by PARPs [45]. Further, CHK1 has been suggested to bind the PAR chain synthesized by PARP1 at stalled replication forks, which facilitates its kinase activity [46]. Besides its role in stalled replication forks, CHK1, together with ATR, is a regulator of the S-phase checkpoint and the global regulation of further origin firing and activation of DNA repair upon replication stress [39]. After HU treatment, we found an almost two-fold lower phosphorylation of CHK1 for BT549 compared to MDA231/PTEN and MDA231. Interestingly, the recruitment and activation of ATR was not affected (Figure 6b). Due to the great impact of ATR in the regulation of stalled replication forks and origin firing, we think that ATR might also be a good target in the treatment of TNBC with high CIN [47].

Finally, the comparison of replication processes in TNBC with low amounts of PTEN and PTEN overexpression provides strong evidence that the amount of PTEN is crucial for replication processes (Figure S8).

We conclude from our data that PTEN might be an important regulator of replication proteins to the chromatin to protect and regulate the action of replication processes. However, the exact process behind this needs further investigation.

With our work, we could offer detailed insight into the importance of PTEN in the maintenance of CIN by regulating DNA replication processes. We consider that the high CIN of PTEN-deficient TNBC predestines it for treatment with PARP1 inhibitors due to the protective role of PTEN during DNA replication.

4. Material and Methods

4.1. Cell Culture, Plasmids and Survival Assays

The breast cancer cell lines BT20, HS578T, GI101, MCF7, MDA231, MDA468 and SKBR3 were cultivated in DMEM and BT474, BT549 and T47D (provided by the Department of Tumor Biology) in RPMI media, both supplemented with 10% FCS, 2 mM glutamine, 100 U/mL penicillin and 100 mg/mL streptomycin at 37 °C and 10% CO_2 or 5% CO_2 respectively. Zsgreen-positive MDA-MB-231 BR control (231BR/CTL) and PTEN-overexpressing (MDA231/PTEN) cells were generated by lentiviral transduction with either control LeGO-SWITCH vector piZs2puro++tTR+ or overexpression vector pPTENiZs2puro++tTR+ [25] and cultured in DMEM supplemented with 1 µg/mL doxycycline. Stable transfectants were selected in DMEM supplemented with 4 µg/mL puromycin. Suitable concentrations of doxycycline as well as puromycin were determined by titration.

For survival assays, 250 cells were seeded in a 6-well plate 6 h before treatment and cells were cultured for 14 days. Cells were fixed and stained with 1% crystal violet (Sigma-Aldrich, St. Louis, MO, USA). Colonies with more than 50 cells were counted and normalized to untreated samples. Each survival curve represents the mean of at least three independent experiments.

4.2. Clinical in Silico Analysis

Gene expression data for *PTEN* and CIN70 genes in the METABRIC dataset (PMID: 27161491) was retrieved from the cBioPortal (PMID: 22588877, PMID: 23550210). For each tumour, the CIN70 score was calculated according to Birkbak et al. (PMID: 21270108) by summation of expression values of all the CIN70 genes. Afterwards, *PTEN* gene expression was compared in the extreme quartiles of CIN70 score. *p*-values were calculated by Student's *t*-test.

4.3. Mutagenesis Assay

PARP1 inhibition was achieved by adding 1 µM Olaparib (Selleck, Houston, TX, USA) for 90 min to the growth medium. For fork stability experiments, cells were treated with 2 mM Hydroxyurea (HU) (Sigma-Aldrich, Darmstadt, Germany) added to the growth medium for four hours. All treatments were performed at 37 °C and in 10% CO_2 or 5% CO_2 atmosphere.

4.4. Western Blotting

Proteins were extracted and concentration was determined via photometry. A total of 40 µg were resolved by SDS-PAGE using a gradient gel [(4–15%), Bio-Rad Laboratories, Feldkirchen, Germany].

Fractionated extracts were generated using the "Subcellular Protein Fractionation Kit for cultured cells" (Thermo Scientific, Waltham, MA, USA), following the Manufacturer's instruction. After harvesting the cells, all incubation and centrifugation was performed at 4 °C. For each step, phosphatase inhibitor (Halt™ Phosphatase Inhibitor Cocktail, Thermo Scientific, Waltham, MA, USA) was added in addition to the protease inhibitor cocktail included in the Kit. The cytoplasmatic, nuclear and

chromatin-bound fractions were isolated, concentration was determined by photometry, and 20 µg were resolved by SDS-PAGE using a gradient gel [(4–15%), Bio-Rad Laboratories, Feldkirchen, Germany].

After transfer to a Nitrocellulose membrane (Licor, Lincoln, NE, USA), proteins were detected by anti-PTEN IgG (9559, 1:2000), anti-Chk1 IgG (2360, 1:750), anti-p-Chk1 IgG (2348, 1:1000), anti-p-ATR (2853, 1:1000) (Cell Signaling Technology, Danvers, MA, USA), anti-ATR IgG (SC1887, 1:1000), anti-PALB2 IgG (A301-2464, 1:1000) and anti-GAPDH IgG (SC25778, 1:1000) (Santa Cruz Biotechnology, Dallas, TX, USA), anti-PARP1 IgG (556362, BD Bioscience, San Jose, CA, USA, 1:1000), anti-H2B IgG (NB100-56347, Novus Biologycals, Littleton, CO, USA, 1:500)or anti-β-actin IgG (Sigma, Darmstadt, Germany, 1:50.000), IRDYE 680 conjugated anti-mouse IgG or IRDYE 800 conjugated anti-rabbit IgG (Licor, Lincoln, NE, USA, 1:7500).

4.5. DNA Fiber Assay

Exponentially growing cells were pulse-labeled with 25 µM CldU (Sigma, Darmstadt, Germany) and 250 µM IdU (Sigma, Darmstadt, Germany) added to the growth medium for the times specified. Where indicated, the cells were exposed to 2 mM HU or 1 µM Olaparib during or in between the pulse labeling, as indicated. Labeled cells were harvested and DNA fiber spreads were prepared from 0.5×10^6 cells/mL as described previously [12]. Slides were incubated in 2.5 M HCl for 80 min and then washed three to five times in PBS, followed by incubation in blocking buffer (2% BSA, 0.1% Tween in PBS) for 1 h. Acid-treated fiber spreads were stained with monoclonal rat anti-BrdU antibody (Bio-Rad, Feldkirchen, Germany) (1:1000) to detect CldU, and monoclonal mouse anti-BrdU antibody (Becton Dickinson, Franklin Lakes, NJ, USA, 1:1500) to detect IdU. Secondary antibodies were goat anti-rat AlexaFluor555 and goat anti-mouse AlexaFluor488 (both Invitrogen, Carlsbad, CA, USA, 1:500). Primary antibodies were diluted in blocking buffer, incubated for 1 h with rat anti-BrdU antibody and mouse anti-BrdU antibody, followed by fixation with 4% paraformaldehyde and extensive washes in PBS and blocking buffer. Secondary antibodies were applied for 1.5 h, washed with PBS and blocking buffer and slides were mounted in Immuno-Fluor mounting medium (MP Biomedicals, Santa Ana, CA, USA). Fiber tracts were examined using an AxioVert 200 M fluorescence microscope (Zeiss, Oberkochen, Germany). Pictures were taken from randomly selected fields with untangled fibers and analyzed using ImageJ software package. For structure analyses, the frequencies of the different classes of fiber tracks were classified as follows: red-green (elongating fork), red (stalled or terminated forks), green-red-red-green (first pulse origin) and green (second pulse origin). At least 300 forks were analyzed for each experiment and the means of at least three independent experiments are represented. For fork speed analyses, the lengths of CldU and IdU tracks were measured and micrometer values were converted into kilobases. A conversion factor for the length of a labeled track of 1 µm = 2.59 kb was used [13]. A minimum of 100 individual fibers were analyzed for each experiment and the means of at least three independent experiments are presented.

4.6. Data Evaluation

Statistical analysis, curve fitting and graphs were performed by means of the Prism software Version 6 (Graph Pad Software, San Diego, CA, USA). Data are given as mean (±SEM) of replicate experiments.

5. Conclusions

Impaired DNA replication occurs in cancer, where it contributes to genomic instability. This vulnerable process is already a target of cancer therapies. Drugs that increase replication stress have become attractive for therapeutic intervention in several cancer types. Our results suggest that the clinical use of PARP1 inhibitors should be extended beyond those tumors with BRCA mutations to a larger group of patients with PTEN mutant tumors, maybe even to the larger group of CIN high tumors.

References

1. Bayani, J.; Selvarajah, S.; Maire, G.; Vukovic, B.; Al-Romaih, K.; Zielenska, M.; Squire, J.A. Genomic mechanisms and measurement of structural and numerical instability in cancer cells. *Semin. Cancer Biol.* **2007**, *17*, 5–18. [CrossRef] [PubMed]

2. Funk, L.C.; Zasadil, L.M.; Weaver, B.A. Living in cin: Mitotic infidelity and its consequences for tumor promotion and suppression. *Dev. Cell* **2016**, *39*, 638–652. [CrossRef] [PubMed]

3. Burrell, R.A.; McClelland, S.E.; Endesfelder, D.; Groth, P.; Weller, M.C.; Shaikh, N.; Domingo, E.; Kanu, N.; Dewhurst, S.M.; Gronroos, E.; et al. Replication stress links structural and numerical cancer chromosomal instability. *Nature* **2013**, *494*, 492–496. [CrossRef] [PubMed]

4. Tijhuis, A.E.; Johnson, S.C.; McClelland, S.E. The emerging links between chromosomal instability (cin), metastasis, inflammation and tumour immunity. *Mol. Cytogenet.* **2019**, *12*, 17. [CrossRef]

5. Hou, S.Q.; Ouyang, M.; Brandmaier, A.; Hao, H.; Shen, W.H. Pten in the maintenance of genome integrity: From DNA replication to chromosome segregation. *Bioessays* **2017**, *39*, 1700082. [CrossRef]

6. Shen, W.H.; Balajee, A.S.; Wang, J.; Wu, H.; Eng, C.; Pandolfi, P.P.; Yin, Y. Essential role for nuclear pten in maintaining chromosomal integrity. *Cell* **2007**, *128*, 157–170. [CrossRef]

7. McEllin, B.; Camacho, C.V.; Mukherjee, B.; Hahm, B.; Tomimatsu, N.; Bachoo, R.M.; Burma, S. Pten loss compromises homologous recombination repair in astrocytes: Implications for glioblastoma therapy with temozolomide or poly(adp-ribose) polymerase inhibitors. *Cancer Res.* **2010**, *70*, 5457–5464. [CrossRef]

8. Bassi, C.; Ho, J.; Srikumar, T.; Dowling, R.J.; Gorrini, C.; Miller, S.J.; Mak, T.W.; Neel, B.G.; Raught, B.; Stambolic, V. Nuclear pten controls DNA repair and sensitivity to genotoxic stress. *Science* **2013**, *341*, 395–399. [CrossRef]

9. Mansour, W.Y.; Tennstedt, P.; Volquardsen, J.; Oing, C.; Kluth, M.; Hube-Magg, C.; Borgmann, K.; Simon, R.; Petersen, C.; Dikomey, E.; et al. Loss of pten-assisted g2/m checkpoint impedes homologous recombination repair and enhances radio-curability and parp inhibitor treatment response in prostate cancer. *Sci. Rep.* **2018**, *8*, 3947. [CrossRef]

10. Li, S.; Shen, Y.; Wang, M.; Yang, J.; Lv, M.; Li, P.; Chen, Z.; Yang, J. Loss of pten expression in breast cancer: Association with clinicopathological characteristics and prognosis. *Oncotarget* **2017**, *8*, 32043–32054. [CrossRef]

11. Dean, S.J.; Perks, C.M.; Holly, J.M.; Bhoo-Pathy, N.; Looi, L.M.; Mohammed, N.A.; Mun, K.S.; Teo, S.H.; Koobotse, M.O.; Yip, C.H.; et al. Loss of pten expression is associated with igfbp2 expression, younger age, and late stage in triple-negative breast cancer. *Am. J. Clin. Pathol.* **2014**, *141*, 323–333. [CrossRef] [PubMed]

12. Beg, S.; Siraj, A.K.; Prabhakaran, S.; Jehan, Z.; Ajarim, D.; Al-Dayel, F.; Tulbah, A.; Al-Kuraya, K.S. Loss of pten expression is associated with aggressive behavior and poor prognosis in middle eastern triple-negative breast cancer. *Breast Cancer Res. Treat.* **2015**, *151*, 541–553. [CrossRef]

13. Khan, F.; Esnakula, A.; Ricks-Santi, L.J.; Zafar, R.; Kanaan, Y.; Naab, T. Loss of pten in high grade advanced stage triple negative breast ductal cancers in african american women. *Pathol. Res. Pract.* **2018**, *214*, 673–678. [CrossRef] [PubMed]

14. Bianchini, G.; Balko, J.M.; Mayer, I.A.; Sanders, M.E.; Gianni, L. Triple-negative breast cancer: Challenges and opportunities of a heterogeneous disease. *Nat. Rev. Clin. Oncol.* **2016**, *13*, 674–690. [CrossRef] [PubMed]

15. Lord, C.J.; Ashworth, A. Parp inhibitors: Synthetic lethality in the clinic. *Science* **2017**, *355*, 1152–1158. [CrossRef]

16. Exman, P.; Mallery, R.M.; Lin, N.U.; Parsons, H.A. Response to olaparib in a patient with germline brca2 mutation and breast cancer leptomeningeal carcinomatosis. *NPJ Breast Cancer* **2019**, *5*, 46. [CrossRef]

17. Thompson, L.L.; Jeusset, L.M.; Lepage, C.C.; McManus, K.J. Evolving therapeutic strategies to exploit chromosome instability in cancer. *Cancers* **2017**, *9*, 151. [CrossRef]

18. Birkbak, N.J.; Eklund, A.C.; Li, Q.; McClelland, S.E.; Endesfelder, D.; Tan, P.; Tan, I.B.; Richardson, A.L.; Szallasi, Z.; Swanton, C. Paradoxical relationship between chromosomal instability and survival outcome in cancer. *Cancer Res.* **2011**, *71*, 3447–3452. [CrossRef]

19. Carter, S.L.; Eklund, A.C.; Kohane, I.S.; Harris, L.N.; Szallasi, Z. A signature of chromosomal instability inferred from gene expression profiles predicts clinical outcome in multiple human cancers. *Nat. Genet.* **2006**, *38*, 1043–1048. [CrossRef]

20. Parplys, A.C.; Seelbach, J.I.; Becker, S.; Behr, M.; Wrona, A.; Jend, C.; Mansour, W.Y.; Joosse, S.A.; Stuerzbecher, H.W.; Pospiech, H.; et al. High levels of rad51 perturb DNA replication elongation and cause unscheduled origin firing due to impaired chk1 activation. *Cell Cycle* **2015**, *14*, 3190–3202. [CrossRef]

21. Liu, C.; Srihari, S.; Lal, S.; Gautier, B.; Simpson, P.T.; Khanna, K.K.; Ragan, M.A.; Le Cao, K.A. Personalised pathway analysis reveals association between DNA repair pathway dysregulation and chromosomal instability in sporadic breast cancer. *Mol. Oncol.* **2016**, *10*, 179–193. [CrossRef] [PubMed]

22. Wilhelm, T.; Olziersky, A.M.; Harry, D.; De Sousa, F.; Vassal, H.; Eskat, A.; Meraldi, P. Mild replication stress causes chromosome mis-segregation via premature centriole disengagement. *Nat. Commun.* **2019**, *10*, 3585. [CrossRef] [PubMed]

23. Schlacher, K.; Wu, H.; Jasin, M. A distinct replication fork protection pathway connects fanconi anemia tumor suppressors to rad51-brca1/2. *Cancer Cell* **2012**, *22*, 106–116. [CrossRef] [PubMed]

24. Yoneda, T.; Williams, P.J.; Hiraga, T.; Niewolna, M.; Nishimura, R. A bone-seeking clone exhibits different biological properties from the mda-mb-231 parental human breast cancer cells and a brain-seeking clone in vivo and in vitro. *J. Bone Miner. Res.* **2001**, *16*, 1486–1495. [CrossRef]

25. Hohensee, I.; Chuang, H.N.; Grottke, A.; Werner, S.; Schulte, A.; Horn, S.; Lamszus, K.; Bartkowiak, K.; Witzel, I.; Westphal, M.; et al. Pten mediates the cross talk between breast and glial cells in brain metastases leading to rapid disease progression. *Oncotarget* **2017**, *8*, 6155–6168. [CrossRef]

26. Daboussi, F.; Courbet, S.; Benhamou, S.; Kannouche, P.; Zdzienicka, M.Z.; Debatisse, M.; Lopez, B.S. A homologous recombination defect affects replication-fork progression in mammalian cells. *J. Cell Sci.* **2008**, *121*, 162–166. [CrossRef]

27. Zeman, M.K.; Cimprich, K.A. Causes and consequences of replication stress. *Nat. Cell Biol.* **2014**, *16*, 2–9. [CrossRef]

28. Parplys, A.C.; Zhao, W.; Sharma, N.; Groesser, T.; Liang, F.; Maranon, D.G.; Leung, S.G.; Grundt, K.; Dray, E.; Idate, R.; et al. Nucks1 is a novel rad51ap1 paralog important for homologous recombination and genome stability. *Nucleic Acids Res.* **2015**, *43*, 9817–9834. [CrossRef]

29. Parplys, A.C.; Kratz, K.; Speed, M.C.; Leung, S.G.; Schild, D.; Wiese, C. Rad51ap1-deficiency in vertebrate cells impairs DNA replication. *DNA Repair* **2014**, *24*, 87–97. [CrossRef]

30. Nikkila, J.; Parplys, A.C.; Pylkas, K.; Bose, M.; Huo, Y.; Borgmann, K.; Rapakko, K.; Nieminen, P.; Xia, B.; Pospiech, H.; et al. Heterozygous mutations in palb2 cause DNA replication and damage response defects. *Nat. Commun.* **2013**, *4*, 2578. [CrossRef]

31. Rehman, F.L.; Lord, C.J.; Ashworth, A. Synthetic lethal approaches to breast cancer therapy. *Nat. Rev. Clin. Oncol.* **2010**, *7*, 718–724. [CrossRef] [PubMed]

32. Arnaudeau, C.; Lundin, C.; Helleday, T. DNA double-strand breaks associated with replication forks are predominantly repaired by homologous recombination involving an exchange mechanism in mammalian cells. *J. Mol. Biol.* **2001**, *307*, 1235–1245. [CrossRef] [PubMed]

33. Wurster, S.; Hennes, F.; Parplys, A.C.; Seelbach, J.I.; Mansour, W.Y.; Zielinski, A.; Petersen, C.; Clauditz, T.S.; Munscher, A.; Friedl, A.A.; et al. Parp1 inhibition radiosensitizes hnscc cells deficient in homologous recombination by disabling the DNA replication fork elongation response. *Oncotarget* **2016**, *7*, 9732–9741. [CrossRef] [PubMed]

34. Mendes-Pereira, A.M.; Martin, S.A.; Brough, R.; McCarthy, A.; Taylor, J.R.; Kim, J.S.; Waldman, T.; Lord, C.J.; Ashworth, A. Synthetic lethal targeting of pten mutant cells with parp inhibitors. *EMBO Mol. Med.* **2009**, *1*, 315–322. [CrossRef]

35. Comen, E.A.; Robson, M. Poly(adp-ribose) polymerase inhibitors in triple-negative breast cancer. *Cancer J.* **2010**, *16*, 48–52. [CrossRef]

36. Toledo, L.I.; Altmeyer, M.; Rask, M.B.; Lukas, C.; Larsen, D.H.; Povlsen, L.K.; Bekker-Jensen, S.; Mailand, N.; Bartek, J.; Lukas, J. Atr prohibits replication catastrophe by preventing global exhaustion of rpa. *Cell* **2013**, *155*, 1088–1103. [CrossRef]

37. Tacconi, E.M.; Badie, S.; De Gregoriis, G.; Reislander, T.; Lai, X.; Porru, M.; Folio, C.; Moore, J.; Kopp, A.; Baguna Torres, J.; et al. Chlorambucil targets brca1/2-deficient tumours and counteracts parp inhibitor resistance. *EMBO Mol. Med.* **2019**, *11*, e9982. [CrossRef]

38. Liao, H.; Ji, F.; Helleday, T.; Ying, S. Mechanisms for stalled replication fork stabilization: New targets for synthetic lethality strategies in cancer treatments. *EMBO Rep.* **2018**, *19*, e46263. [CrossRef]

39. Conti, C.; Seiler, J.A.; Pommier, Y. The mammalian DNA replication elongation checkpoint: Implication of chk1 and relationship with origin firing as determined by single DNA molecule and single cell analyses. *Cell Cycle* **2007**, *6*, 2760–2767. [CrossRef]

40. Rickman, K.; Smogorzewska, A. Advances in understanding DNA processing and protection at stalled replication forks. *J. Cell Biol.* **2019**, *218*, 1096–1107. [CrossRef]

41. Wang, G.; Li, Y.; Wang, P.; Liang, H.; Cui, M.; Zhu, M.; Guo, L.; Su, Q.; Sun, Y.; McNutt, M.A.; et al. Pten regulates rpa1 and protects DNA replication forks. *Cell Res.* **2015**, *25*, 1189–1204. [CrossRef] [PubMed]

42. Zou, L.; Elledge, S.J. Sensing DNA damage through atrip recognition of rpa-ssdna complexes. *Science* **2003**, *300*, 1542–1548. [CrossRef] [PubMed]

43. Schlacher, K.; Christ, N.; Siaud, N.; Egashira, A.; Wu, H.; Jasin, M. Double-strand break repair-independent role for brca2 in blocking stalled replication fork degradation by mre11. *Cell* **2011**, *145*, 529–542. [CrossRef] [PubMed]

44. Ying, S.; Hamdy, F.C.; Helleday, T. Mre11-dependent degradation of stalled DNA replication forks is prevented by brca2 and parp1. *Cancer Res.* **2012**, *72*, 2814–2821. [CrossRef] [PubMed]

45. Ronson, G.E.; Piberger, A.L.; Higgs, M.R.; Olsen, A.L.; Stewart, G.S.; McHugh, P.J.; Petermann, E.; Lakin, N.D. Parp1 and parp2 stabilise replication forks at base excision repair intermediates through fbh1-dependent rad51 regulation. *Nat. Commun.* **2018**, *9*, 746. [CrossRef]

46. Min, W.; Bruhn, C.; Grigaravicius, P.; Zhou, Z.W.; Li, F.; Kruger, A.; Siddeek, B.; Greulich, K.O.; Popp, O.; Meisezahl, C.; et al. Poly(adp-ribose) binding to chk1 at stalled replication forks is required for s-phase checkpoint activation. *Nat. Commun.* **2013**, *4*, 2993. [CrossRef]

47. Lecona, E.; Fernandez-Capetillo, O. Targeting atr in cancer. *Nat. Rev. Cancer* **2018**, *18*, 586–595. [CrossRef]